

A11102 616271

NAT'L INST OF STANDARDS & TECH R.I.C.



A11102616271

Cruz, J. E./Assessment of error bounds for  
QC100 .U5753 NO.1300 1986 V198 C.1 NBS-P

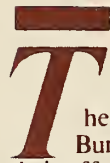
# NBS TECHNICAL NOTE 1300

U.S. DEPARTMENT OF COMMERCE/National Bureau of Standards

## Assessment of Error Bounds for Some Typical MIL-STD-461/462 Types of Measurements

J.E. Cruz  
E.B. Larsen

QC  
100  
.U5753  
NO.1300  
1986  
C.2



The National Bureau of Standards<sup>1</sup> was established by an act of Congress on March 3, 1901. The Bureau's overall goal is to strengthen and advance the nation's science and technology and facilitate their effective application for public benefit. To this end, the Bureau conducts research and provides: (1) a basis for the nation's physical measurement system, (2) scientific and technological services for industry and government, (3) a technical basis for equity in trade, and (4) technical services to promote public safety. The Bureau's technical work is performed by the National Measurement Laboratory, the National Engineering Laboratory, the Institute for Computer Sciences and Technology, and the Institute for Materials Science and Engineering.

### *The National Measurement Laboratory*

Provides the national system of physical and chemical measurement; coordinates the system with measurement systems of other nations and furnishes essential services leading to accurate and uniform physical and chemical measurement throughout the Nation's scientific community, industry, and commerce; provides advisory and research services to other Government agencies; conducts physical and chemical research; develops, produces, and distributes Standard Reference Materials; and provides calibration services. The Laboratory consists of the following centers:

- Basic Standards<sup>2</sup>
- Radiation Research
- Chemical Physics
- Analytical Chemistry

### *The National Engineering Laboratory*

Provides technology and technical services to the public and private sectors to address national needs and to solve national problems; conducts research in engineering and applied science in support of these efforts; builds and maintains competence in the necessary disciplines required to carry out this research and technical service; develops engineering data and measurement capabilities; provides engineering measurement traceability services; develops test methods and proposes engineering standards and code changes; develops and proposes new engineering practices; and develops and improves mechanisms to transfer results of its research to the ultimate user. The Laboratory consists of the following centers:

- Applied Mathematics
- Electronics and Electrical Engineering<sup>2</sup>
- Manufacturing Engineering
- Building Technology
- Fire Research
- Chemical Engineering<sup>2</sup>

### *The Institute for Computer Sciences and Technology*

Conducts research and provides scientific and technical services to aid Federal agencies in the selection, acquisition, application, and use of computer technology to improve effectiveness and economy in Government operations in accordance with Public Law 89-306 (40 U.S.C. 759), relevant Executive Orders, and other directives; carries out this mission by managing the Federal Information Processing Standards Program, developing Federal ADP standards guidelines, and managing Federal participation in ADP voluntary standardization activities; provides scientific and technological advisory services and assistance to Federal agencies; and provides the technical foundation for computer-related policies of the Federal Government. The Institute consists of the following centers:

- Programming Science and Technology
- Computer Systems Engineering

### *The Institute for Materials Science and Engineering*

Conducts research and provides measurements, data, standards, reference materials, quantitative understanding and other technical information fundamental to the processing, structure, properties and performance of materials; addresses the scientific basis for new advanced materials technologies; plans research around cross-country scientific themes such as nondestructive evaluation and phase diagram development; oversees Bureau-wide technical programs in nuclear reactor radiation research and nondestructive evaluation; and broadly disseminates generic technical information resulting from its programs. The Institute consists of the following Divisions:

- Ceramics
- Fracture and Deformation<sup>3</sup>
- Polymers
- Metallurgy
- Reactor Radiation

<sup>1</sup>Headquarters and Laboratories at Gaithersburg, MD, unless otherwise noted; mailing address Gaithersburg, MD 20899.

<sup>2</sup>Some divisions within the center are located at Boulder, CO 80303.

<sup>3</sup>Located at Boulder, CO, with some elements at Gaithersburg, MD.

NE-56  
QC100  
U5753  
PL 1300  
1986  
2.2

# Assessment of Error Bounds for Some Typical MIL-STD-461/462 Types of Measurements

J.E. Cruz  
E.B. Larsen

Electromagnetic Fields Division  
Center for Electronics and Electrical Engineering  
National Engineering Laboratory  
National Bureau of Standards  
Boulder, Colorado 80303

Sponsored by  
U.S. Army Aviation Systems Command  
DRSAV-QE  
St. Louis, Missouri 63120



---

U.S. DEPARTMENT OF COMMERCE, Malcolm Baldrige, Secretary

NATIONAL BUREAU OF STANDARDS, Ernest Ambler, Director

Issued October 1986

National Bureau of Standards Technical Note 1300  
Natl. Bur. Stand. (U.S.), Tech Note 1300, 108 pages (Oct. 1986)  
CODEN:NBTNAE

U.S. GOVERNMENT PRINTING OFFICE  
WASHINGTON: 1986

---

For sale by the Superintendent of Documents, U.S. Government Printing Office, Washington, DC 20402



## Contents

	Page
List of Tables.....	v
List of Figures.....	vi
1. Overall Introduction.....	1.1
2. Generating a Known EM Field in a Parallel-Plate Transmission Line...	2.1
2.1 Introduction.....	2.1
2.2 TEM Cell with a 50 $\Omega$ Impedance, 50 $\Omega$ Termination, and 377 $\Omega$ E/H Ratio.....	2.2
2.3 Parallel-Plate Line with Open Sides and 377 $\Omega$ E/H Ratio.....	2.5
2.3.1 Characteristic Impedance and Input Impedance of a Stripline.....	2.6
2.3.2 Field Level and Uniformity in a Stripline.....	2.9
2.3.3 Effect of Screenroom Resonances on Field Strength.....	2.10
2.4 Operation of a Parallel-Plate Line in the Open-Circuit Mode or Short-Circuit Mode.....	2.11
2.5 Use of E- and H-Field Probes as Transfer Standards.....	2.12
2.6 References.....	2.13
Tables 2-1 to 2-8.....	2.15
Figures 2-1 to 2-14.....	2.23
3. EM Field of a Single-Wire Transmission Line in a Screenroom.....	3.1
3.1 Introduction.....	3.1
3.2 Experimental Configuration of a Typical Long-Wire Antenna.....	3.2
3.3 Evaluation of a Long-Wire Antenna.....	3.3
3.3.1 Field Uniformity Along Axis of Long-Wire.....	3.3
3.3.2 Measured vs Calculated Field Beneath the Long-Wire.....	3.4
3.4 Conclusions and Recommendations.....	3.6
3.5 References.....	3.6
Figures 3-1 to 3-7.....	3.7
4. Calibration of Antenna Factors for EMI Antennas.....	4.1
4.1 Introduction.....	4.1
4.2 Measurement of Antenna Factors in a Screenroom.....	4.5
4.3 Measurement of Antenna Factors at an Open Field Site.....	4.6
4.3.1 Standard Antenna Method.....	4.6
4.3.2 Standard Field Method.....	4.8
4.4 Experimental Measurements of Antenna Factors.....	4.10
4.4.1 Biconical Dipoles.....	4.10
4.4.2 Vertical Monopoles.....	4.12
4.5 Discussion of Antenna Factor Measurement Accuracy in Shielded Enclosures.....	4.13
4.6 Error Bounds of Screenroom Measurements.....	4.14
4.7 Conclusions.....	4.14
4.8 References.....	4.15
Figures 4-1 to 4-19.....	4.17
5. Measurement of Broadband Impulsive Signals.....	5.1
5.1 Introduction.....	5.1
5.2 Calibration of an EMI Receiver and Measurement of an Impulse Generator Using the Video Pulse Technique of MIL-STD-462.....	5.2
5.3 Measurement of an IG by the NBS FFT Calibration System.....	5.6
5.4 Approximations of IG Output in Terms of the Measured Area of the Pulses.....	5.8
5.5 References.....	5.10

CONTENTS (Continued)

	Page
Tables 5-1 to 5-4.....	5.11
Figures 5-1 to 5-6.....	5.15
6. Overall Summary, Conclusions, and Recommendations.....	6.1
6.1 Field of a Parallel-Plate Transmission Line.....	6.1
6.2 Use of an Electrically Small Transfer Probe.....	6.2
6.3 Field of a Single-Wire Transmission Line.....	6.2
6.4 Calibration of Antenna Factors for EMI Antennas.....	6.3
6.5 Measurement of Broadband Impulsive Signals.....	6.5
7. Acknowledgments.....	7.1

## List of Tables

	Page
2-1. Measured input impedance of the NBS MIL-STD-462 stripline in an unshielded laboratory, with 83 $\Omega$ termination.....	2.15
2-2. Measured input impedance of the NBS MIL-STD-462 stripline in an unshielded laboratory, with 120 $\Omega$ termination.....	2.16
2-3. Measured input impedance of the NBS MIL-STD-462 stripline in center of NBS screenroom, with 83 $\Omega$ termination.....	2.17
2-4. Measured input impedance of the NBS MIL-STD-462 stripline in center of NBS screenroom, with 120 $\Omega$ termination.....	2.18
2-5. Measured characteristic impedance of MIL-STD-462 stripline in NBS screenroom.....	2.19
2-6. Measured E-field error in center of MIL-STD-462 stripline.....	2.20
2-7. Measured E-field error along center line of MIL-STD-462 stripline, at 30 MHz.....	2.21
2-8. Calculated cavity-mode resonances for the empty NBS screenroom, first four modes.....	2.22
5-1 Response of an ideal receiver to various types of input signals.....	5.11
5-2 Calibration of receiver impulse bandwidth (IBW) and impulse generator spectrum amplitude $S(f)$ using MIL-STD-462 technique, bands 1-4.....	5.12
5-3 Calibration of receiver impulse bandwidth (IBW) and impulse generator spectrum amplitude $S(f)$ using MIL-STD-462 technique, bands 5-8.....	5.13
5-4 Spectrum amplitude of the commercial impulse generator, measured with the NBS FFT calibration system.....	5.14

## List of Figures

		Page
2-1.	Isometric sketch of a typical TEM cell used to generate standard E and H fields.....	2.23
2-2.	Side view of a typical TEM cell.....	2.24
2-3.	Cross-sectional view of a TEM cell.....	2.24
2-4.	Isometric sketch of a typical MIL-STD-462 parallel-plate transmission line.....	2.25
2-5.	Cross-sectional view of the NBS MIL-STD-462 parallel-plate transmission line.....	2.25
2-6.	Instrumentation for measuring the E-field level in the MIL-STD-462 stripline.....	2.26
2-7.	Measured input impedance of the MIL-STD-462 stripline in the center of the NBS screenroom.....	2.27
2-8.	Measured characteristic impedance of the MIL-STD-462 stripline in the NBS screenroom.....	2.27
2-9.	Measured E-field error in center of stripline. Position A in screenroom, with no ground strap.....	2.28
2-10.	Measured E-field error in center of stripline. Position B in screenroom.....	2.28
2-11.	Measured E-field error along length of stripline at 30 MHz, 83 $\Omega$ termination. Position A in screenroom, with no ground strap.....	2.29
2-12.	Measured E-field error along length of stripline at 30 MHz, 100 $\Omega$ termination. Position B in screenroom.....	2.29
2-13.	A parallel-plate cage system for generating a known E-field, 0.01 to 40 MHz.....	2.30
2-14.	Typical response of an EFM-5 probe vs frequency, at a field strength of 20 dBV/m (10 V/m).....	2.31
3-1.	The long-wire antenna in a shielded enclosure.....	3.7
3-2.	Signal generator drives intermediate feeder line to long-wire antenna.....	3.8
3-3.	Signal generator coaxial line feeds long-wire directly.....	3.8
3-4.	Electric field uniformity of long-wire antenna along the length of the chamber at 1 MHz.....	3.9



	Page
3-5. Electric field uniformity of long-wire antenna along the length of the chamber at 15 MHz.....	3.9
3-6. Electric field uniformity of long-wire antenna along the length of the chamber at 30 MHz.....	3.10
3-7. Calculated-to-measured field versus distance below the long-wire for selected frequencies from 1 to 30 MHz.....	3.10
4-1. Test setup required by MIL-STD-461A for determination of antenna factors.....	4.17
4-2. Instrumentation used at NBS open-field site to calibrate monopole antenna factors.....	4.17
4-3. Antenna factor of a typical biconical dipole taken from the manufacturer's manual for a far-field separation distance.....	4.18
4-4. Antenna factor of a typical biconical dipole taken from the manufacturer's manual for a separation distance of 1 m.....	4.18
4-5. Antenna factor of a typical biconical dipole taken from the manufacturer's manual for a separation distance of 3 m.....	4.19
4-6. Antenna factor of a typical biconical dipole taken from the manufacturer's manual for a separation distance of 15 m and an antenna height of 3 m.....	4.19
4-7. Antenna factor of Biconical No. 1 for a "far-field" separation distance, as measured at NBS.....	4.20
4-8. Antenna factor of Biconical No. 2 for a "far-field" separation distance, as measured at NBS.....	4.20
4-9. Placement of biconical antennas in the NBS screenroom, position 1.....	4.21
4-10. Antenna factors for biconical dipole calibrated in the NBS screenroom at spacings of 1 and 3 m.....	4.22
4-11. Placement of biconical antennas in the NBS screenroom, position 2.....	4.23
4-12. Placement of biconical antennas in the NBS screenroom, position 3.....	4.24
4-13. Measurement results of three screenroom placements with an antenna separation distance of 1 m.....	4.25

4-14.	Difference between antenna factors measured in a screenroom and on the NBS field site for a biconical dipole.....	4.26
4-15.	Difference between field strength measured with a calibrated transfer probe (EFM-5) and that measured with a biconical antenna calibrated by the MIL-STD-461A two-antenna method.....	4.26
4-16.	Antenna factor for typical 1.04 m vertical monopole taken from the manufacturer's manual.....	4.27
4-17.	Free-space antenna factor of two vertical monopoles as calibrated at the NBS open-field site.....	4.27
4-18.	Antenna factor for 1.04 m vertical monopole calibrated in the NBS screenroom at different antenna spacings.....	4.28
4-19.	Antenna factor for 1.04 m vertical monopole calibrated in the NBS screenroom at different antenna locations for a 1 m antenna separation.....	4.28
5-1.	Instrumentation for testing the MIL-STD-461/462 approach for measuring impulse bandwidth of a receiver and spectrum amplitude of an impulse generator.....	5.15
5-2.	Photographs of the receiver impulse response envelopes (video pulses) measured at NBS.....	5.16
5-3.	Instrumentation for the NBS automatic FFT pulse measurement system.....	5.17
5-4.	Photograph of sampling oscilloscope trace of the IG output pulse (top) and plot of the pulse supplied to the computer for the FFT (bottom).....	5.18
5-5.	Graphs of the IG spectrum amplitude measured by two methods, MIL-STD-462 and the NBS FFT pulse measurement system.....	5.19
5-6.	Sketches of the spectrum amplitude of three common pulse waveforms.....	5.20

Assessment of Error Bounds for Some Typical  
MIL-STD-461/462 Types of Measurements

J. E. Cruz and E. B. Larsen

Electromagnetic Fields Division  
National Bureau of Standards  
Boulder, Colorado 80303

This report deals with the instrumentation and equations for several systems used by the U.S. Army for electromagnetic compatibility (EMC) testing and calibrations. Most testing for MIL-STD-461/462 is performed in a shielded enclosure (screenroom) rather than an open field site, which leads to uncertainty in the measurement of emissions from electronic equipment, or the susceptibility of equipment to radiation. Assessment of error bounds by the National Bureau of Standards (NBS) is covered in this report, and suggestions are given for improving the measurements.

Four areas of concern were studied as follows: (a) electromagnetic (EM) fields generated in a parallel-plate transmission line (stripline), (b) EM fields beneath a single-wire transmission line in a screenroom (long-wire line), (c) determination of antenna factors for electromagnetic interference (EMI) antennas located in a screenroom, and (d) calibration of EMI receivers to measure broadband impulsive signals. Most EMC antennas at NBS are calibrated at an open field site or in an anechoic chamber. This report presents antenna factors determined in a typical screenroom using the two-antenna method, and comparison with those determined at an open field site. The video pulse technique prescribed in MIL-STD-462 for calibrating EMI receivers was also evaluated. Four different methods were tested for comparison with the MIL-STD approach. They are defined and discussed in this report.

Keywords: antenna factor; electromagnetic compatibility; field strength standards; impulse spectrum amplitude; military standards; screenroom measurements

## 1. Overall Introduction

This report deals with the instrumentation and equations for several systems used by the U.S. Army for electromagnetic compatibility (EMC) testing and calibrations. The report relates to Military Standards 461, 462, and 463 which are standards issued by the U.S. Department of Defense (DOD) for use by all departments and agencies within DOD. MIL-STD-461A is titled "Electromagnetic interference characteristics, requirements for equipment." It is



dated August 1, 1968, and supersedes MIL-STD-461. MIL-STD-462 was issued by DOD on July 31, 1967, and is titled "Electromagnetic interference characteristics, measurement of." MIL-STD-463 was issued on June 9, 1966, and is titled "Definitions and systems of units, electromagnetic interference technology." This report (NBS Tech. Note 1300) deals only with MIL-STD-461A and MIL-STD-462, and will generally be referred to here as MIL-STD-461/462.

Most EMC testing for MIL-STD-461/462 is performed in a shielded enclosure (screenroom) rather than at an open field site because of lower cost, shielding from ambient fields, and convenience. This MIL-STD, which is used in the procurement of many military and other government systems, has several recognized problems. Possible errors and large uncertainties can occur in the measurement of electromagnetic (EM) emissions from electronic equipment, or the susceptibility of this equipment to EM radiation. The uncertainty is increased when performing the measurements inside a screenroom where multiple reflections and antenna impedance perturbations occur. Assessment of the error bounds by the National Bureau of Standards (NBS) is covered in this report, and the data should provide insight into the problems associated with this type of testing. A few suggestions are also given for improving the measurement procedures prescribed in MIL-STD-462. However, these improvements are now being quantified and will be covered in greater detail in a future report.

Four areas of concern were studied at NBS for determining the error bounds of MIL-STD-461/462 testing, as follows: (a) EM fields generated in a parallel-plate transmission line (stripline); (b) EM fields beneath a single-wire transmission line in a screenroom (long-wire line); (c) determination of antenna factors for electromagnetic interference (EMI) antennas located in a screenroom, and (d) calibration of EMI receivers to measure broadband impulsive signals.

The parallel-plate stripline parameters (input impedance, characteristic impedance, and field uniformity) were measured at various locations of the stripline inside the NBS screenroom, using MIL-STD-462 techniques. The MIL-STD also describes a laboratory method of producing a field having known E and H magnitudes in a shielded room by a long-wire antenna. The objective of NBS testing was to measure the field level and uniformity, and compare this with



theoretically calculated values. Equations for computing the E- and H-field magnitudes in the enclosure are included in this report.

Most EMC antennas at NBS are calibrated at an open field site or in an anechoic chamber, using the standard antenna or standard field method. Because these antenna factors are not necessarily applicable to making measurements in a screenroom, the errors for measuring emissions with the calibrated antenna can be quite large. This report presents antenna factors determined in a typical screenroom using the two-antenna method, and comparison with those determined at the NBS open field site. Experimental data show the variability of antenna factor as a function of frequency and location in the screenroom, thereby providing an indication of error bounds.

The video pulse technique prescribed in MIL-STD-462 for calibrating EMI receivers was also evaluated at NBS. This approach involves application of a train of identical repetitive pulses to the EMI receiver. As specified in the MIL-STD, the area and maximum amplitude of the receiver response envelope are measured. From those measurements the receiver impulse bandwidth (IBW) and spectrum amplitude of the impulse generator (IG) are determined. The IBW of an EMI receiver is used for measurement of broadband interference. It can be determined by several different approaches. The spectrum amplitude of an impulse generator as a function of frequency,  $S(f)$ , can also be measured by several approaches. Four different methods were evaluated at NBS for comparison with the MIL-STD approach. They are defined and discussed in this report.



## 2. Generating a Known EM Field in a Parallel-Plate Transmission Line

### 2.1 Introduction

Chapters 2 and 3 of this report deal with the instrumentation and design equations for several systems used to generate calculable electric (E) and magnetic (H) fields for EMC testing. These "standard" electromagnetic fields with known magnitude are used to (a) test the susceptibility of electronic equipment to EM fields, (b) calibrate E- and H- field probes for measuring and mapping fields, and (c) expose biological specimens in a known EM environment.

The type of instrumentation employed at NBS to generate a standard field depends on the signal frequency, desired field intensity, and size of the device under test (DUT). In general, transverse electromagnetic (TEM) cells or other TEM transmission lines are used at frequencies up to about 200 MHz. A series of four waveguide transmission cells can be used at frequencies between 100 and 750 MHz. At frequencies above 200 MHz, NBS usually generates a known calibrating field in an anechoic chamber, using the transmitted field of an open-ended waveguide launcher or a pyramidal horn antenna. However, the production of radiated standard fields in anechoic chambers is described elsewhere [2-1,2-2] and will not be covered in this report. Most of the EMC testing for MIL-STD-461/462 is still performed within a shielded enclosure (screenroom). The screenroom is preferred to an open site because of its lower cost, shielding from the effects of interfering (ambient) fields, and its overall convenience--especially during inclement weather.

All of the standard field generators discussed here have been in use for about 50 years. However, some of the newer EMC engineers are not familiar with the principles and operation of these devices. Therefore it seems useful to summarize the design parameters and mathematical basis for several common E- and H-field synthesizers.

Much has been written in the past 15 years about the design, construction, and use of so-called TEM cells. Therefore, little discussion is included here about these TEM lines when operated in their usual mode and terminated in their characteristic impedance, which is usually  $50 \Omega$ . The main advantage of TEM cells is that electrically-small antennas such as E- and H-field probes can be calibrated in a shielded environment, in a fairly uniform EM field having a free-space wave impedance ( $Z_f$ ) of  $377 \Omega$ . One disadvantage of TEM cells is the inverse proportionality between their physical size and

upper useful frequency limit. Another limitation is the large power (and consequent cost) required to generate a high field intensity, for the usual case where the cell characteristic impedance ( $Z_C$ ) and terminating load resistance ( $Z_L$ ) are only 50  $\Omega$ . Therefore, it is often advantageous to use other field generating configurations for EMC applications.

The following types of EM field simulators are described in chapters 2 and 3 of this report:

- (1) TEM cell with a characteristic impedance ( $Z_C$ ) of 50  $\Omega$ , operated in its normal mode with a terminating load impedance ( $Z_L$ ) of 50  $\Omega$  (discussed only briefly);
- (2) parallel-plate transmission line (stripline) with a characteristic impedance ( $Z_C$ ) of 75-200  $\Omega$ , but having a free-space wave impedance ( $Z_W$ ) of 377  $\Omega$ , where  $Z_W$  is the E/H field strength ratio;
- (3) stripline or TEM cell operated in the open-circuit mode to produce an intense E-field with a high wave impedance or in the short-circuit mode to produce an intense H-field with a low wave impedance; and
- (4) "long-wire" antenna chamber, made in a typical screenroom by installing a horizontal wire as the "center" conductor of a TEM line, having a  $Z_C$  value of 200-600  $\Omega$ .

## 2.2 TEM Cell with a 50 $\Omega$ Impedance, 50 $\Omega$ Termination, and 377 $\Omega$ E/H Ratio

A TEM cell is essentially a triplate transmission line with the sides closed in to prevent radiation of rf energy into the environment, and to provide electrical isolation of equipment being tested for susceptibility to EM fields. Much has been published describing their design and principles of operation [2-2,2-3,2-4,2-5].

An isometric view, a side view, and a cross section view of a typical TEM cell are shown in figures 2-1, 2-2, and 2-3, respectively. The cell consists of a length of rectangular "coaxial" transmission line made of flat metal plates, with the cell septum acting as the center conductor. The two ends of



the cell have tapered dimensions to adapt to standard coaxial connectors. The line and tapered transitions are generally designed to have a nominal characteristic impedance of 50  $\Omega$  in order to obtain a low voltage standing wave ratio (VSWR) in a 50  $\Omega$  system. RF energy is conducted through the line from a 50  $\Omega$  transmitter connected at the input port to a 50  $\Omega$  terminating load ( $Z_L$ ) connected at the output port. The electric field level at the test point in the cell, midway between the center of the septum and either (outer) wall, is given by

$$E = \frac{V}{b} = \frac{\sqrt{P Z_C}}{b}, \quad (2-1)$$

where  $E$  = electric field strength at the test point, V/m,  
 $V$  = RMS voltage on the septum (center conductor), V,  
 $b$  = separation distance between the septum and outer walls, m,  
 $P$  = net power flow through the cell, W, and  
 $Z_C$  = real part of the cell's characteristic impedance  $\approx 50 \Omega$ .

The TEM or principal mode of operation produces only E- and H-fields that are transverse (perpendicular) to the direction of energy flow (propagation). Such waves can carry energy at frequencies down to dc, while the higher order (waveguide) modes have large attenuation below a so-called cutoff frequency. A transmission line must have two separate conductors to support a TEM wave. The wave traveling through the cell has a wave impedance (E/H ratio) of approximately 377  $\Omega$ , the same as a far-zone plane wave propagating in free space. Therefore, the H-field is given by

$$H = E/Z_f \approx E/377, \quad (2-2)$$

where  $H$  = magnetic field strength at the test point, A/m, and  
 $Z_f$  = wave impedance of free space  $\approx 377 \Omega$ .

An approximate equation for the characteristic impedance of a rectangular transmission line is [2-6,2-7]:

$$Z_C = \frac{377}{4 \left[ \frac{a}{b} - \frac{2}{\pi} \ln \left( \sinh \frac{\pi g}{2b} \right) \right] - k}, \quad (2-3)$$

where  $a$ ,  $b$ , and  $g$  are shown in figure 2-3 and  $k$  is related to the fringing

capacitance between the edges of the septum and the side walls. For large gaps ( $g/a > 0.2$ ) this fringing term is negligible. As an example, consider the TEM cell used in the Fields Characterization Laboratory at NBS. The dimensions shown in figure 2-3 are  $2a = 1.2$  m,  $2b = 0.6$  m, and  $w = 0.81$  m. In this case,  $k$  of eq (2-3) is negligible and the calculated value of  $Z_c$  is  $50.1 \Omega$ .

An expression for calculating  $Z_c$  of a triplate transmission line with open sides, in which the upper and lower (grounded) plates have infinite width, is given by eq (20) in reference [2-8] as

$$Z_c = \frac{377}{4 \left[ \frac{w}{2b} + \frac{2}{\pi} \ln 2 \right]} \quad (2-4)$$

The calculated value of  $Z_c$  for an open triplate line having a plate spacing ( $b = 0.3$  m) and septum width ( $w = 0.81$  m) equal to that of the above NBS TEM cell is  $52.6 \Omega$ . Note that this is only slightly higher than the  $50 \Omega$  value for the TEM cell with closed sides.

The upper useful frequency of a TEM cell is limited by field distortions which are caused by waveguide-mode resonances that occur at frequencies above the empty cell's multimode cutoff. Because of the tapered section at either end of the cell, the resonant length is not well defined. As a first approximation, the overall cell length is often considered to be the wavelength of the lowest frequency resonance [2-2]. In other words, for good operation the spacing between the cell plates, the width of the septum, and the length of the nontapered section should all be less than  $\lambda/2$ . Thus it is generally not possible to use a TEM cell for calibrating or taking data with most EMI antennas.

The estimated measurement uncertainty in establishing EM fields in a TEM cell operating in the fundamental (TEM) mode ranges from  $\pm 0.5$  dB to  $\pm 2$  dB, depending on the shape of the cell (width to height ratio) and the quality of design. Details for calculating the electric field distribution inside a TEM cell and procedures for performing radiated susceptibility tests are given elsewhere [2-6,2-9,2-10].

It is important that the size of the device to be tested does not exceed approximately one-third of the plate spacing of the cell [2-11,2-12]. This is because the device tends to short out the test field in the region it occupies

between the plates, increasing the field amplitude. Field strength errors and perturbations caused by placing equipment inside the cell can be partially corrected by measuring the field in the test region near the DUT with a small calibrated E-field probe, and making appropriate corrections. This procedure is discussed in reference [2-9].

### 2.3 Parallel-Plate Line with Open Sides and 377 $\Omega$ E/H Ratio

One major limitation of a TEM cell is the inverse proportionality between its physical size and upper useful frequency. As mentioned, the spacing between the cell conductors, the width of the septum, and length of the uniform (nontapered) line section should all be less than  $\lambda/2$ . Thus, when designing an rf chamber for exposing relatively large samples, rather than for calibrating a small measurement probe, it is often not possible or convenient to use a TEM cell. Another disadvantage is the large power required for a given field intensity, if the characteristic impedance and load resistance are only 50  $\Omega$ . The required power, however, is about 10-20 dB less than that required for radiated field methods performed in an anechoic chamber or at an open field site.

Any sharp bends or inhomogeneities in a transmission line tend to promote higher-order waveguide modes. For example, the side walls of a TEM cell perpendicular to the septum permit higher-order modes to propagate at lower frequencies than in a parallel-plate line having open sides [2-13]. Also, it is sometimes advantageous for other reasons to use open parallel plates or a transmission line having a characteristic impedance other than 50  $\Omega$ , as discussed in section 2.4.

If a parallel-plate transmission line is terminated in its characteristic impedance, the E/H ratio has a free-space value of 377  $\Omega$ . Also, similar to a plane wave in free space, the E, H and propagation vectors are all mutually orthogonal. That is, the E and H vectors are perpendicular to each other and both are perpendicular to the propagation vector of the traveling wave.

Figure 2-4 is a sketch of a parallel-plate transmission line (stripline) which is useful for generating known E- and H-fields at frequencies up to 30 or 40 MHz. This type of calibrating line is specified in MIL-STD-462 [2-14] and SAE Standard AIR-1209 as a test chamber for radiated susceptibility (RS) measurements on small equipment at frequencies between 14 kHz and 30 MHz.



Notice 3 of the MIL-STD permits the installation of a "long-wire" antenna in a screenroom, for RS testing of equipment that is too large for the stripline (see chapter 3 of this report).

The expression for calculating the E- and H-field intensity existing at the test point midway between two flat conducting plates of a stripline is the same as that for a TEM cell, which is given by eqs (2-1) and (2-2). In this case,

E = electric field strength midway between the two plates, V/m,

V = RMS voltage difference between the plates, V, and

b = plate spacing, m.

Evaluation of a typical MIL-STD-461/462 parallel plate line at NBS was accomplished in three phases, as follows:

(a) measurement of the characteristic impedance and input impedance to the stripline for various values of terminating resistance and for various locations of the stripline inside the NBS screenroom, at frequencies from 1 to 100 MHz;

(b) calibration of a small transfer probe suitable for checking the E field generated within the stripline, and

(c) measurement of the absolute level and uniformity of the generated field strength at frequencies from 2 to 100 MHz using the above calibrated probe.

### 2.3.1 Characteristic Impedance and Input Impedance of a Stripline

The general expression for the characteristic impedance of a transmission line is given by eq (2-5), where the approximation given applies to a low loss line.

$$Z_C = \sqrt{\frac{R + j\omega L}{G + j\omega C}} \approx \sqrt{\frac{L}{C}}, \quad (2-5)$$

where R = resistance of the line per unit length,  $\Omega/m$ ,

G = conductance of the line per unit length, S/m,



L = inductance of the line per unit length, H/m, and  
C = capacitance of the line per unit length, F/m.

The required value of load impedance for terminating a parallel-plate line in its characteristic impedance ( $Z_C$ ), which results in a minimum voltage standing wave ratio (VSWR), depends mainly on the plate spacing and width. The  $Z_C$  value of an open-sided line is also affected by its surroundings, especially if the line is located in a shielded enclosure (high Q cavity) such as a screen room. Therefore, the optimum value of terminating resistor for a parallel-plate line should be verified experimentally from tests of the E-field uniformity along the line, with a small dipole probe, as discussed in section 2.3.2 [2-15]. The parallel-plate transmission line of figure 2-4, as fabricated according to MIL-STD-462, has measured values of characteristic impedance which range from 80 to 160  $\Omega$ , as will be shown later. Similar striplines with smaller dimensions are also in use. These are useful at frequencies up to 50 or 100 MHz, depending on size.

MIL-STD-462 specifies the use of a stripline having a plate spacing of 0.457 m (1.5 ft) and an upper plate width of 0.610 m (2 ft), as shown in figure 2-5. This stripline is used for making radiated susceptibility (RS04) tests of electronic equipment in a known EM field. The width of the lower plate in figure 2-5 is 0.305 m (1 ft) greater, on one side, than the upper plate. The lower plate thus has a total width of 0.914 m (3 ft). The MIL-STD and the SAE documents state that the expected  $Z_C$  value for this line is 83  $\Omega$ . Several equations are given in the literature for calculating the characteristic impedance of parallel-plate lines. For example, Sensor and Simulation Note XXI by Baum [2-8] gives an equation for  $Z_C$  of a balanced parallel-plate line or a single-plate line above an infinite ground plane. The characteristic impedance of a two-plate line in free space is

$$Z_C = (377) \left(\frac{b}{w}\right) \left\{1 + \frac{b}{\pi w} \left[1 + \ln\left(\frac{2\pi w}{b}\right)\right]\right\}^{-1}. \quad (2-6)$$

If the extra 0.305 m (1 ft) width in the lower plate of the MIL-STD-462 line is ignored, the calculated value for  $Z_C$  using eq (2-6) is 162  $\Omega$ . If it is assumed that the lower plate extends to infinity on each side (infinite width), the theoretical value of  $Z_C$  is half the above value, or 81  $\Omega$ . This is close to the 83  $\Omega$  value given by the MIL-STD.

Volume 4 of White's series of books on EMI/EMC [2-16] contains a graph (fig. 4.19 on p. 4.34) of the characteristic impedance of parallel-plate lines. If the lower plate width ( $w$ ) is equal to or greater than three times the width of the upper plate, the graph in [2-16] indicates that  $Z_C$  of the MIL-STD-462 line would be  $113 \Omega$ . The theoretical  $Z_C$  of the line would thus be greater than  $113 \Omega$  (rather than  $83 \Omega$ ) because the lower plate width is less than  $3w$ .

Another equation given in the literature for calculating  $Z_C$  of a strip-line, in which  $w/b$  is restricted to a value between 1 and 10, is [2-17]

$$Z_C = \frac{377}{(w/b) + 2.42 - 0.44 (b/w) + (1 - b/w)^6} \quad (2-7)$$

According to eq (2-7), the theoretical  $Z_C$  value for a MIL-STD-461 line, assuming infinite width in the lower plate, is  $110 \Omega$ . Thus the actual MIL-STD line should have a  $Z_C$  nearly double this value. It can be seen that the theoretically calculated values of  $Z_C$  for a stripline having an upper plate width of  $0.610 \text{ m}$  ( $2 \text{ ft}$ ) and a plate spacing of  $0.457 \text{ m}$  ( $1.5 \text{ ft}$ ) range from about  $80$  to  $160 \Omega$ , depending on the assumptions used.

A parallel-plate transmission line was fabricated at NBS according to the specifications and dimensions given in MIL-STD-462. Measurements were done to determine experimentally the optimum value of terminating load resistor  $R_L$  for this line to see how closely this compares with the specified value of  $83 \Omega$ . These measurements were performed with an automatic network analyzer, which determines  $Z_C$  from measurements of the line input reactance as a function of signal frequency, for two cases. In one case the line was terminated with a good short circuit and in the other case with an open circuit. That is,

$$Z_C = \sqrt{L_0/C_0}, \quad (2-8)$$

where  $Z_C$  = characteristic impedance of the transmission line,  $\Omega$ ,  
 $L_0$  = short-circuit inductance, H, and  
 $C_0$  = open-circuit capacitance, F.

In measuring the line inductance, two short copper straps were soldered between the tapered end of the upper plate and the ground plate. The straps were connected in place of the three parallel resistors previously connected

to terminate the line. Figure 2-6 shows the instrumentation used for measuring  $Z_C$ ,  $Z_{in}$  and the E-field uniformity within the MIL-STD-462 stripline.

Measurements were made of the input impedance of the stripline, with the line terminated in two different values of resistance ( $83 \Omega$  and  $120 \Omega$ ). The stripline was supported on wood sawhorses at a height 1 m above the floor. These data are given in tables 2-1, 2-2, 2-3 and 2-4 for frequencies ranging from 1 to 100 MHz. The data show that the measured input impedance varies with frequency for both values of terminating resistance. The optimum value of terminating resistance appears to be in the neighborhood of  $120 \Omega$  rather than the  $83 \Omega$  specified in MIL-STD-462. Graphs of the data from tables 2-3 and 2-4 for frequencies up to 50 MHz are shown in figure 2-7.

The measured values of line characteristic impedance are given in table 2-5 for three different locations of the line inside the NBS screenroom. Position A corresponds to placement of the stripline near and parallel to the long wall of the room at a height 1 m above the floor. A copper grounding strap 10 cm wide was connected in some of the tests between the grounded plate of the line and the copper-clad table. Position B is the same as position A except that the stripline was placed on the floor so that the grounded side of the line was capacitively coupled to the grounded floor of the screenroom. Position C refers to the stripline mounted on sawhorses along the center line of the screenroom, with the grounded plate of the line at a height 1 m above the floor. Position D is the same as position C except that the stripline was lowered to the floor level. Table 2-5 shows that the measured characteristic impedance of the transmission line varies greatly with frequency, but for the lower frequencies it has a value of about  $100 \Omega$ . Graphs of the measured line  $Z_C$  for frequencies up to 50 MHz are shown in figure 2-8 for three positions of the stripline in the screenroom.

### 2.3.2 Field Level and Uniformity in a Stripline

The main criterion for a good standard-field setup is the uniformity of the generated field as a function of frequency. It is also important to know how closely the test field approximates a uniform plane wave with a wave impedance (E/H ratio) equal to that of free space, which is  $377 \Omega$ . Measurements were made with a calibrated NBS E-field probe (EFM-5) having dipole antennas 5 cm in length [2-18]. A block diagram of the setup used is given in



figure 2-6. The field level chosen for these tests was about 5 V/m. The tests were done to compare the actual measured field with the values calculated from eq (2-1) given previously,  $E = V/b$ .

For most of the tests, the EFM-5 probe was placed midway (vertically) between the two plates and in the center (horizontally) of the line, as indicated in figure 2-6. The electric field uniformity was checked as a function of signal frequency using two different values of terminating resistance (83 and 100  $\Omega$ ). The value of R in figure 2-6, used to terminate the coaxial cable leading to the stripline in 50  $\Omega$ , was 145  $\Omega$  when the stripline termination was 83  $\Omega$ . The measured dc input resistance for this case was 54  $\Omega$ . The value of R was changed to 100  $\Omega$  when the stripline was terminated in 100  $\Omega$ , and the measured dc input resistance for this case was 51  $\Omega$ . Measurements of electric field strength at the probe position, versus signal frequency, were made for two different locations of the stripline in the empty screenroom. The large walk-in doors to the room were closed when taking field strength data.

The measured values of electric field strength at the center of the stripline are shown in table 2-6 and figures 2-9 and 2-10 for both values of terminating resistance. It can be seen that the standard field values calculated from eq (2-1) are correct within  $\pm 2$  dB at all frequencies up to 40 MHz. The measured values of E-field at 30 MHz as a function of position along the line are given in table 2-7 and figures 2-11 and 2-12. It can be seen that the field level is correct within 2.3 dB and uniform within  $\pm 0.5$  dB over the 2 m length of line at this frequency. The use of a broadband step-up transformer at the stripline input would result in higher E-field magnitudes for a given amount of rf power than that obtained with the instrumentation of figure 2-6.

### 2.3.3 Effect of Screenroom Resonances on Field Strength

The characteristic impedance of a stripline with open sides is influenced by the proximity of nearby metal surfaces and the Q of the enclosure (screenroom) in which it is located. The effect of room resonances on the behavior of the stripline is clearly evident by the excursions in impedance and measured field strength at frequencies above 40 MHz. These resonance effects would occur at lower frequencies if a larger screenroom were used. The NBS screenroom was initially evaluated for EM shielding effectiveness in



the frequency range of 10 kHz to 1000 MHz, using MIL-STD-285 as a guide. However, the data are not included in this report.

Test methods RE02 and RS02 in MIL-STD-462 require that E- and H-field tests be performed on electronic equipment for radiated emissions and susceptibility. It is generally necessary to make these measurements inside a screenroom. Because of reflections from conducting surfaces, it is difficult to make measurements that correlate with open-site data. At higher frequencies there are field strength anomalies due to cavity-mode resonances of the room. The resonant frequencies of an empty rectangular screenroom are given by

$$F = 150 \sqrt{\left(\frac{a}{\ell}\right)^2 + \left(\frac{b}{w}\right)^2 + \left(\frac{c}{h}\right)^2}, \quad (2-9)$$

where  $F$  = frequency, MHz,  
 $a, b, c$  = cavity mode integers, only one of which can be zero, and  
 $\ell, w, h$  = length, width, height of the screenroom, m, and  $\ell > w > h$ .

For the NBS screenroom,  $\ell = 7.202$  m,  $w = 3.362$  m, and  $h = 2.805$  m. In this case, the lowest-frequency cavity-mode resonance is the 110 mode, where  $a = 1$ ,  $b = 1$ , and  $c = 0$ . The calculated frequency of this mode is

$$F = 150 \sqrt{\left(\frac{1}{7.202}\right)^2 + \left(\frac{1}{3.362}\right)^2} = 49.24 \text{ MHz}. \quad (2-10)$$

The next higher-frequency mode is the 101 mode, which has a calculated frequency of 57.39 MHz. Table 2-8 gives a list of all the possible cavity-mode resonances for mode integers up to 4. The lowest resonance at 49.24 MHz is associated with a transverse electric (TE) wave traveling in the  $\ell$  direction.

#### 2.4 Operation of a Parallel-Plate Line in the Open-Circuit Mode or Short-Circuit Mode

A parallel-plate stripline (or a TEM cell) can be operated without a resistive termination for frequencies up to 30 or 40 MHz. When the line is open circuited it acts as a parallel-plate capacitor rather than a transmission line, and produces a field with a high wave impedance (high E/H ratio). High-level E-fields can then be produced by connecting a broadband step-up transformer at the input terminal of the line.

Figure 2-13 is a sketch of a system using open-ended parallel plates to generate a known electric field. The expression for calculating the E-field intensity at the point P midway between the flat metal plates is the same as that for a stripline or TEM cell, namely eq (2-1). The uncertainty of the calculated field is also about the same. The wave impedance, however, is greater than  $377 \Omega$ . A high level E-field can thus be produced with a low power source, especially if the line is resonated by means of an inductor, as shown in the figure. For example, a field level of 1000 V/m can generally be achieved at the resonant frequency with a 1 W power source. At higher frequencies (above 20 or 30 MHz) approaching self resonance of the system, similar to a MIL-STD-462 stripline, it is not possible to calculate the field level from eq (2-1). It is then necessary to measure the field strength at the calibrating point with a small transfer probe that has been calibrated previously in a small stripline or a TEM cell, as explained in section 2.5 of this report. By contrast, when a MIL-STD-462 stripline (or a TEM cell) is short circuited, it acts as a single-turn loop and produces a field having a very low wave impedance. This configuration is useful for producing a high-level H-field with a low E/H ratio.

## 2.5 Use of E- and H-Field Probes as Transfer Standards

The term "transfer standard" refers to an electrically small antenna (rf probe). This can be a short dipole for sensing E-fields or a small loop for H-fields that has a known response over a given range of frequency and amplitude. Such a probe can be used to measure the field strength as a function of frequency in a transmission line. A typical calibration curve for a 5 cm dipole probe (EFM-5) is shown in figure 2-14.

As mentioned in section 2.3.2, tests of field level vs frequency and position in a MIL-STD-462 stripline can be made with this type of probe. Such transfer probes can also be used to improve the construction and operation of standard-field chambers, for example, by optimizing the value of terminating load impedance. The optimum value should be determined experimentally for each measurement situation and location of the line with respect to its surrounding objects, screenroom walls, etc.

Transmission line chambers can often be used at frequencies above those for which the theoretical equations apply. In this case the field strength is

determined or checked with a transfer probe that has been calibrated previously in a smaller chamber, or which has been calibrated at a lower frequency but is known to have a flat response up to the frequency of interest. For example, the E- or H-field in a screenroom that has been converted into a long-wire chamber can usually be determined more accurately with a transfer probe than by relying on theoretical equations.

## 2.6 References

- [2-1] Kummer, W. H.; Gillespie, E. S. Antenna measurements--1978. Proc. IEEE. 66(4): 483-507; 1978 April.
- [2-2] Ma, M. T.; Kanda, M.; Crawford, M. L.; Larsen, E. B. A review of electromagnetic compatibility/interference measurement methodologies. Proc. IEEE. 73(3): 388-411; 1985 March.
- [2-3] Crawford, M. L. Generation of standard EM fields using TEM transmission cells. IEEE Trans. on EMC. EMC-16(4): 189-195; 1974 November.
- [2-4] Crawford, M. L. Generation of standard EM fields for calibration of power density meters 20 kHz to 1000 MHz. Nat. Bur. Stand. (U.S.) NBSIR 75-804; 1975 January.
- [2-5] Mitchell, J. C. A radio frequency radiation exposure apparatus. Brooks Air Force Base, School of Aerospace Medicine, Technical Report SAM-TR-70-43; 1970 July.
- [2-6] Tippet, J. C.; Chang, D.C. Radiation characteristics of dipole sources located inside a rectangular coaxial transmission line. Nat. Bur. Stand. (U.S.) NBSIR 75-829; 1976 January.
- [2-7] Chen, T. S. Determination of the capacitance, inductance, and characteristic impedance of rectangular lines. IRE Trans. on MTT. MTT-8(5): 510-519; 1960 September.
- [2-8] Baum, C. E. Note XXI. Impedances and field distributions for parallel plate transmission line simulators. Electromagnetic Pulse Sensor and Simulation Notes. Vol. 1, DASA Report 1880-1; 1967 April.
- [2-9] Crawford, M. L.; Workman, J. L. Using a TEM cell for EMC measurements of electronic equipment. Nat. Bur. Stand. (U.S.) Tech. Note 1013; Revised 1981 July. 65 p.
- [2-10] Crawford, M. L. Improving the repeatability of EM susceptibility measurements of electronic components when using TEM cells. International Congress Exposition; 1983 February 28-March 4; Detroit, MI; and SAE Handbook; 1984.

- [2-11] Kanda, M. Electromagnetic-field distortion due to a conducting rectangular cylinder in a transverse electromagnetic cell. IEEE Trans. on EMC. EMC-24(3): 294-301; 1982 August.
- [2-12] Kanda, M. Analytical and numerical techniques for analyzing an electrically short dipole with a nonlinear load. IEEE Trans. Ant. and Prop. AP-28: 71-78; 1980 January.
- [2-13] Weil, C. M.; Joines, W. T.; Kinn, J. F. Frequency range of large-scale TEM mode rectangular strip lines. Microwave Journal: 93-100; 1981 November.
- [2-14] Military Standard, Electromagnetic Interference Characteristics, Measurement of. MIL-STD-462; 1967 July 31.
- [2-15] Roseberry, B. E.; Schulz, R. B. A parallel-strip line for testing RF susceptibility. IEEE Trans. on EMC. EMC-7: 142-150; 1965 June.
- [2-16] White, D. R. J. EMC Handbook, Vol. 4, EMI test instrumentation and systems. Maryland: Don White Consultants, Inc.; 1971.
- [2-17] Gardiol, F. E.; Zurcher, J. F. HP-65 program computes microstrip impedance. Microwaves: 186; 1977 December.
- [2-18] Larsen, E. B.; Ries, F. X. Design and calibration of the NBS isotropic electric-field monitor (EFM-5), 0.2 to 1000 MHz. Nat. Bur. Stand. (U.S.) Tech. Note 1033; 1981 March. 103 p.



Table 2-1. Measured input impedance of the NBS MIL-STD-462 stripline in an unshielded laboratory, with 83  $\Omega$  termination.

<u>Frequency</u> MHz	<u>Resistance</u> $\Omega$	<u>Reactance</u> $\Omega$	<u>Impedance</u> $\Omega$	<u>Ratio</u> $Z_{in}/83$
1	83	5	83	1.00
1.5	83	7	83	1.00
2	83	10	84	1.01
2.5	84	12	85	1.02
3	85	15	86	1.04
3.5	87	15	88	1.06
4	84	18	86	1.04
4.5	84	25	88	1.06
5	88	26	92	1.11
5.5	91	28	95	1.14
6	89	28	93	1.12
6.5	93	36	100	1.20
7	98	38	105	1.27
7.5	101	39	108	1.30
8	105	41	113	1.36
8.5	107	41	115	1.39
9	111	43	119	1.43
9.5	116	43	124	1.49
10	121	42	128	1.54
15	157	22	159	1.92
20	147	-32	150	1.81
25	111	-26	114	1.37
30	97	-9	97	1.17
35	93	-1	93	1.12
40	86	11	87	1.05
45	114	28	117	1.41
50	119	10	119	1.43
55	105	19	107	1.29
60	108	40	115	1.39
65	168	59	178	2.14
70	132	-28	135	1.63
75	118	-14	119	1.43
80	97	10	98	1.18
85	93	29	97	1.17
90	135	59	147	1.77
95	147	16	148	1.78
100	127	12	128	1.54

Table 2-2. Measured input impedance of the NBS MIL-STD-462 stripline in an unshielded laboratory, with 120  $\Omega$  termination.

Frequency MHz	Resistance $\Omega$	Reactance $\Omega$	Impedance $\Omega$	Ratio $Z_{in}/120$
1	120	-2	120	1.00
2	118	-3	118	0.98
3	116	-7	116	0.97
4	108	-3	108	0.90
5	115	-2	115	0.96
6	108	1	108	0.90
7	114	1	114	0.95
8	115	0	115	0.96
9	115	0	115	0.96
10	115	-2	115	0.96
11	113	-2	113	0.94
12	112	-1	112	0.93
13	109	-3	109	0.91
14	110	5	110	0.92
15	113	4	113	0.94
16	114	4	114	0.95
17	115	4	115	0.96
18	118	3	118	0.98
19	118	-1	118	0.98
20	116	-4	116	0.97
21	111	-8	111	0.93
22	102	-1	102	0.85
23	103	8	103	0.86
24	108	12	109	0.91
25	110	13	111	0.93
26	114	16	115	0.96
27	120	16	121	1.01
28	124	13	125	1.04
29	125	12	126	1.05
30	126	11	126	1.05
35	126	-21	128	1.07
40	91	-28	95	0.79
45	89	5	89	0.74
50	100	15	101	0.84
55	93	15	94	0.78
60	97	45	107	0.89
65	128	71	146	1.22
70	203	-19	204	1.70
75	120	-38	126	1.05
80	93	-8	93	0.78
85	89	19	91	0.76
90	110	54	123	0.92
95	137	28	140	1.17
100	135	37	140	1.17

Table 2-3. Measured input impedance of the NBS MIL-STD-462 stripline in center of NBS screenroom, with 83  $\Omega$  termination.

<u>Frequency</u> <u>MHz</u>	<u>Resistance</u> <u><math>\Omega</math></u>	<u>Reactance</u> <u><math>\Omega</math></u>	<u>Impedance</u> <u><math>\Omega</math></u>	<u>Ratio</u> <u><math>Z_{in}/83</math></u>
1	83	4	83	1.00
1.5	83	6	83	1.00
2	83	9	83	1.00
2.5	84	12	85	1.02
3	85	15	86	1.04
3.5	87	15	88	1.06
4	84	18	86	1.04
4.5	84	25	88	1.06
5	88	26	92	1.11
5.5	91	28	95	1.14
6	89	28	93	1.12
6.5	93	36	100	1.20
7	98	38	105	1.27
7.5	101	39	108	1.30
8	105	41	113	1.36
8.5	107	41	115	1.39
9	111	43	119	1.43
9.5	116	43	124	1.49
10	121	42	128	1.54
15	157	22	159	1.92
20	147	-32	150	1.81
25	111	-26	114	1.37
30	97	-9	97	1.17
35	93	-1	93	1.12
40	86	11	87	1.05
45	114	28	117	1.41
50	119	10	119	1.43
55	105	19	107	1.29
60	108	40	115	1.39
65	168	59	178	2.14
70	132	-28	135	1.63
75	118	-14	119	1.43
80	97	10	98	1.18
85	93	29	97	1.17
90	135	59	147	1.77
95	147	16	148	1.78
100	127	12	128	1.54

Table 2-4. Measured input impedance of the NBS MIL-STD-462 stripline in center of NBS screenroom, with 120  $\Omega$  termination.

<u>Frequency</u> <u>MHz</u>	<u>Resistance</u> <u><math>\Omega</math></u>	<u>Reactance</u> <u><math>\Omega</math></u>	<u>Impedance</u> <u><math>\Omega</math></u>	<u>Ratio</u> <u><math>Z_{in}/120</math></u>
1	120	-2	120	1.00
2	118	-3	118	0.98
3	116	-7	116	0.97
4	108	-3	108	0.90
5	115	-2	115	0.96
6	108	1	108	0.90
7	114	1	114	0.95
8	115	0	115	0.96
9	115	0	115	0.96
10	115	-2	115	0.96
11	113	-2	113	0.94
12	112	-1	112	0.93
13	109	-3	109	0.91
14	110	5	110	0.92
15	113	4	113	0.94
16	114	4	114	0.95
17	115	4	115	0.96
18	118	3	118	0.98
19	118	-1	118	0.98
20	116	-4	116	0.97
21	111	-8	111	0.93
22	102	-1	102	0.85
23	103	8	103	0.86
24	108	12	109	0.91
25	110	13	111	0.93
26	114	16	115	0.96
27	120	16	121	1.01
28	124	13	125	1.04
29	125	12	126	1.05
30	127	10	127	1.06
35	126	-21	128	1.07
40	91	-28	95	0.79
45	89	5	89	0.74
50	100	15	101	0.84
55	93	15	94	0.78
60	97	45	107	0.89
65	128	71	146	1.22
70	203	-19	204	1.70
75	120	-38	126	1.05
80	93	-8	93	0.78
85	89	19	91	0.76
90	110	54	123	1.03
95	137	28	140	1.17
100	135	37	140	1.17



Table 2-5. Measured characteristic impedance of MIL-STD-462 stripline in NBS screenroom.

Frequency, MHz	Characteristic Impedance, ohms		
	Position A	Position C	Position D
2	102	111	110
4	101	132	108
6	100	122	107
8	105	117	105
10	142	121	105
12	100	119	102
14	88	112	99
16	63	94	57
18	392	312	155
20	135	143	126
22	120	129	118
24	113	134	114
26	106	136	108
28	99	134	102
30	86	135	93
32	40	123	50
34	154	151	423
36	209	103	145
38	148	169	130
40	136	143	125
42	125	139	118
44	113	138	106
46	68	132	83
48	279	836	375
50	74	41	76
55	91	51	65
60	362	115	325
65	138	124	347
70	316	131	216
75	137	217	117
80	99	78	807
85	55	74	78
90	143	305	77
95	295	193	64
100	159	168	196

Table 2-6. Measured E-field error in center of MIL-STD-462 stripline

Frequency MHz	Stripline error with 83 $\Omega$ termination, dB		Stripline error with 100 $\Omega$ termination, dB		
	Position A*	Position B	Position A*	Position A**	Position B
2	0.0	0.6	0.2	0.8	0.7
4	-	0.6	0.6	1.3	0.8
6	0.0	0.5	0.3	1.8	0.9
8	-	0.3	0.7	1.1	2.8
10	0.0	0.5	0.8	1.6	1.2
12	-	0.2	0.8	0.8	1.4
14	0.0	0.6	0.8	1.3	1.2
16	-	0.3	0.1	-0.1	1.3
18	0.1	0.8	0.7	0.7	1.2
20	-	1.0	0.9	1.1	1.3
22	0.8	1.5	0.8	1.1	1.6
24	-	0.4	1.4	0.7	-0.2
26	1.8	1.4	0.9	1.6	-0.1
28	-	1.6	1.2	1.5	-0.1
30	2.6	2.1	0.9	1.4	-0.1
32	-	1.4	1.0	1.2	-0.4
34	2.1	1.5	0.5	0.8	-0.8
36	-	1.0	0.1	0.1	-0.9
38	1.2	0.6	0.2	-0.2	-1.2
40	-	-0.2	-0.8	-0.7	-1.7
42	1.6	-0.2	1.8	-1.2	-1.2
44	-	-1.1	-2.0	-1.0	-1.6
46	-4.5	-2.4	-4.2	-3.7	-2.8
48	-10.5	-6.1	-12.3	-12.4	-12.2
50	9.1	-3.7	8.7	8.7	3.7
52	-	1.7	5.6	5.8	1.8
54	3.0	1.1	3.6	3.9	0.9
56	-	0.0	3.1	3.3	-0.8
58	-	0.5	2.3	2.8	0.0
60	3.5	0.4	2.5	2.2	1.3

\*No ground strap

\*\*With strap

Table 2-7. Measured E-field error along center line of MIL-STD-462 stripline, at 30 MHz

Distance from center of stripline, cm	Stripline error with 83 $\Omega$ termination, dB		Stripline error with 100 $\Omega$ termination, dB		
	Position A*	Position B	Position A*	Position A**	Position B
-90	2.6	2.0	0.9	0.9	-0.2
-75	2.8	2.1	1.0	1.0	-0.2
-60	2.8	2.1	1.0	1.0	-0.2
-45	2.9	2.2	1.0	1.0	-0.2
-30	2.9	2.2	1.0	1.0	-0.2
-15	2.9	2.3	1.0	1.1	-0.2
0	2.9	2.3	1.0	1.1	-0.1
15	2.8	2.2	1.0	1.1	-0.1
30	2.7	2.1	1.0	1.1	0.0
45	2.6	2.1	1.1	1.1	0.1
60	2.4	2.0	1.1	1.1	0.1
75	2.2	1.9	1.1	1.1	0.2
90	2.0	1.7	1.1	1.1	0.3
105	1.8	1.6	1.1	1.0	0.3

\*No ground strap

\*\*With strap

Table 2-8. Calculated cavity-mode resonances for the empty NBS screenroom, first four modes.

<u>Resonance Number</u>	<u>Mode Integers</u>	<u>Frequency, MHz</u>	<u>Resonance Number</u>	<u>Mode Integers</u>	<u>Frequency, MHz</u>
1	1 1 0	49.24	57	4 0 3	180.77
2	1 0 1	57.39	58	3 3 2	182.37
3	2 1 0	61.04	59	2 4 0	183.26
4	2 0 1	67.79	60	0 2 3	183.57
5	0 1 1	69.64	61	1 2 3	184.75
6	1 1 1	72.69	62	4 1 3	186.19
7	3 1 0	76.78	63	0 4 1	186.3
8	2 1 1	81.15	64	1 4 1	187.47
9	3 0 1	82.24	65	2 2 3	188.24
10	1 2 0	91.63	66	3 4 0	189.09
11	3 1 1	93.56	67	4 3 2	190.51
12	4 1 0	94.51	68	2 4 1	190.9
13	2 2 0	98.48	69	3 2 3	193.92
14	4 0 1	99.0	70	3 4 1	196.5
15	0 2 1	104.03	71	4 4 0	196.95
16	1 2 1	106.09	72	4 2 3	201.59
17	4 1 1	108.59	73	4 4 1	204.08
18	3 2 0	108.93	74	0 4 2	208.06
19	1 0 2	108.96	75	0 3 3	208.93
20	2 2 1	112.06	76	1 4 2	209.1
21	2 0 2	114.78	77	1 3 3	209.97
22	0 1 2	115.88	78	2 4 2	212.19
23	1 1 2	117.74	79	2 3 3	213.04
24	3 2 1	121.35	80	1 0 4	214.92
25	4 2 0	122.08	81	3 4 2	217.24
26	2 1 2	123.14	82	2 0 4	217.92
27	3 0 2	123.87	83	3 3 3	218.07
28	3 1 2	131.66	84	0 1 4	218.51
29	4 2 1	133.28	85	1 1 4	219.5
30	1 3 0	135.46	86	2 1 4	222.44
31	4 0 2	135.57	87	3 0 4	222.84
32	0 2 2	139.29	88	4 4 2	224.12
33	2 3 0	140.18	89	4 3 3	224.93
34	1 2 2	140.84	90	3 1 4	227.27
35	4 1 2	142.72	91	4 0 4	229.55
36	0 3 1	144.14	92	0 2 4	231.77
37	2 2 2	145.38	93	1 2 4	232.7
38	1 3 1	145.63	94	4 1 4	233.85
39	3 3 0	147.71	95	2 2 4	235.48
40	2 3 1	150.03	96	0 4 3	239.97
41	3 2 2	152.66	97	3 2 4	240.04
42	3 3 1	157.1	98	1 4 3	240.87
43	4 3 0	157.66	99	2 4 3	243.56
44	1 0 3	161.77	100	4 2 4	246.29
45	4 2 2	162.3	101	3 4 3	247.97
46	2 0 3	165.75	102	0 3 4	252.33
47	4 3 1	166.48	103	1 3 4	253.19
48	0 1 3	166.52	104	4 4 3	254.02
49	1 1 3	167.81	105	2 3 4	255.74
50	0 3 2	171.33	106	3 3 4	259.95
51	2 1 3	171.65	107	4 3 4	265.73
52	3 0 3	172.17	108	0 4 4	278.58
53	1 3 2	172.59	109	1 4 4	279.35
54	2 3 2	176.32	110	2 4 4	281.67
55	3 1 3	177.85	111	3 4 4	285.5
56	1 4 0	179.68	112	4 4 4	290.77



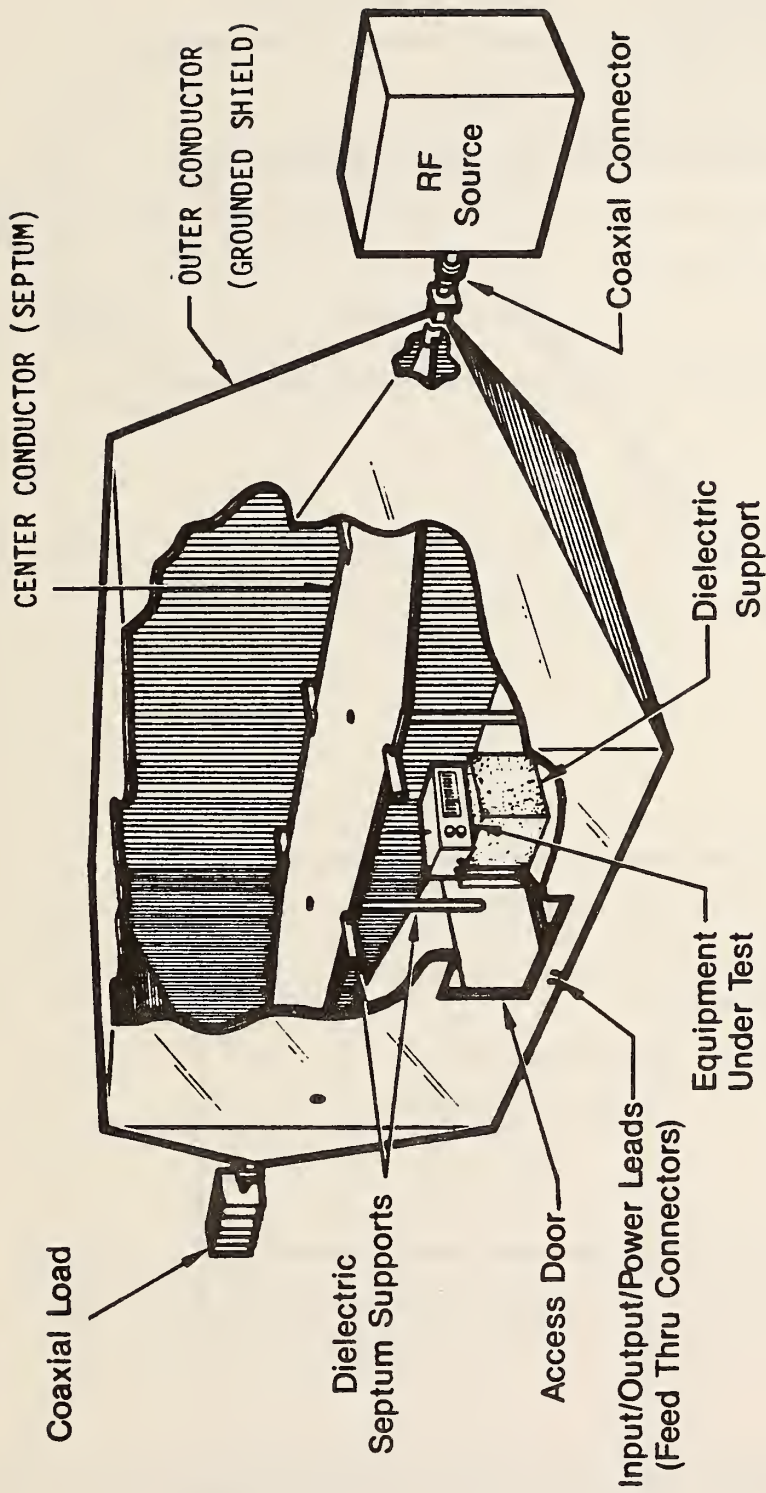


Figure 2-1. Isometric sketch of a typical TEM cell used to generate standard E and H fields.

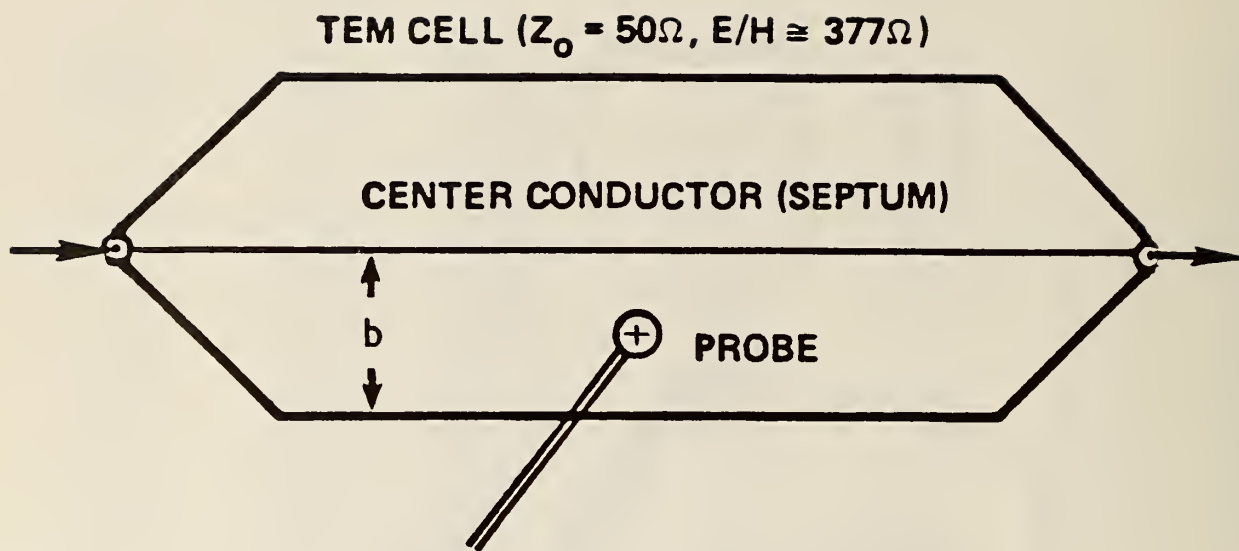


Figure 2-2. Side view of a typical TEM cell.

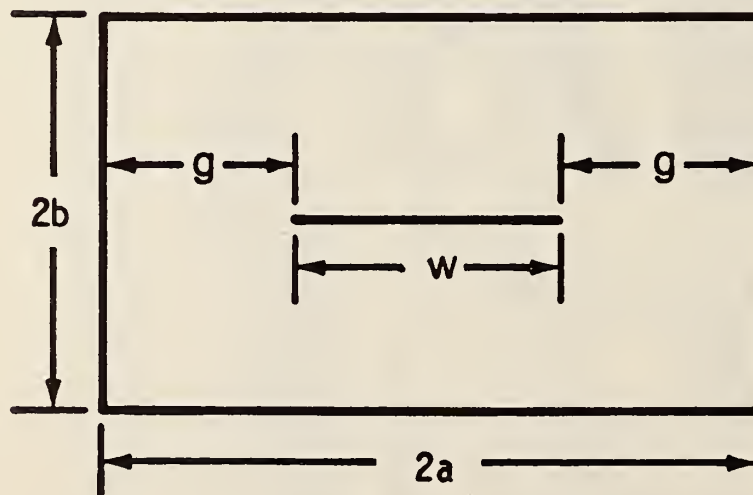


Figure 2-3. Cross-sectional view of a TEM cell.

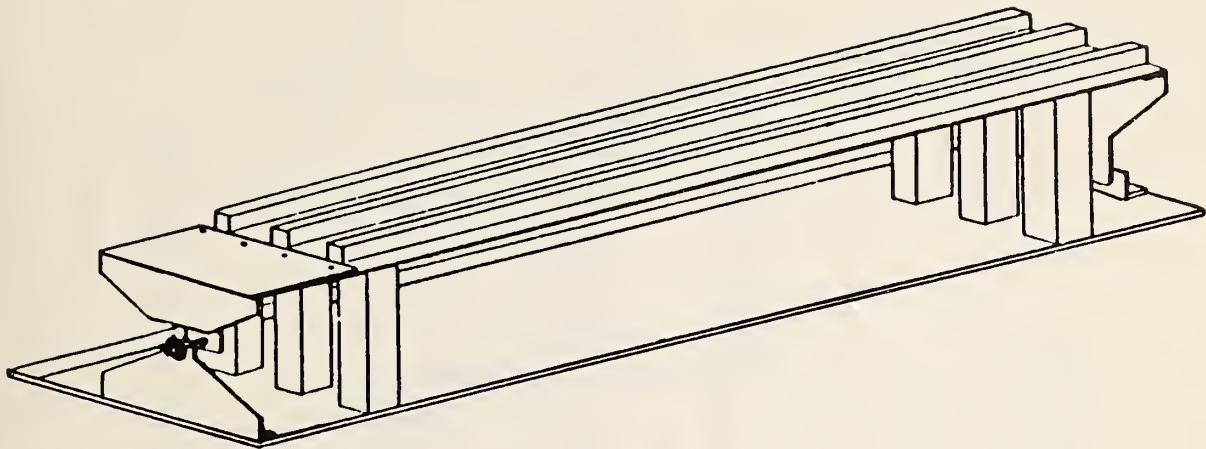


Figure 2-4. Isometric sketch of a typical MIL-STD-462 parallel-plate transmission line.

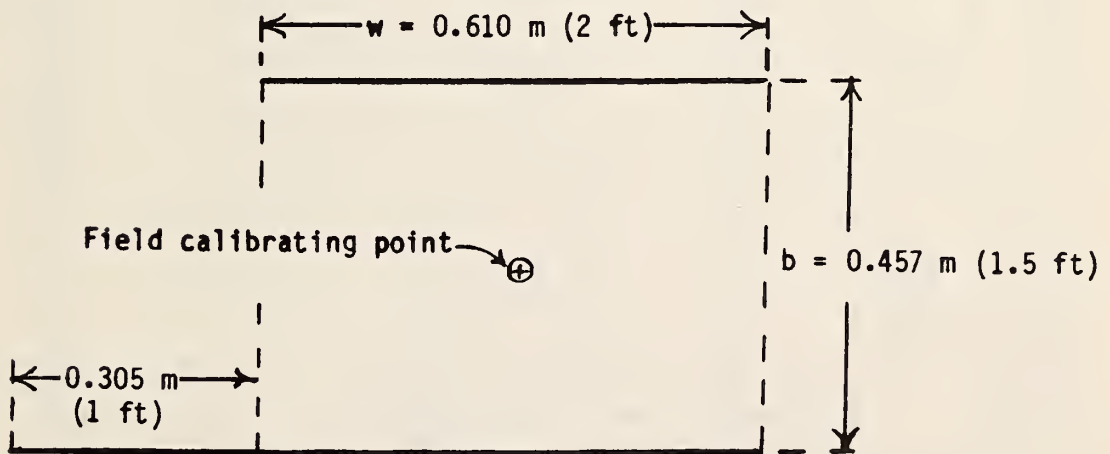


Figure 2-5. Cross-sectional view of the NBS MIL-STD-462 parallel-plate transmission line.

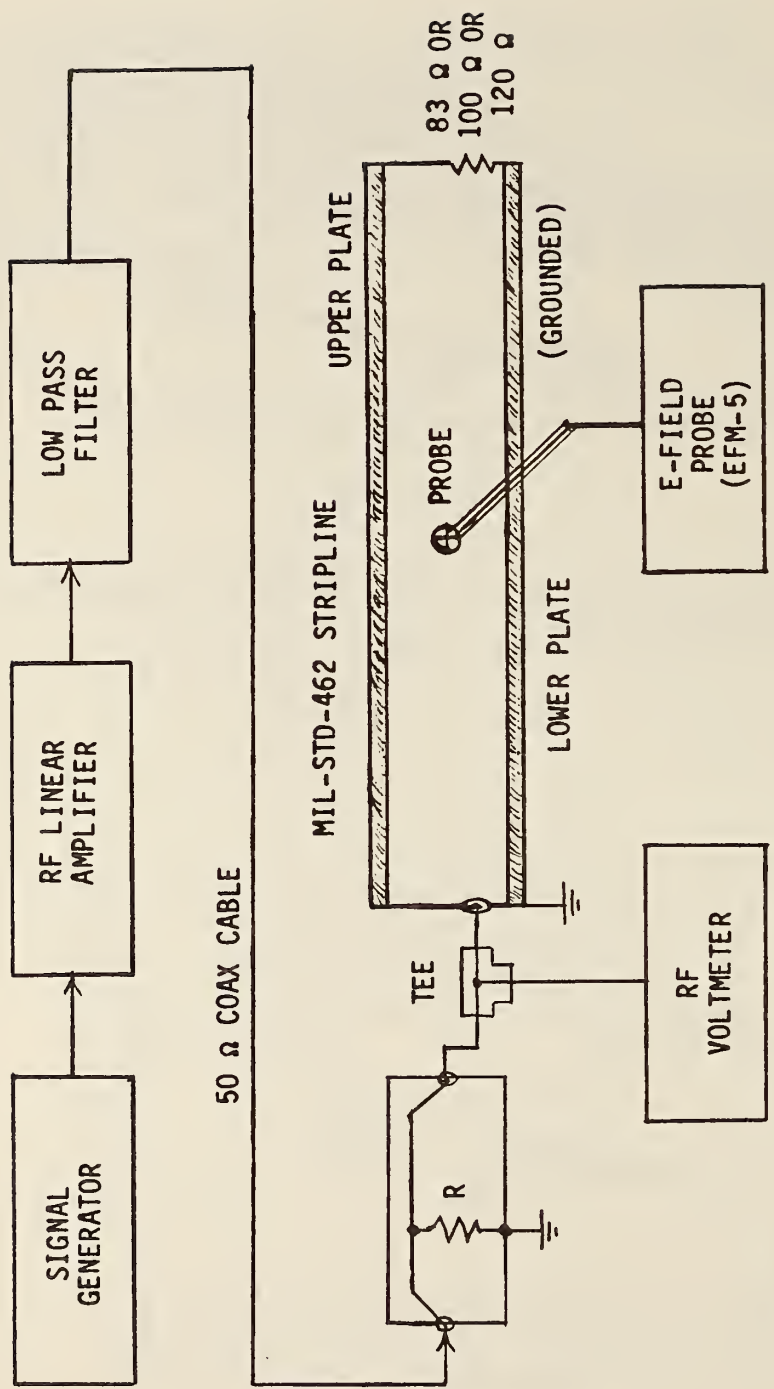


Figure 2-6. Instrumentation for measuring the E-field level in the MIL-STD-462 stripline.



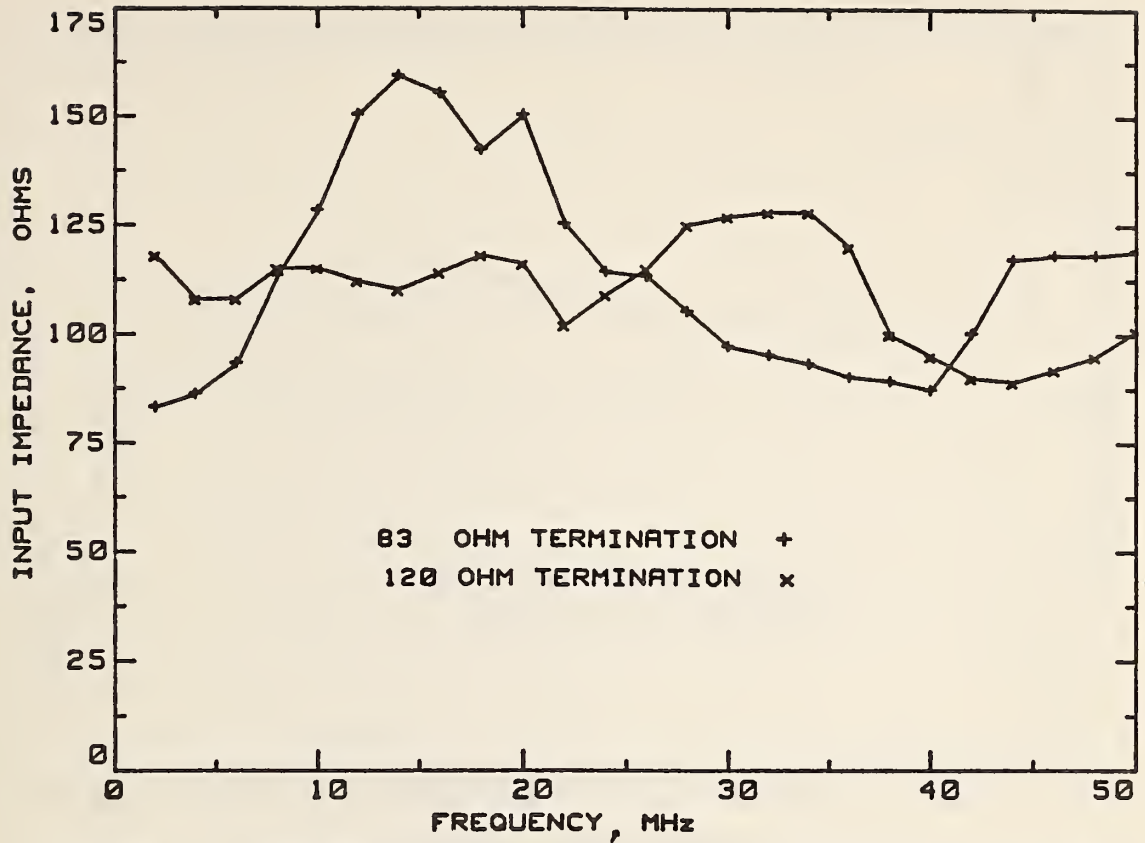


Figure 2-7. Measured input impedance of the MIL-STD-462 stripline in the center of the NBS screenroom.

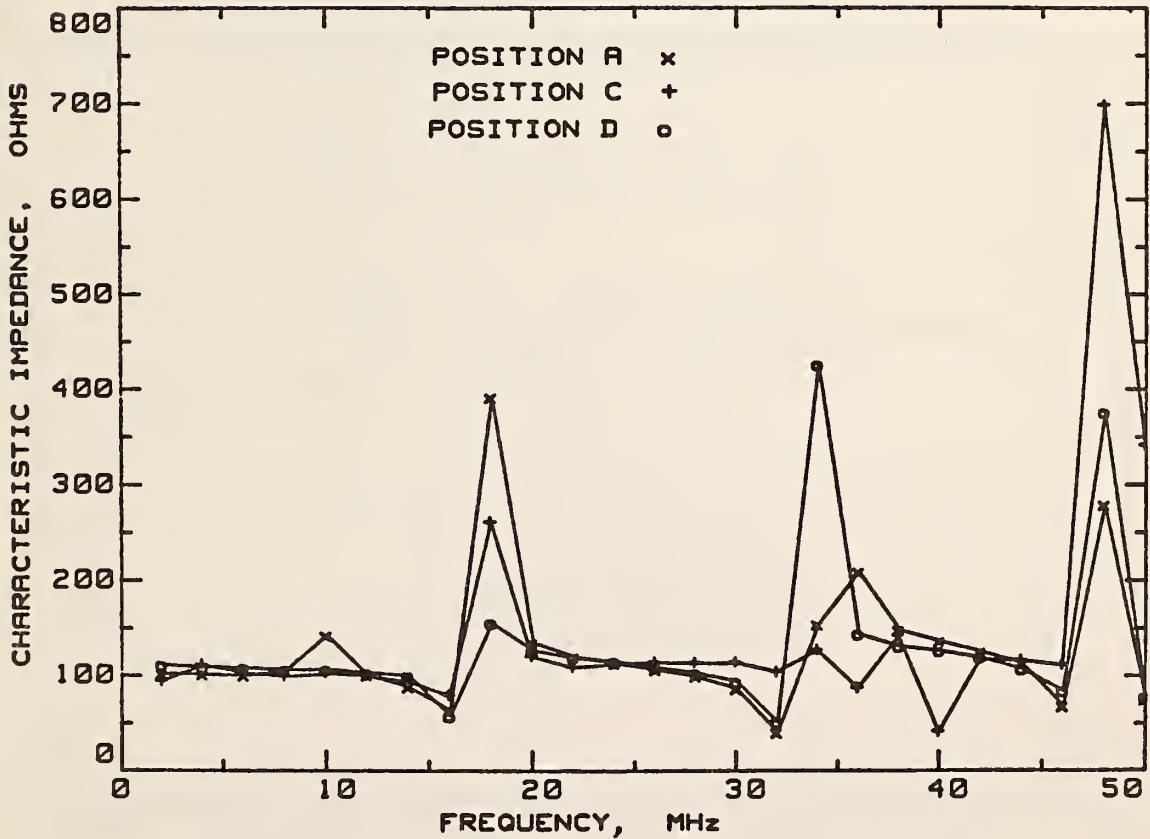


Figure 2-8. Measured characteristic impedance of the MIL-STD-462 stripline in the NBS screenroom.

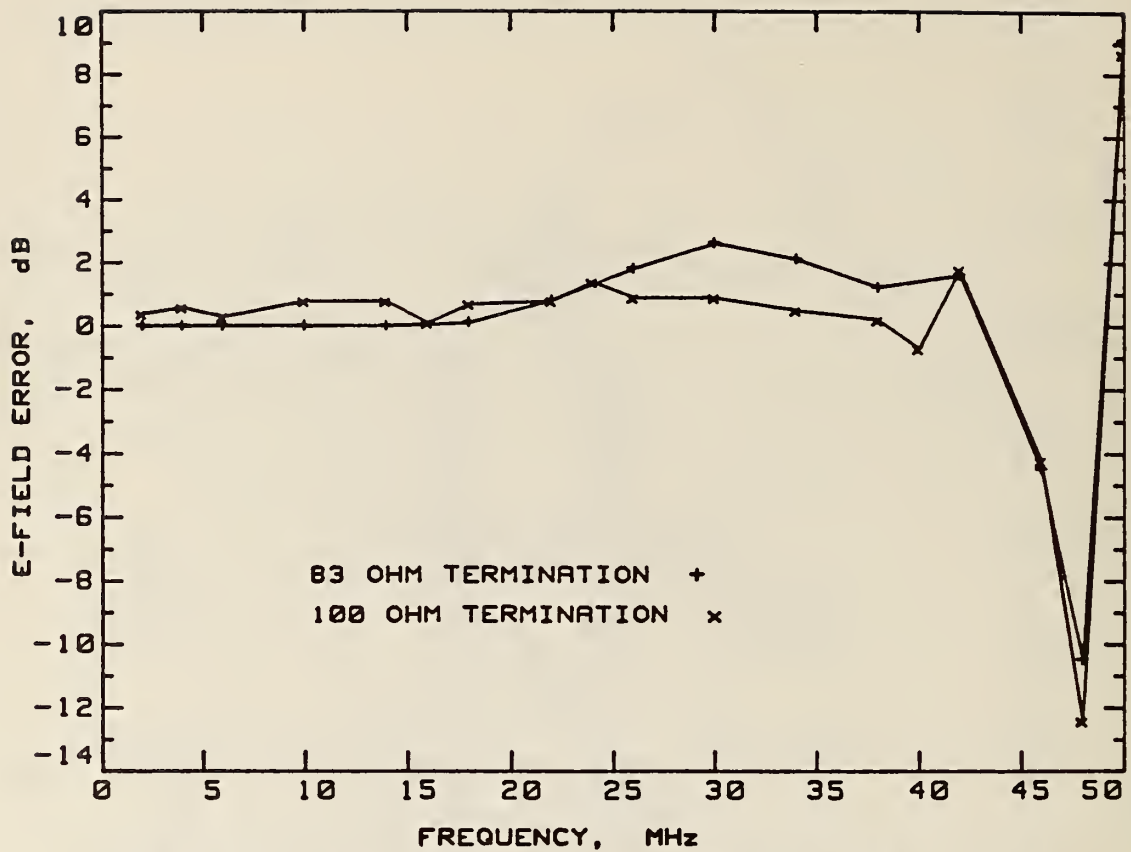


Figure 2-9. Measured E-field error in center of stripline.  
Position A in screenroom, with no ground strap.

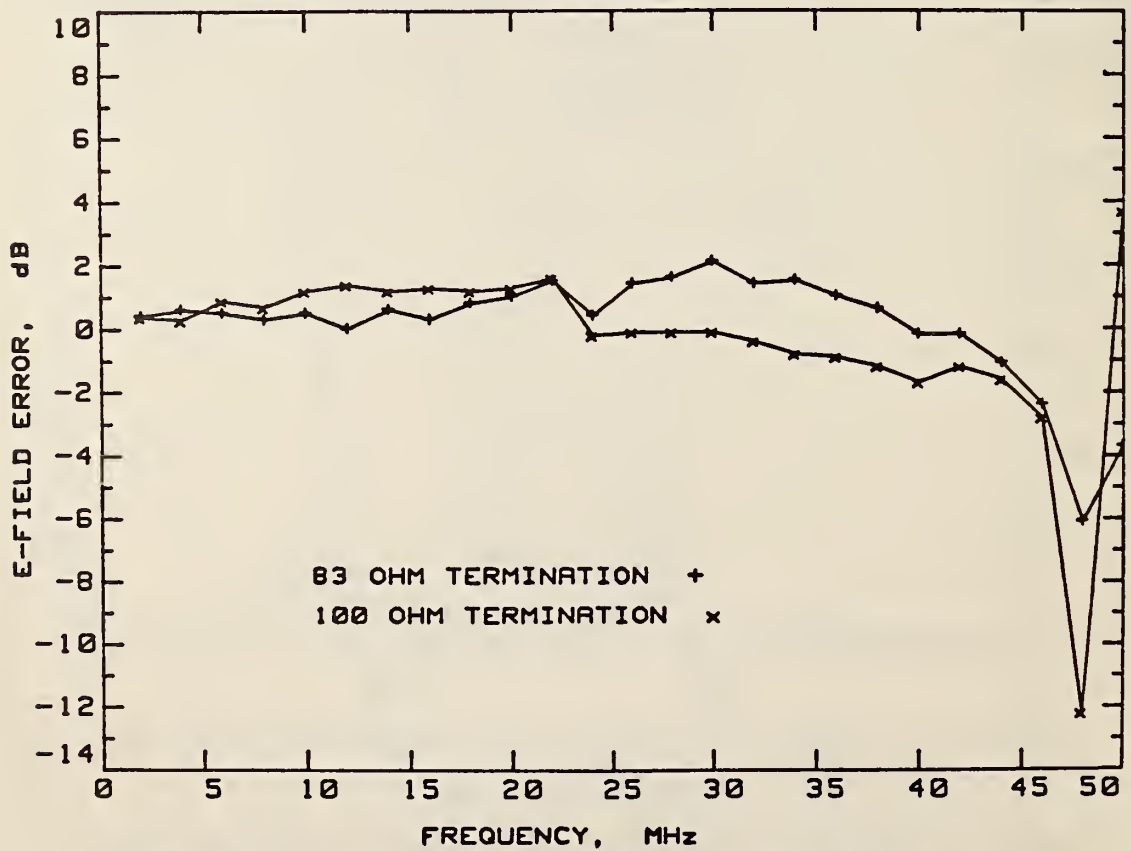


Figure 2-10. Measured E-field error in center of stripline.  
Position B in screenroom.

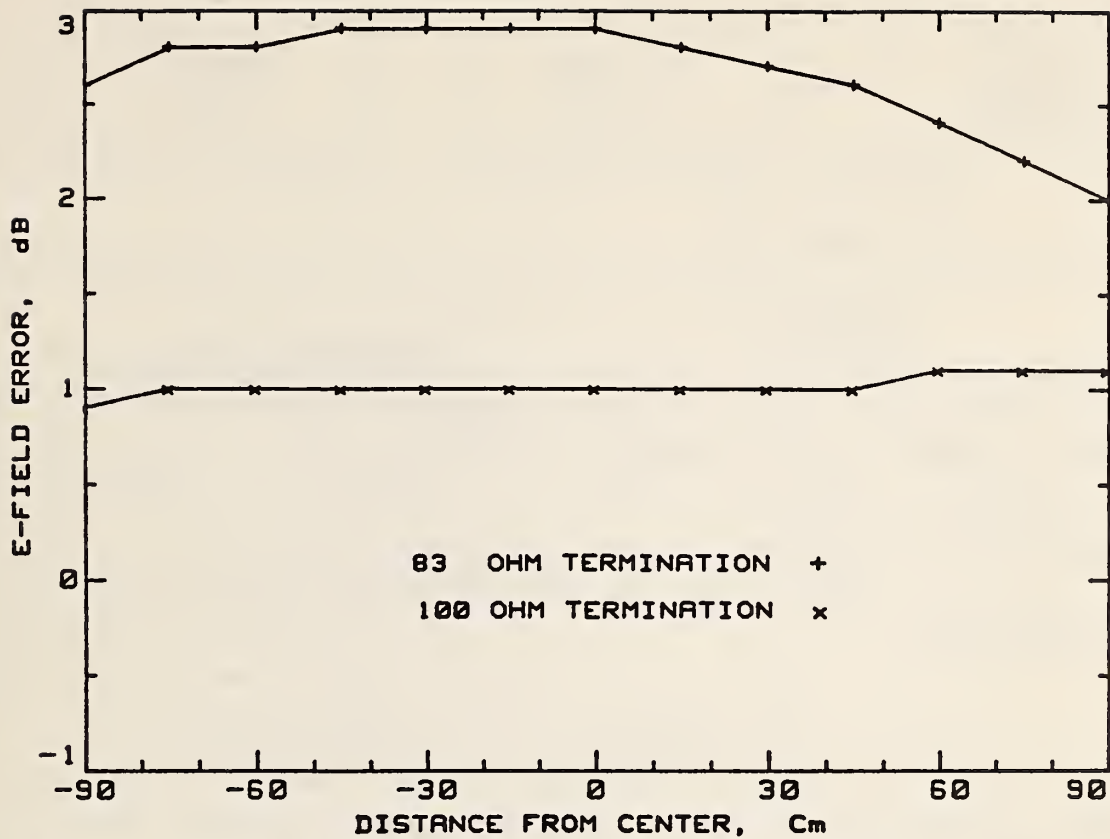


Figure 2-11. Measured E-field error along length of stripline at 30 MHz, 83  $\Omega$  termination. Position A in screenroom, with no groundstrap.

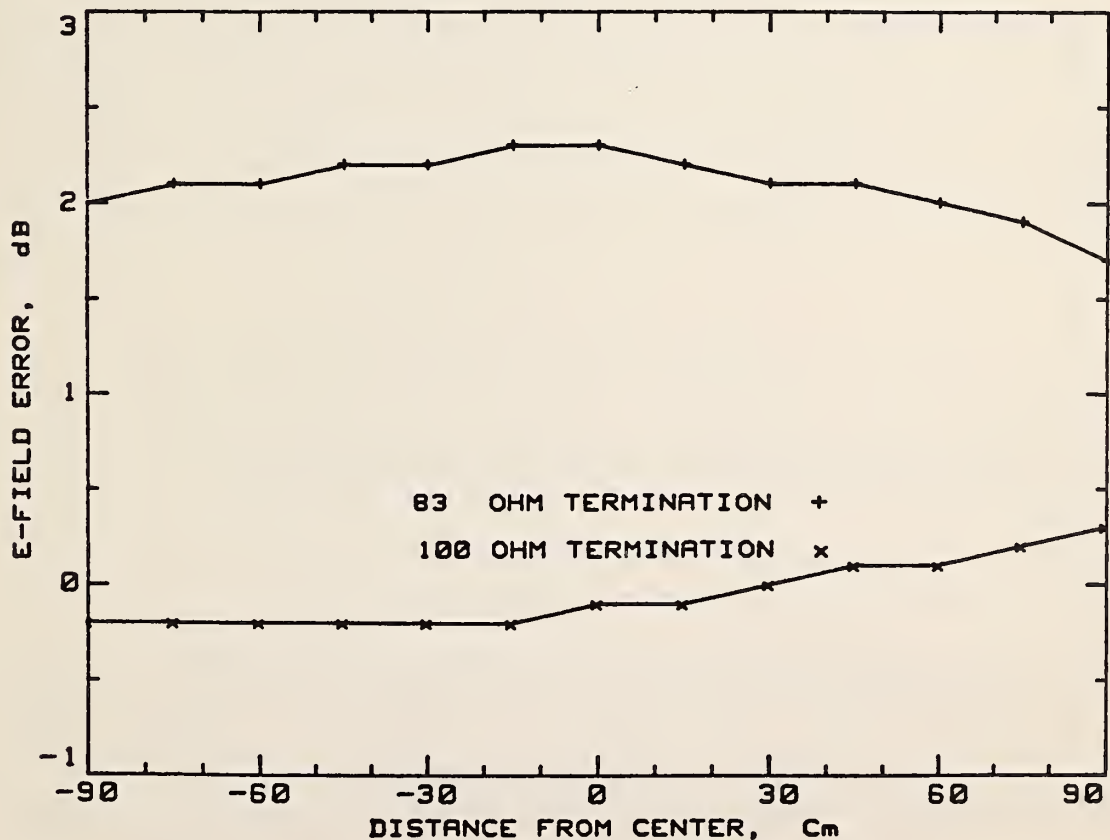


Figure 2-12. Measured E-field error along length of stripline at 30 MHz, 100  $\Omega$  termination. Position B in screenroom.

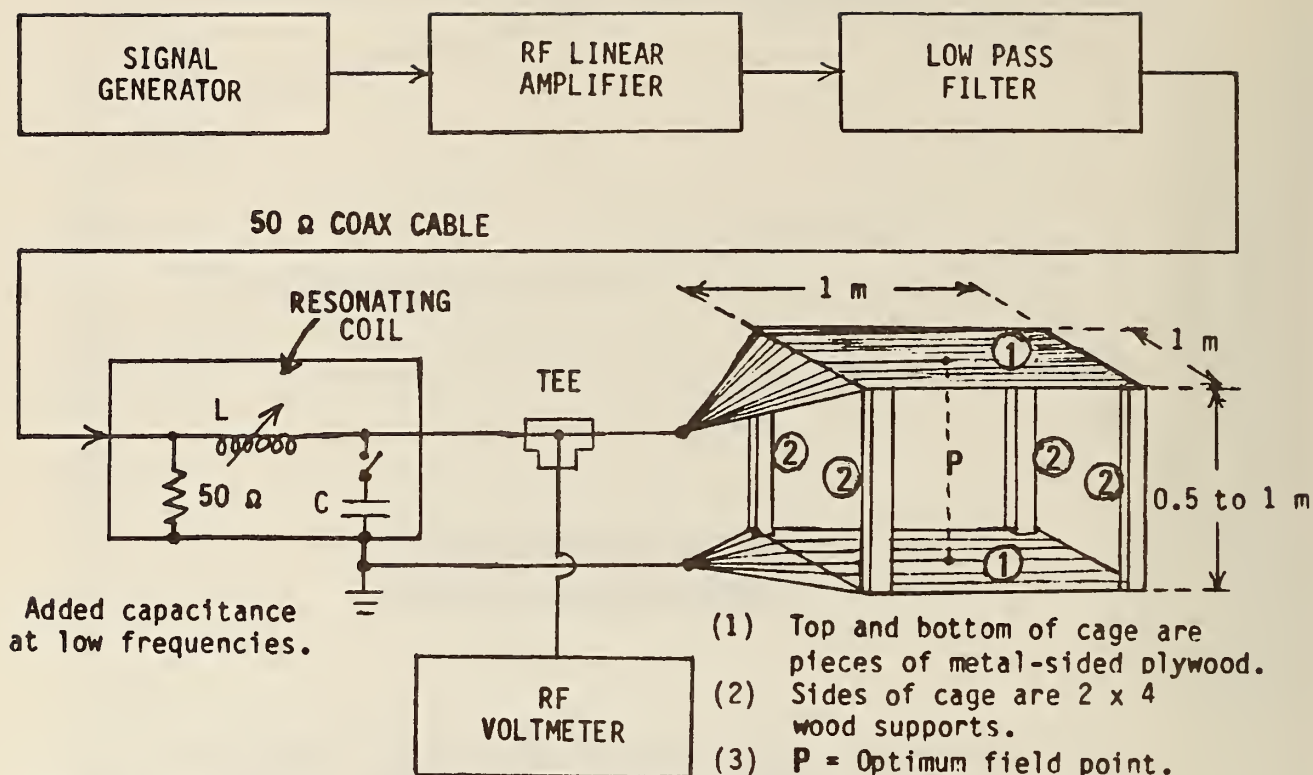


Figure 2-13. A parallel-plate cage system for generating a known E-field, 0.01 to 40 MHz.

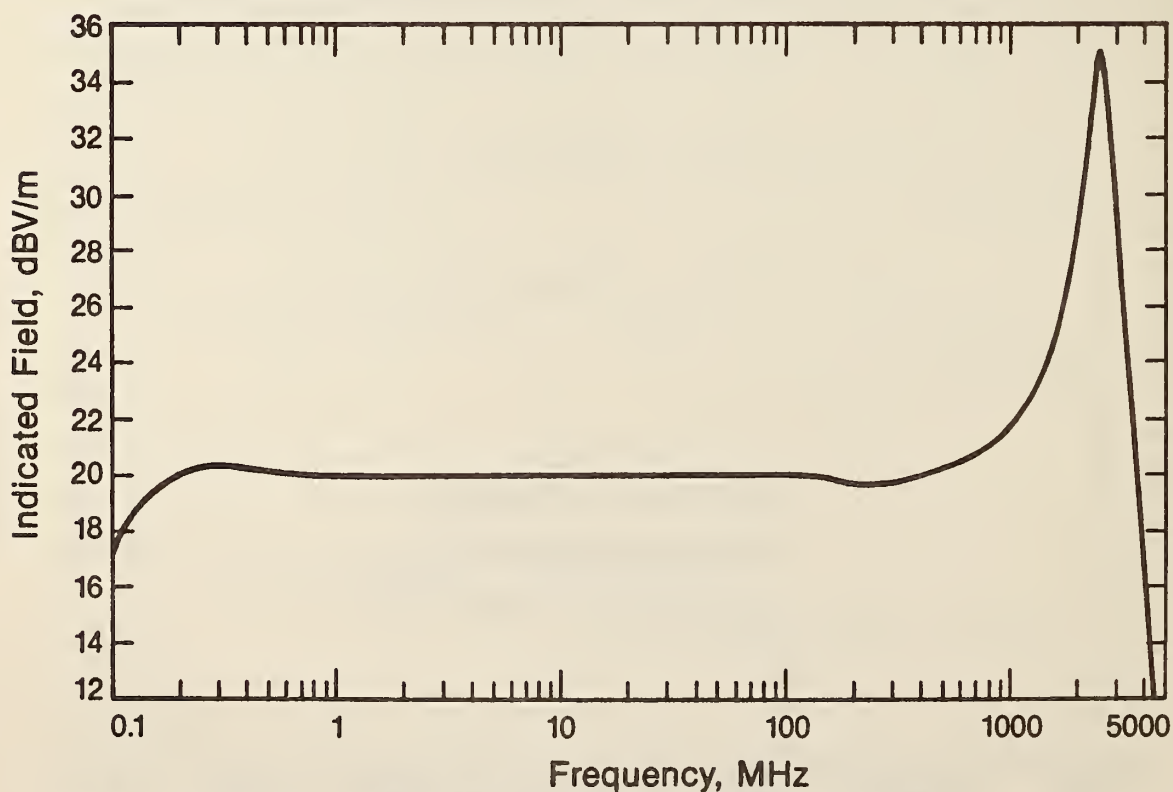


Figure 2-14. Typical response of an EFM-5 probe vs frequency, at a field strength of 20 dBV/m (10 V/m).



### 3. EM Field of a Single-Wire Transmission Line in a Screenroom

#### 3.1 Introduction

The long-wire antenna is used in a shielded enclosure when test items are too large to be placed in a parallel-plate line or other standard-field chamber. This long-wire antenna is illustrated in figure 3.1 installed in a shielded enclosure as per MIL-STD-461/462 specifications. The objective in testing the long-wire antenna at NBS was to determine the electromagnetic field uniformity and compare the measured field with theoretically calculated values.

MIL-STD 461/462 describes a laboratory method of simulating, in a shielded room, a radiated field having vertical polarization and controllable properties of electromagnetic (E and H) field strength. The long-wire antenna provides a means for applying a known field to test the susceptibility of electronic equipment at frequencies up to about 30 MHz. This long-wire antenna, as shown in figure 3-1, is the center conductor of a chamber formed by the walls of the shielded room which act as the outer conductor. This "coaxial" transmission line is terminated in its characteristic impedance, so that standing waves are minimized and the field intensity is fairly constant with respect to frequency and position along the line.

Two techniques are used for matching the generator impedance to the characteristic impedance of the long-wire transmission line as follows:

(1) An intermediate impedance-matched line is connected between the long-wire input and a short 50 ohm coaxial line from the signal generator, as shown in figure 3-2. If the characteristic impedance of this intermediate line is  $R_1$  and is matched by a parallel combination of  $R_2$  and  $R_3$ , where  $R_2$  is the terminating impedance of the long-wire line (equal to its characteristic impedance  $Z_0$ ), the delivered voltage to the long-wire line is  $(R_1/50)(V_t)$ , where the delivered voltage,  $V_t$ , will generate an

electromagnetic field proportional to the increased voltage. This technique requires that the 50 ohm short cable from the signal generator be less than  $0.025\lambda$  in length at its highest frequency of operation to minimize standing waves in the system.

(2) Instead of using a special intermediate transmission line, a 50 ohm coaxial feed line is used, as shown in figure 3-3. The 50 ohm coaxial line is terminated with  $R_3$  such that the parallel combination of  $R_2$  and  $R_3$  yields 50 ohms. The electromagnetic field in this case is proportional to  $V_t$ . The first technique has the advantage of generating more voltage in the long-wire antenna, while the second technique has the advantage of simplicity in construction.

Haber [3-1] describes a method for calibrating loop antennas in a shielded enclosure using the long-wire as its H field generator. His approach involves generating a known field by an energized wire mounted near the ceiling of the enclosure. Other formulas for computing the E and H field magnitudes in the enclosure have been published. For example, Bond [3-2] considers the system to be equivalent to an infinitely long wire under a perfectly conducting plane of infinite extent. Terman and Pettit [3-3] use a similar solution to Bond but include an image antenna below the plane of the floor.

The premise for using the long-wire antenna is that the field strength in the chamber is calculable and susceptibility measurements can be made using the field equations specified by MIL-STD 461/462.

### 3.2 Experimental Configuration of a Typical Long-Wire Antenna

The long-wire antenna is shown in figure 3-1 as installed in a shielded room. A No. 10 wire was used in the NBS room, suspended from the two end walls of the room, driven at one end and terminated at the other. The resistors,  $R_2$  and  $R_3$  remain fixed, once calculated.

The internal dimensions of the NBS shielded enclosure are 7.0 meters long by 3.7 meters wide by 2.4 meters high. These dimensions are minimum

values for MIL-STD 461/462 emission and susceptibility testing. The (center conductor) wire was suspended 0.65 meters from the ceiling. With this geometrical configuration, the characteristic impedance of the long-wire antenna can be calculated using the equation

$$Z_0 = 138 \log_{10} \left[ \frac{4a}{D} \right], \quad \Omega, \quad (3-1)$$

where  $a$  = distance of wire to ceiling, m,  
 $D$  = diameter of wire, m.

According to the MIL-STD, this equation for the characteristic impedance can be used when the distance of the wire to the ceiling is less than one third the room height. Using equation (3-1), the characteristic impedance of the long-wire antenna was determined to be 422  $\Omega$ .

Technique (2), as discussed by White [3-4], was used to determine experimentally the final values of  $R_2$  and  $R_3$  for optimum termination of the long-wire antenna. With the installation of these optimum values for  $R_2$  and  $R_3$ , construction of the long-wire is complete. Final experimental determination of the optimum impedance was 380  $\Omega$  for  $R_2$  and 57  $\Omega$  for  $R_3$ .

### 3.3 Evaluation of a Long-Wire Antenna

#### 3.3.1 Field Uniformity Along Axis of Long-Wire.

To measure the field uniformity of the long-wire antenna chamber, an EFM-5 probe, developed at the National Bureau of Standards, was used [3-5]. This probe was calibrated in a TEM cell and used as a transfer standard for measuring the fields of the long-wire antenna [3-6]. The probe has three mutually orthogonal dipoles to sense the field and can be used to measure the "total" E field or the three mutually-perpendicular field components (vertical, horizontal, propagation path). Because of its design and small size, the EFM-5 does not disturb the field being measured. The EFM-5 was

used mainly to measure the vertical field component directly beneath the center conductor of the long-wire.

Figure 3-4 shows the measured field uniformity along the center line of the screenroom chamber at 1 MHz. Figure 3-5 shows the field uniformity at 15 MHz and figure 3-6 at 30 MHz. The field deviation along the axis of the chamber was taken with respect to the field measured at the midpoint of the chamber. Figure 3-4 shows that the deviation was less than  $\pm 0.3$  dB at 1 MHz, figure 3-5 shows a deviation less than  $\pm 1$  dB at 15 MHz, and figure 3-6 shows a deviation of + 0 to - 3 dB at 30 MHz. The voltage standing wave on the long-wire antenna at these frequencies is clearly shown.

Figures 3-4, 3-5, and 3-6 indicate that a fairly uniform field can be achieved in the long-wire antenna chamber. However, terminating the antenna with a resistor equal to its measured characteristic impedance, as specified and described in MIL-STD 461/462, is important. It is also important that the field uniformity be measured, using a transfer probe that does not distort the field being measured. The measurement error of the EFM-5 is estimated to be less than  $\pm 1/2$  dB when calibrated at the measurement frequencies used in the long-wire antenna screenroom. Using such a transfer probe standard also has the advantage of checking the absolute value of the field, as a function of frequency and location in the screenroom.

### 3.3.2 Measured vs Calculated Field Beneath the Long-Wire

Experimental investigations of the fields in a screenroom, as energized by a single wire transmission line, indicate that the field uniformity as a function of distance below the long-wire is quite poor. The accuracy of the calculated electric field intensity below the line depends on careful optimization of the line terminating impedance. Equations to determine E and H and the approximate required values of  $R_2$  and  $R_3$  are given in the literature [MIL-STD-461 and IEEE Standards on Receivers]. In the derivation of these equations it is assumed that a pure resistance is an adequate



termination for the long-wire transmission line. It is also assumed that if the line height is greater than 2/3 the room height, the presence of the side walls and floor of the screenroom can be ignored when calculating the characteristic impedance of the line. The theoretical field strength at a distance d (figure 3-1) below the center of the screenroom long-wire is then given approximately by:

$$E \approx \frac{60 V}{(Z_0 + Z_g)} \left[ \frac{1}{d} - \frac{1}{d + 2a} - \frac{1}{d - 2b} + \frac{1}{d - 2a - 2b} + \frac{1}{d + 2a + 2b} - \frac{1}{d - 2a + 4b} + \frac{1}{d + 4a + 2b} + \frac{1}{d - 4a - 4b} \right], \quad (3-2)$$

and  $H \approx E/377$

where

E=electric field strength at a distance d below the center of the long-wire, V/m,

H=magnetic field strength at the same point, A/m,

V=RMS voltage input to the transmission line, V,

$Z_0$ =characteristic impedance of the line,  $\Omega$ ,

$Z_g$ =impedance of the generator,  $\Omega$ ,

a=distance from the wire to the ceiling, m,

b=distance from the wire to the floor, m,

d=distance from the wire to the field point P, m.

Equation (3-2) was used to calculate the electric field, and this was compared with the measured field (using the EFM-5 transfer standard) for signal frequencies of 1, 2, 3, 5, 7.5, 15, 22 and 30 MHz. The vertical component of electric field was used for these comparisons, at several distances below the center of the long-wire. The differences between calculated and measured field strength (in dB) were plotted against distance. This distance ranged from 0.2 meters to 0.8 meters below the center of the long-wire. The measured field was taken as the 0 dB reference when compared to the calculated field.

Figure 3-7 is a plot of this calculated-to-measured field difference versus distance below the long-wire antenna. It shows that the difference between the calculated field using eq (3-2) and the measured field varies both as a function of distance and frequency. The data show that the calculated E-field has a greater error as the distance from the center conductor increases.

### 3.4 Conclusions and Recommendations

The data indicate that the average vertical electric field strength produced in the long-wire antenna chamber is uniform within 3 dB along the length of the line in the frequency range where the screenroom does not have any resonances (up to 30 MHz) provided that care has been exercised to terminate the long-wire antenna in its characteristic impedance (to eliminate standing waves). However, it is recommended that a transfer standard probe such as a calibrated EFM-5 be used for measuring the uniformity of the field and for checking the absolute value of the field.

The error in the calculated field of the long-wire antenna using equation (3-2) varies with both position and frequency. It is recommended that a calibrated transfer probe be used to check the absolute value of the field strength at any desired location in the chamber.

### 3.5 References

- [3-1] Haber, F. Generation of Standard Fields in Shielded Enclosures, IRE Proc., Vol 42, No. 11 1954.
- [3-2] Bond, D.S. Radio Direction Finders, McGraw-Hill Book Co. Inc., New York, N.Y., pp 221-229 1944.

[3-3] Terman, F.E. and Pettit, J. M., *Electronic Measurements*, McGraw-Hill Book Co. Inc., New York, N. Y., pp 405-406 1952.

[3-4] White D. *Electromagnetic Interference and Compatibility, EMC Handbook*, Vol. 4, pp 4.7-4.13, Don White Consultants 1971.

[3-5] Larsen, E.B., and Ries, F.X. *Design and Calibration of the NBS Isotropic Electric-Field Monitor (EFM-5), 0.2 to 1000 MHz*, U.S. Nat. Bur. of Standards, NBS Tech. Note No. 1033, 104 pages March 1981.

[3-6] Crawford, M.L. *Generation of standard EM fields using TEM transmission cells*, *IEEE Trans. Electromag. compat.*, EMC-16 No. 4, pp 189-195 November 1974.

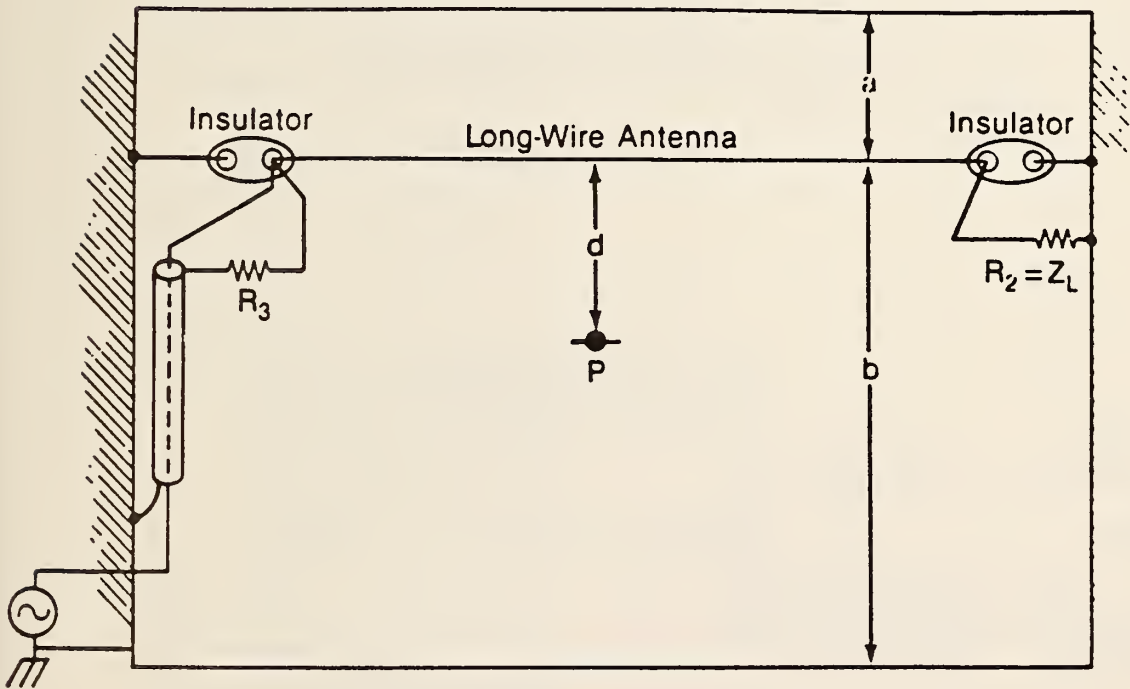


Figure 3-1. The long-wire antenna in a shielded enclosure.

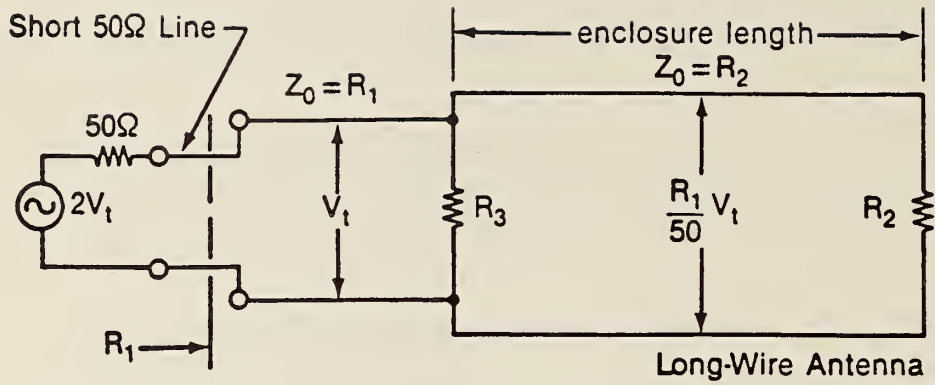


Figure 3-2. Signal generator drives intermediate feeder line to long-wire antenna.

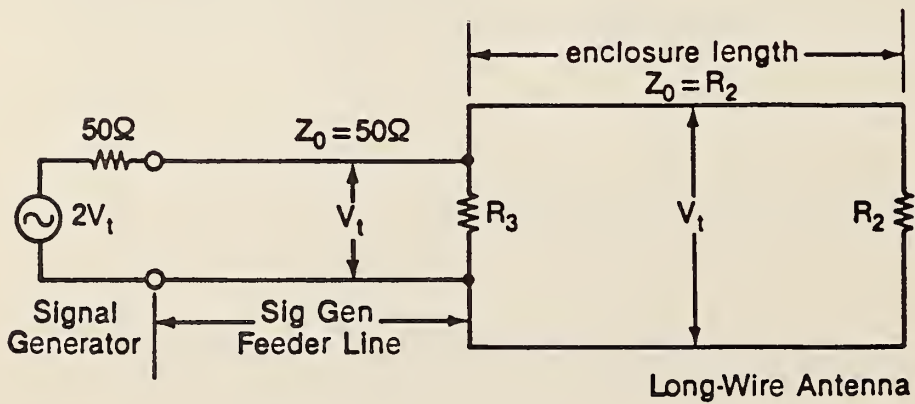


Figure 3-3. Signal generator coaxial line feeds long-wire directly.



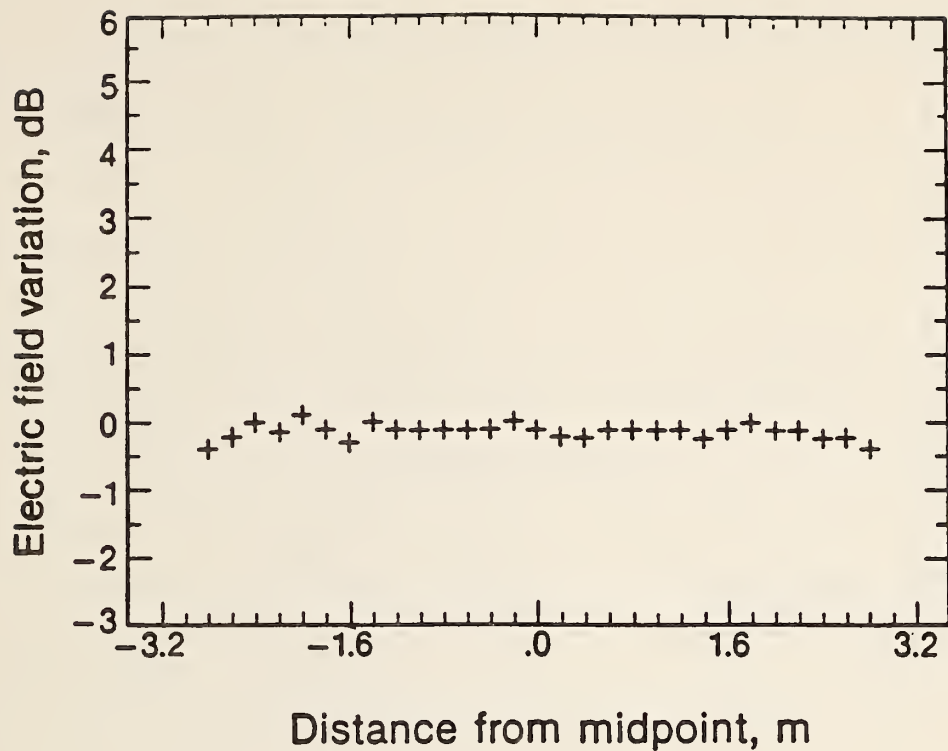


Figure 3-4. Electric field uniformity of long-wire antenna along the length of the chamber at 1 MHz.

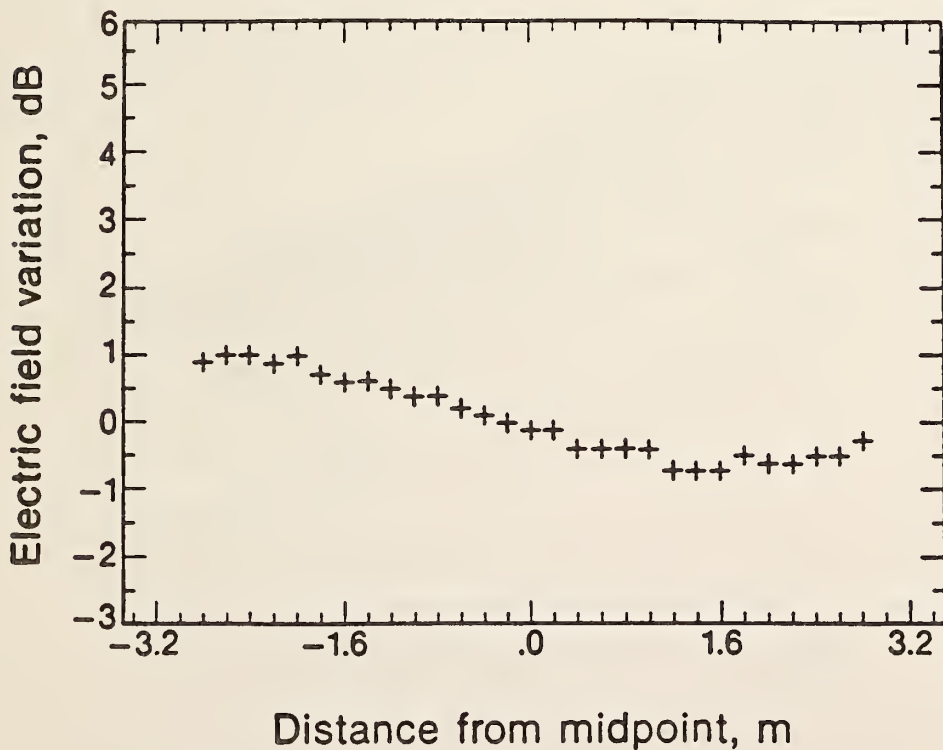


Figure 3-5. Electric field uniformity of long-wire antenna along the length of the chamber at 15 MHz.

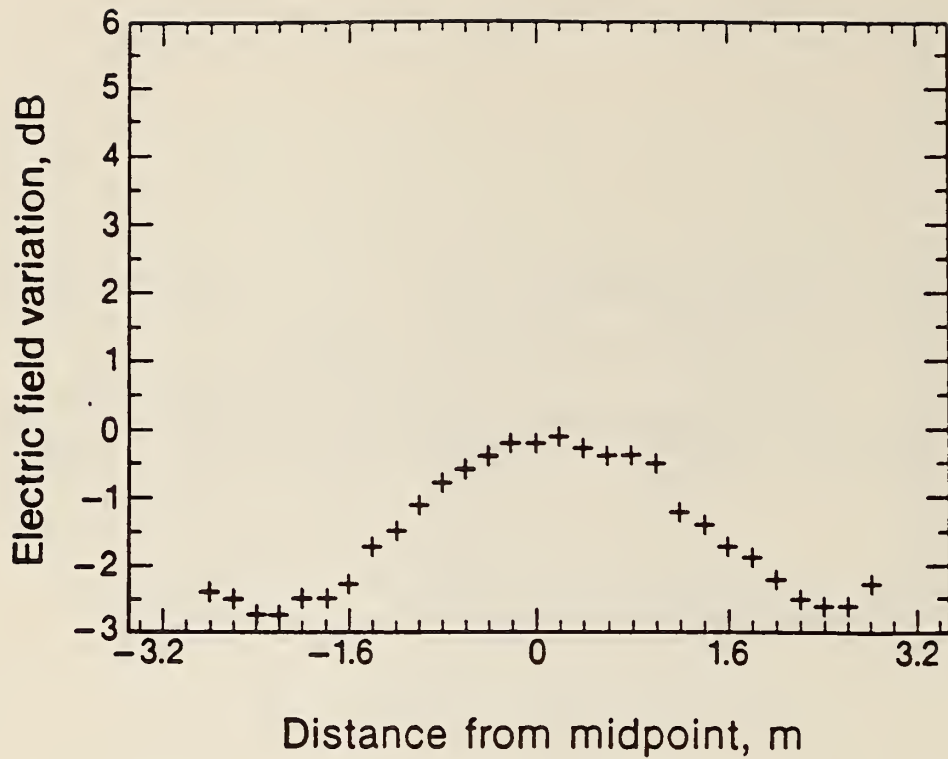


Figure 3-6. Electric field uniformity of long-wire antenna along the length of the chamber at 30 MHz.

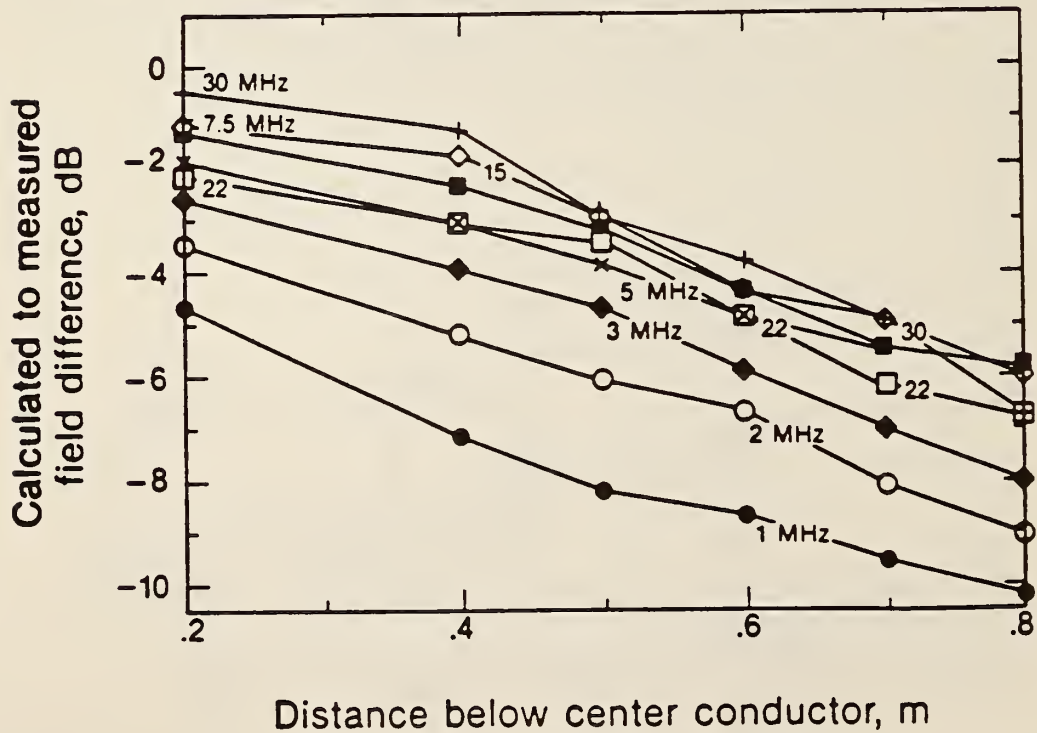


Figure 3-7. Calculated-to-measured field versus distance below the long-wire for selected frequencies from 1 to 30 MHz.

## 4. Calibration of Antenna Factors for EMI Antennas

### 4.1 Introduction

The measurement of electromagnetic fields in a shielded enclosure (screenroom) has serious problems because of uncertain antenna factors and multipath reflections from conductive surfaces. Most electromagnetic interference antennas at NBS are calibrated in a known field at an open site or anechoic chamber, using the standard antenna or standard field method. Because the resulting antenna factors are not necessarily applicable for making measurements in a screenroom, the errors for measuring field strength with the calibrated antenna can be quite large. This report presents the results for antenna factors determined in a screenroom using the two-antenna method. These antenna factors are compared with antenna factors determined at an open field site. Experimental data are presented to show the variability of antenna factor as a function of frequency and location in the screenroom, thereby providing an indication of error bounds. The historical background of screenroom measurements is referenced. A technique is offered for making more accurate field measurements in a screenroom.

The accuracy of measurements in a shielded enclosure has been investigated in terms of near-field effects [4-1], theoretical considerations for making RFI measurements in a shielded enclosure [4-2], and wall reflections [4-3]. Other errors when making measurements in a shielded room are caused by: antenna VSWR, antenna height above the floor, dimensions of the enclosure, and antenna detuning by walls and ceilings. Added to these are instrument errors, and systematic and random errors involved in making the measurement. Because of the many sources of errors, it is not a simple task to make accurate measurements in a shielded enclosure. Each of the above variables requires extensive analysis for improving accuracy. All of these measurement errors indicate that a

substantially different method from presently established procedures must be developed.

The following sections will discuss: historical papers dealing with evaluation of measurements in screenrooms, error bounds of antenna factors measured in a screenroom, and reliability of measured antenna factors for making screenroom measurements.

As background information, a description is given of electromagnetic (EM) measurements, measurement philosophy, measurement theory, and measurement errors in a screenroom. For many reasons, a screenroom is often used to perform electromagnetic radiation measurements, especially at frequencies below 1 GHz. However, a screenroom produces measurement problems due to multiple reflections, resonances, and distortion of the electromagnetic fields. Measurement results are influenced by the size of the enclosure, location of the test equipment, spacing of the equipment under test (EUT) and the type of transmitting or receiving equipment.

The frequency and amplitude of screenroom resonances are determined by the dimensions and geometry of the room, conductivity of the enclosure surfaces, and by objects inside the enclosure. For an empty rectangular enclosure the resonant frequencies can be calculated from eq (2-9 of this report which is

$$f=150\sqrt{\left(\frac{a}{\ell}\right)^2 + \left(\frac{b}{w}\right)^2 + \left(\frac{c}{h}\right)^2}, \quad (4-1)$$

where F= frequency, MHz.,  
a,b,c= cavity integers, only one which can be zero, and  
 $\ell,w,h$ = length, width, height of the screenroom, m

The resonant characteristics of a shielded enclosure are different for each test in which the equipment under test in the enclosure is physically different or in a different location. Errors as great as 50 dB may be



present in screenroom field strength measurements, depending on frequency and the characteristics of the individual enclosure.

Stuckey, Free and Robertson [4-1] have investigated the near-field effects on measurement accuracies in a shielded enclosures. They have postulated a theory "which accounts for the observed inaccuracies in terms of a near-field measurement effect which is present in a shielded enclosure environment and absent in the corresponding open-field environment". This near-field coupling hypothesis is used to explain the measurement differences between the open-field and screenroom configurations at frequencies below the first resonance of the enclosure. According to their hypothesis, "the coupling between two antennas includes inductive coupling and capacitive coupling as well as the normal coupling involving the radiated field". Their data show a deviation of about  $\pm 40$  dB between the open-field and screenroom environment. Their evidence supports their near-field coupling hypothesis. However, they suggest that additional investigation of the near-field coupling phenomena is needed.

Krstansky and Standley [4-3] developed a theory of EMC measurements in screenrooms. They applied electromagnetic theory to the problem of obtaining reliable and meaningful screenroom EMC measurements. They divided the electromagnetic problem of determining the field distribution inside a rectangular enclosure, into three separate and unique parts depending on the operating frequency and enclosure dimensions, as follows:

Case 1,  $\omega < \omega_1$ , where  $\omega_1$  is the lowest resonant frequency

Case 2,  $\omega \approx \omega_k$ , where  $\omega_k$  is a given resonant frequency

Case 3,  $\omega > \omega_k$ , for k sufficiently large.

Their conclusion for case 1 was that "the size of the enclosure, as well as source and receiver locations, is extremely critical. Hence a specification as to the allowable field strength at a given distance from an equipment under test is virtually meaningless unless the screenroom

dimensions are included in the specification". They consider case 2 to be the most serious problem area in that as  $\omega$  approaches some  $\omega_k$  value, the fields become quite large. The exact value of  $\omega_k$  depends primarily on the screenroom dimensions and location of objects within the enclosure, and measurements made in one enclosure do not necessarily repeat in another enclosure. For case 3 the density of  $\omega_k$  values become so large that single mode resonances are usually not observed and the theoretical field distribution becomes very complex. "A possible solution to this problem is a statistical procedure involving mode mixing techniques". However, "a detailed investigation of this approach is required to prove its superiority over current methods".

In making EMC measurements, the antenna factor of any antenna varies with the conditions under which the antenna is used [4-4]. Antenna factor is defined as the ratio of the standard (known) calibrating field to the rf voltage delivered to the receiver by the antenna being calibrated when the antenna is terminated in a resistance of 50 ohms. It is given by the eq

$$K = \frac{E}{V_{50}}, \quad (4-2)$$

where  $E$  = the electric field strength incident upon the receiving antenna, and  
 $V_{50}$  = measured voltage at the input of the 50  $\Omega$  measuring device to which the antenna is connected.  
 Usually the antenna factor is given in dB and written in the form

$$K, \text{dB} = 20 \log\left(\frac{E}{V_{50}}\right). \quad (4-3)$$

Eqs (4-2) and (4-3) do not take into consideration the angles of incidence and polarization diversity of the received signal with respect to the transmitted signal. Mutual coupling between antennas should be accounted

for when the antennas are closely spaced. In a screenroom there are multiple reflections due to the walls, floor, and ceiling. In addition, the mutual impedance between the receiving and transmitting antennas may be significant. Finally, resonances and nulls caused by enclosure interaction with the antennas make the error of using the ideal free-space antenna factor unreasonably large.

#### 4.2 Measurement of Antenna Factors in a Screenroom

To determine antenna factors in a screenroom, the two antenna method as described in MIL-STD-461A was used. Figure 4-1 shows the instrumentation and configuration used for making the measurements. This procedure requires two antennas with "identical" characteristics (identical loading effects, and equal impedance and gains). However, the observed antenna gain is a function of position in the screenroom; hence the measured antenna factor is also a function of position.

In the two-antenna method, the transmitter output level is adjusted to obtain a received signal,  $V_R$ , from the receiving antenna. The receiver and signal generator cables are then disconnected from the antennas and directly connected to each other to get the direct signal,  $V_T$ . The ratio of these two levels is used to find the "realized gain" or effective gain,  $G_{eff}$  of the two identical antennas being calibrated using the eq

$$G_{eff} = (4\pi d/\lambda)(V_R/V_T), \quad (4-4)$$

where  $d$  = distance between the two antennas shown in figure 4.1, m,

$V_R$  = radiated signal received by the receiving antenna, V,

$V_T$  = direct signal of the transmitted antenna via the

coupled cables, V,

$\lambda = 300/f, \text{MHz}$ , = free-space wavelength, m.

It should be noted that a measurement of "true gain" requires a knowledge of antenna impedance or that the antennas and loads be conjugately

matched in impedance, with lossless matching networks. However, after measuring the "effective gain" by the two antenna method, the antenna factor is calculated using the eq [4-5]

$$K = 9.73 / (\lambda \sqrt{G_{\text{eff}}}) \quad (4-5)$$

Substituting for  $G_{\text{eff}}$  from eq (4-4) into (4-5) one gets,

$$K = 9.73 / 2 \sqrt{\pi \lambda d (V_R / V_T)}$$

Substituting  $(300/f, \text{MHz})$  for  $\lambda$  and taking 20 times the log of K, one gets,

$$K, \text{dB} = 10 \log \left[ \frac{(f, \text{MHz}) (V)_T}{(d) (V_R)} \right] - 16 \quad (4-6)$$

Using eq (4-6) and the instrumentation of figure 4-1, one can determine an "in situ" antenna factor for two identical antennas at two specific locations in a given shielded enclosure.

#### 4.3 Measurement of Antenna Factors at an Open Field Site

To determine antenna factors at an open field site, the two techniques normally used are the "standard field" and the "standard antenna" method. At NBS the standard antenna approach is used for calibrating dipoles or similar antennas in which the horizontal component of electric field is to be determined. The standard field method is used for calibrating monopoles or antennas in which the vertical component of electric field is desired.

##### 4.3.1 Standard Antenna Method

The antenna factors are normally determined at an open field site. The calibration is performed by radiating a field of convenient magnitude using a transmitting half-wave dipole or a log periodic antenna (at frequencies above 80 MHz) [4-6, 4-7]. The calibrations are done at a separation distance of at least  $2\lambda$  between the transmitting and receiving antennas. The receiving antennas are normally set at a height of 3 meters. The



transmitting antenna voltage is held at a constant level. The electric field is detected by the standard  $\lambda/2$  dipole. The antenna being calibrated is then substituted, in the same location, and its response recorded.

The NBS standard receiving dipoles used to measure the magnitude of electric field strength consist of self-resonant dipoles with a high impedance balanced voltmeter built across the center gap of the antenna. The balanced voltmeter uses a Schottky diode detector, an R-C filter network, and a high resistance transmission line. The dc output of the filter is measured with a high impedance (100 M $\Omega$ ) voltmeter.

The antenna voltmeter dc-to-rf voltage transfer function is measured, and from the dc output of the antenna the resulting rf voltage at the essentially open-circuit dipole terminals can be determined. The calibrating field strength at the measurement location is obtained from the eq

$$E_s = \frac{V_{oc}}{L_{eff}}, \quad (4-7)$$

where  $E_s$  = strength of the standard field, V/m,  
 $V_{oc}$  = open-circuit rf voltage of standard dipole, V,  
 $L_{eff}$  = standard dipole effective length, m,  
 $= (\lambda/\pi)[\tan(\pi L/2\lambda)]$ ,  
 $\lambda$  = free-space wavelength, m, and  
 $L$  = length of standard (self resonant) dipole, m.

Antenna factor is defined as the ratio of the standard calibrating field to the rf voltage delivered to a 50 ohm receiver by the antenna being calibrated. This antenna factor (K), expressed in dB, is defined in eq (4-3) and is determined from the standard field in eq (4-7). Measuring

the rf voltage and using eqs (4-7) and(4-3) one can obtain the antenna factor from

$$K, \text{ dB} = 20 \log(E_s/V_{50}) = 20 \log\left[\frac{V_{oc}}{V_{50}L_{eff}}\right]. \quad (4-8)$$

#### 4.3.2 Standard Field Method

The antenna factors of vertical monopoles are calibrated by immersing the receiving monopole antenna in a known field above the NBS groundscreen and about 20 meters from the transmitting vertical monopole. A block diagram of the instrumentation used for this type of calibration is given in figure 4-2. The receiving antenna output at the end of the transmission line is applied to a calibrated 50 ohm spectrum analyzer having a VSWR  $\bar{\bar{< 1.05$ . This spectrum analyzer is used as a frequency-selective voltmeter to measure the received rf voltage ( $V_{50}$ ) at each frequency tested.

The calibration of vertical monopole antennas at NBS is done at an outdoor field site which has approximately a 30 x 60 meter conducting mesh stretched over a concrete slab. The strength of the calibrating field is calculated at each frequency in terms of the base current in a thin transmitting vertical monopole antenna. The vertical component of E field, as a function of base current and position, is given by the eq

$$E_o = \left[\frac{30I_o}{\sin(\beta h)}\right] \left[\frac{e^{-j\beta r_1}}{r_1} + \frac{e^{-j\beta r_2}}{r_2} - 2\cos(\beta h)\left(\frac{e^{-j\beta r_o}}{r_o}\right)\right] \quad (4-9)$$

where  $E_o$  = vertical component of standard E field, RMS V/m,

$I_o$  = monopole antenna base current, A,

$h$  = height of transmitting monopole, m,

$\beta$  =  $2\pi/\text{wavelength}$  in meters,

$r_1$  = distance from top of transmitting monopole to field point, m,

$r_2$  = distance from image of top of monopole (in ground) to field point, m,

$r_o$  = distance from bottom of monopole to field point, m.

Eq (4-9) is number (10-72) on page 323 of Jordan [4-8].

The base current of the transmitting monopole is measured directly or obtained from the eq

$$I_o = \frac{V_o}{Z_{in}} \quad (4-10)$$

where:

$I_o$  = monopole current, A,

$V_o$  = measured base voltage of the transmitting monopole, V,

$Z_{in}$  = magnitude of the monopole input impedance,  $\Omega$ .

At frequencies up to 30 MHz, a 2.5 m transmitting monopole is used to generate a standard field. At frequencies above 30 MHz, the monopole height is reduced to a value of  $\lambda/4$ . At frequencies below one-tenth of the self-resonant  $\lambda/4$  frequency, the radiation resistance is negligible and the input impedance is a capacitive reactance. The capacitance of a thin electrically-short whip can be calculated from the eq

$$C = \frac{55.63 h}{\ln(h/a) - 1} \quad (4-11)$$

where  $C$  = monopole input capacitance, pF,

$h$  = monopole height, m,

$a$  = monopole radius, m.

The above eq is number (11) on page 306 of Schelkunoff [4-9].

At frequencies above one-tenth the self-resonant frequency, the input impedance of the monopole ( $Z_{in}$ ) is calculated from Schelkunoff's "mode" theory using eq (108), page 433 of reference [4-9]. The impedance values of this eq have been verified for the 2.5 meter whip by measuring with a commercial vector impedance meter. Eq (4-10) has been experimentally verified at frequencies near self-resonance by measuring the transmitting monopole base current with a calibrated vacuum thermocouple. Another check of calculated E field has been made at the resonant frequency with a small

active probe which was calibrated in the known field of a TEM cell. The rf voltage on the transmitting monopole ranges from 3 volts at self-resonant frequencies to 300 volts at frequencies well below resonance.

The antenna factor (K), in dB, is determined from the eq

$$K = E_o - V, \quad (4-12)$$

where  $E_o$  = field strength calculated from eq (8), dB $\mu$ V/meter,  $V$   
= pickup rf voltage delivered to the calibrated 50 ohm  
spectrum analyzer, dB $\mu$ V.

#### 4.4 Experimental Measurements of Antenna Factors

Two types of antennas were used for the measurement of antenna factors; monopoles (104 cm rods) and broadband dipoles (biconicals). These antennas are used for emission and susceptibility tests at frequencies from 10 kHz to 200 MHz. The antenna factors of the monopoles and broadband dipoles were measured at an outdoor field site using the standard techniques developed by NBS for calibrations. Additional measurements of the two types of antennas were made in the NBS screenroom using the MIL-STD-461A two antenna method. All of the antenna factor values for the antennas are given in graphical form, as described in the following section.

##### 4.4.1 Biconical Dipoles

Figure 4-3 is the antenna factor graph given in the manufacturer's manual for a typical biconical dipole. It is seen that the antenna factor as a function of frequency varies from a minimum value of 7 dB, at its resonance dip, to a maximum value of 18 dB. Figures 4-4 to 4-6 show antenna factor curves as given in the antenna manufacturer's manual. Figure 4-4 is for an antenna separation distance of 1 m, figure 4-5 is for a separation of 3 m, and figure 4-6 is for use in the far-field. All three figures are probably intended by the manufacturer for use at an open field site (free space) because the antenna factor variation is only from 4 dB (minimum value) to 18 dB maximum. Figures 4-7 and 4-8 give the far-field values of antenna factor measured at NBS for the 2 biconical antennas purchased from



the manufacturer. These were calibrated at the outdoor NBS field site, using the standard antenna method, with each antenna located at a distance of 15 m from a transmitting dipole. The height above ground was 3 m for both transmitting and receiving antennas. A height of 3 m is theoretically sufficient to reduce the ground proximity effects to a negligible value. As shown in figures 4-7 and 4-8 , the two biconical antennas have measured values of antenna factor which are nearly identical and can thus be used legitimately as an identical pair for making two-antenna gain calibrations as described in section 4.4. The total range of measured antenna factor is from 4 dB (minimum) to 17 dB (maximum).

Figure 4-9 is a sketch of the screenroom layout for measuring the gain ( $G_{\text{eff}}$ ) of two biconical antennas in the NBS screenroom. The two antennas were located on the center line (long dimension) of the screenroom with both antennas at a height of 1 m above the floor. The dipoles were parallel to each other and adjusted for horizontal polarization as indicated in the figure. Two different separation distances were checked, 1 m and 3 m. Figure 4-10 gives the two antenna factor curves for the separation distances of 3 m and 1 m. The effect of screenroom resonances and reflections on the measurement of antenna factor for a separation distance of 3 m is from -2.3 dB (minimum) to 54.9 dB (maximum). The range for a 1 m separation distance is 4.8 dB (minimum) to 50.1 dB (maximum). The reduced variation at a closer separation distance is apparently due to reduction of screenroom (cavity) Q by the close proximity of the receiving antenna with its associated power absorption.

Figure 4-11 shows a sketch of the screenroom layout with the two biconical antennas spaced 1 m apart but with their centerline rotated 90 degrees in the screenroom. Figure 4-12 shows another room configuration which was tested for the effect of screenroom reflections on measured antenna factor. Figure 4-13 gives the measurement results for the three screenroom configurations of figures 4-9, 4-11, 4-12. The data of figure 4-13 were obtained with a separation distance of 1 m between the antennas. The

data clearly indicate the screenroom resonance effects and multipath reflection variability as a function of antenna placement.

Figure 4-14 compares the difference in antenna factor in dB for a biconical antenna as measured in a screenroom and on the open field site. This graph indicates that using the open-field-site antenna factors as permitted in MIL-STD-461A will give a greater error in field strength measurements in a screenroom than using the antenna factors as measured in-situ.

Using the NBS designed EFM-5 [4-10], calibrated in a TEM cell [4-11], the electric field at the receiving antenna location was measured in conjunction with measurement of the antenna factor of the biconical antenna by the two-antenna method. Using this antenna factor, the field was determined from eq (4-12) and compared with the applied field as measured with the EFM-5. This applied field was kept constant while making the antenna factor measurements. Figure 4-15 is a plot of the difference between field strength measured with the calibrated EFM-5 probe and that measured with the biconical antenna calibrated by the MIL-STD-461 two-antenna method. The plot indicates that the electric field as determined from the measured screenroom antenna factors can differ as much as 7 dB from the electric field measured with a calibrated EFM-5 probe, over the frequency range of 20 to 140 MHz.

#### 4.4.2 Vertical Monopoles

Figure 4-16 is a typical graph of antenna factor for a vertical monopole as given in the manufacturer's manual. Two of these antennas were calibrated at the outdoor NBS field site, using the standard field method. Each antenna was located at a distance of 20 m from the transmitting monopole. The height (length) of the transmitting monopole was 2.45 m. The receiving monopole base was 1 m above ground. Figure 4-17 shows that the two calibrated monopoles have measured antenna factors which are nearly identical and can thus be used for determining antenna factor by the two

antenna method. The antenna factors measured on the ground screen varied from about 12 dB (minimum) to about 42 db (maximum).

The gains of the two vertical monopoles were measured in the screenroom using the two antenna technique as described previously for the biconical antennas. Again, two separation distances of 1 and 3 m were used. Figure 4-18 gives the two antenna factor curves for separation distances of 1 and 3 m. The antenna factor range for the 1 m separation is 10.3 dB (minimum) to 55.2 dB (maximum). The range for the 3 m separation is 24.9 dB (minimum) to 86.8 dB (maximum).

Figures 4-9, 4-11, and 4-12 show a sketch of the screenroom layout with the two biconicals spaced 1 m apart to test the effect of screenroom interaction on the antennas. Using figures 4-9, 4-11, and 4-12 for reference placement, the two vertical monopoles were placed in the same position as those occupied by the biconicals. Figure 4-19 gives the measurement results of the three screenroom configurations. The figure demonstrates the screenroom nulls and coupling effects inside the enclosure as a function of antenna placement.

#### 4.5 Discussion of Antenna Factor Measurement Accuracy in Shielded Enclosures

Figures 4-10, 4-13, 4-18, and 4-19 show that measurements in a screenroom environment differ significantly from measurements made at an open field site (figures 4-3, 4-4, 4-5, 4-6, 4-7, 4-8, 4-16, and 4-17). Variations of antenna factor for frequencies at or above the first resonance of the enclosure can be attributed to the screenroom resonances and to multi-path reflections in the screenroom. Variations of antenna factor at frequencies below the first resonance of the screenroom, where the dimensions of the enclosure are small compared to the wavelength, are caused primarily by coupling of the two antennas via the enclosure walls and normal coupling of the two antennas due to the radiated field.

#### 4.6 Error Bounds of Screenroom Measurements

The data presented above show the variability of measured antenna factors in a screenroom as a function of frequency, antenna placement, and distance between the antennas. The error can vary from 0 to 40 dB as a function of any of the parameters given in the previous sentence. The measurements also indicate that antenna factors determined in a screenroom by the MIL-STD-461A two-antenna method are not an accurate parameter for subsequently measuring an electric field. The errors in the measured field strength inside a screenroom using the antenna factor eq of MIL-STD-461A can be greater than  $\pm 7$  dB for biconical antennas in the 20 to 140 MHz frequency range.

#### 4.7 Conclusions

Large measurement errors can occur in a screenroom because of room resonances, multiple reflections, distorted radiated fields, and errors in the antenna factors as measured by the MIL-STD-461A technique. It has been shown that measurement results depend greatly on the size of the enclosure, location of the test setup in the screenroom, and location of the antennas. Field strength measurements made with the calibrated antennas in the enclosure may have large errors. The correlation of these measurements, to open-field or other shielded enclosure measurements with different dimensions and geometries, is small.

Determination of an in-situ antenna factor in a screenroom or using antenna factors which have been determined in a free space environment do not lead to accurate field strength measurements in a screenroom. To establish accurately-known electromagnetic fields in a screenroom, a transfer standard such as a calibrated EFM-5 probe should be used to check and measure the field. These small transfer probes do not interfere with or distort the electric field being measured [4-10].



Further theoretical and experimental work needs to be done in the measurement of radiated EM fields, such as loading the screenroom with absorbing material in a systematic manner and studying the behavior of the dampened waves.

#### 4.8 References

- [4-1] Stuckey, C.W. Free, W.R., Robinson, D.W. Preliminary interpretation of near-field effects on measurements, IEEE-EMC Symposium Record, June 1969, Asbury Park NJ.
- [4-2] Free, W.R. Radiated EMI measurements in shielded enclosures, IEEE-EMC Symposium Record, July 1967, Washington DC.
- [4-3] Krstansky, J.J., Standley, R.D. Theory of RFI measurements in shielded enclosures, 8th Annual IEEE Symposium on EMC, Jan. 1966, San Francisco, Ca.
- [4-4] Bennett, W.S. Antenna factors in EMC measurements, IEEE International symposium on EMC, Arlington Va., 1983
- [4-5] MIL-STD-461A; Military Standard, Electromagnetic Interference Characteristics, requirements for equipment; pp 10-11, August 1, 1985
- [4-6] Greene, F.M. NBS field-strength standards and measurements (30 Hz to 1000 MHz). Proc. IEEE, Vol. 55, pp 970-981; June 1967.
- [4-7] Taggart, H.E. and Workman, J.L. Calibration principles and procedures for field strength meters (30 Hz to 1 GHz). National Bureau of Standards Tech Note 370; March 1969.
- [4-8] Jordan E.C. Electromagnetic waves and radiating systems, Prentice-Hall, Inc., 1950

- [4-9] Schelkunoff S.A. and Friis, H.T. Antennas, theory and practice, John Wiley and Sons, Inc., 1952.
- [4-10] Larsen, E.B., and Ries F.X. Design and calibration of the NBS Isotropic Electric-Field Monitor (EFM-5), 0.2 to 1000 MHz, U.S. Nat. Bur. of Standards, NBS Tech. Note No. 1033, 104 pages March 1981.
- [4-11] Crawford, M.L. Generation of standard EM; fields using TEM transmission cells, IEEE Trans. Electromag. compat., EMC-16 No. 4, pp 189-195 November 1970

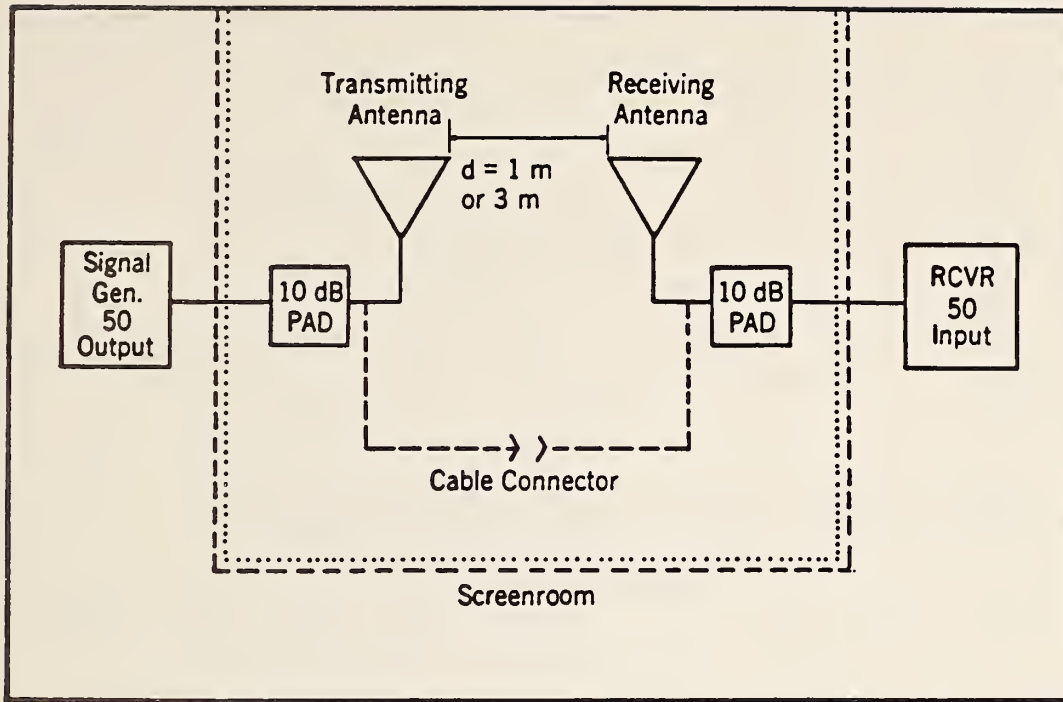


Figure 4-1. Test setup required by MIL-STD-461A for determination of antenna factors.

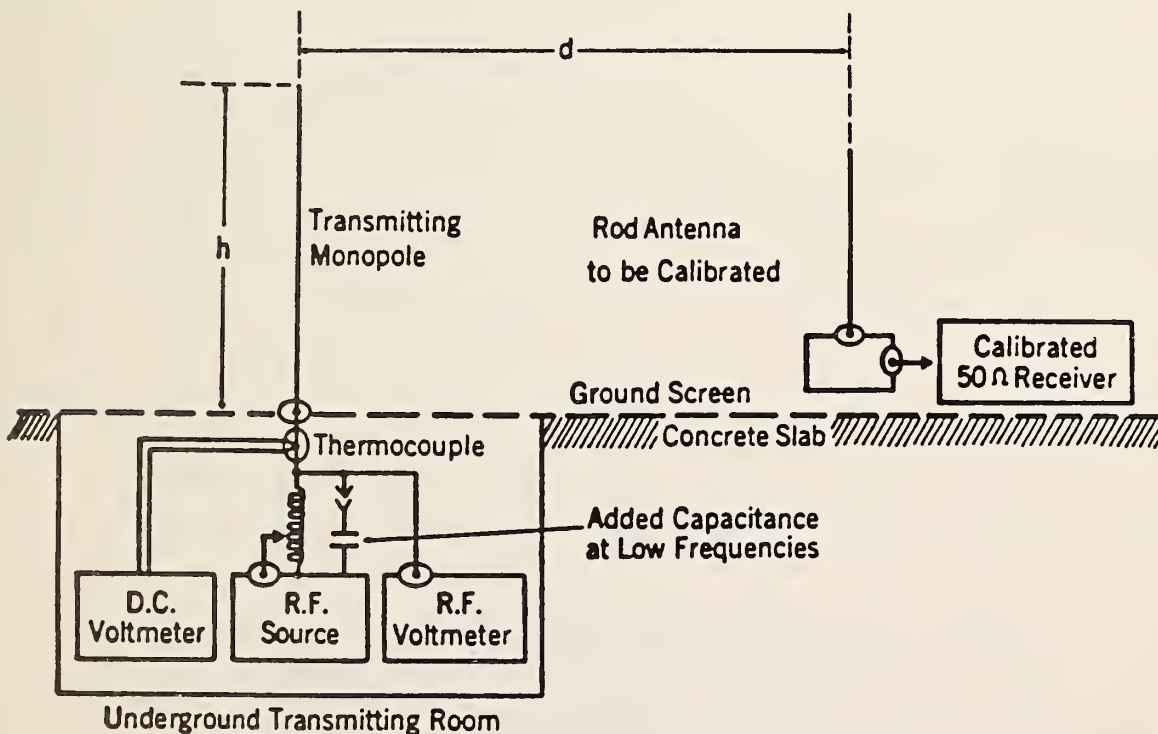


Figure 4-2. Instrumentation used at NBS open-field site to calibrate monopole antenna factors.

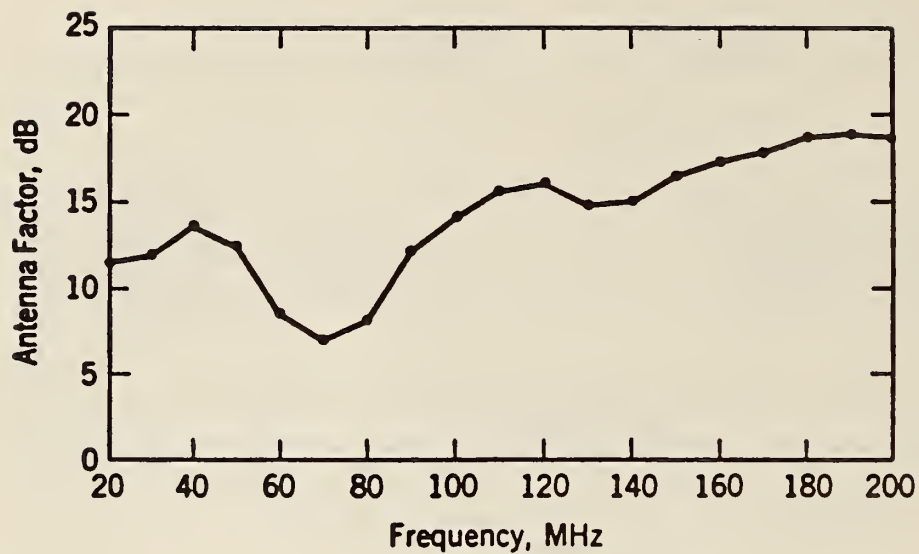


Figure 4-3. Antenna factor of a typical biconical dipole taken from the manufacturer's manual for a far-field separation distance.

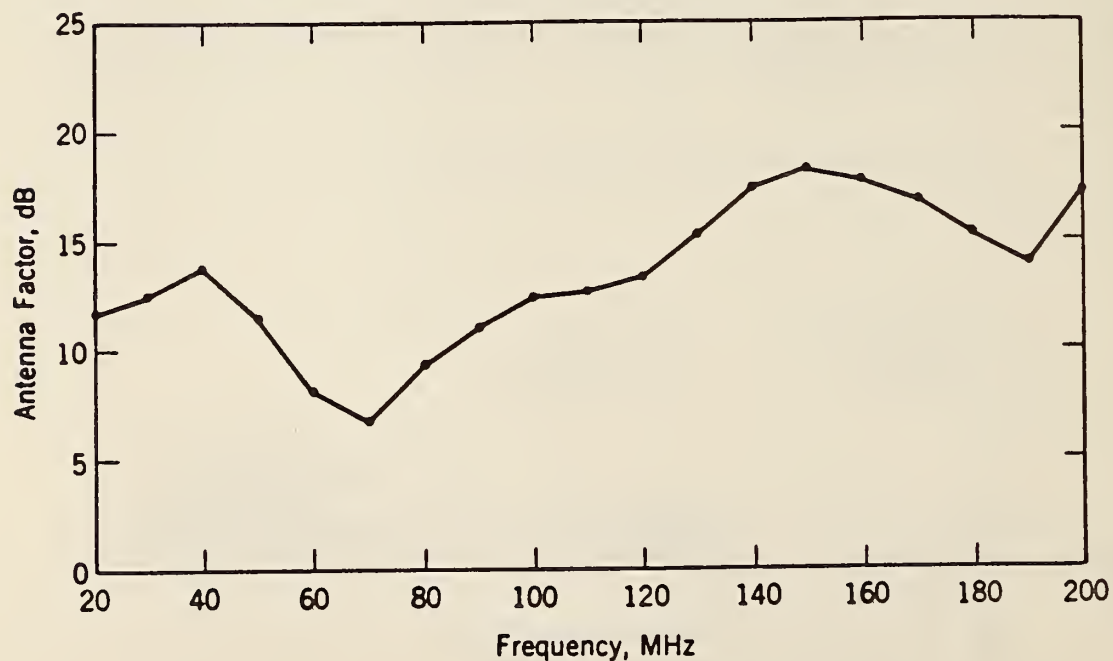


Figure 4-4. Antenna factor of a typical biconical dipole taken from the manufacturer's manual for a separation distance of 1 m.



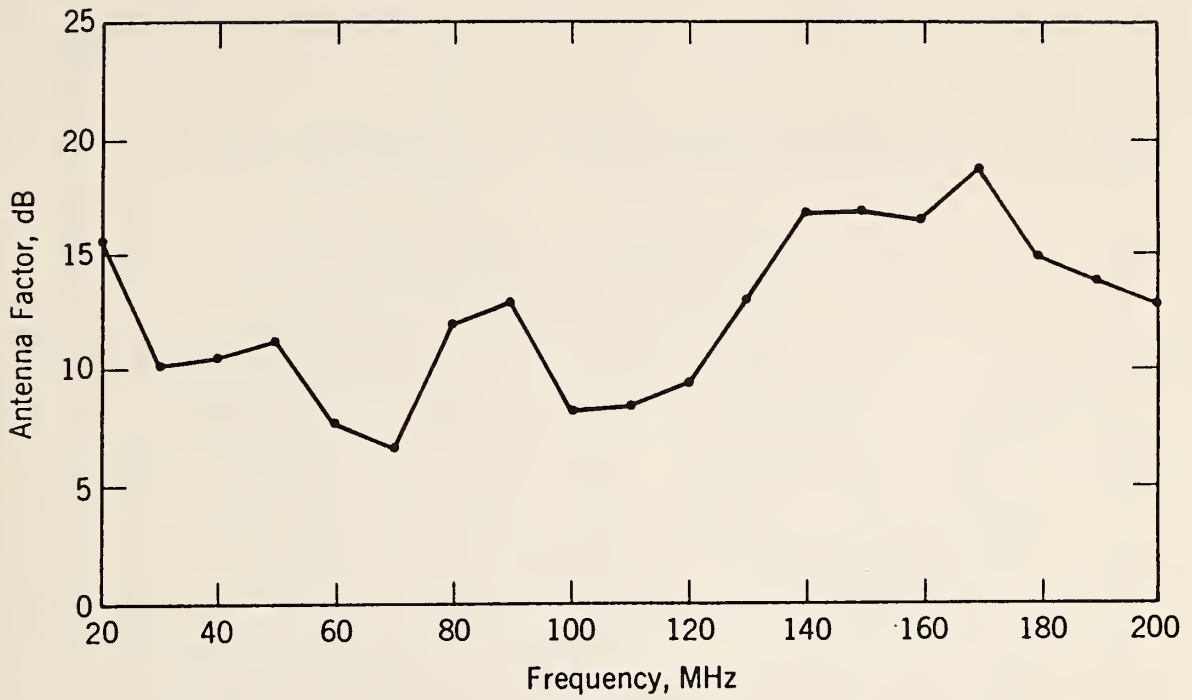


Figure 4-5. Antenna factor of a typical biconical dipole taken from the manufacturer's manual for a separation distance of 3 m.

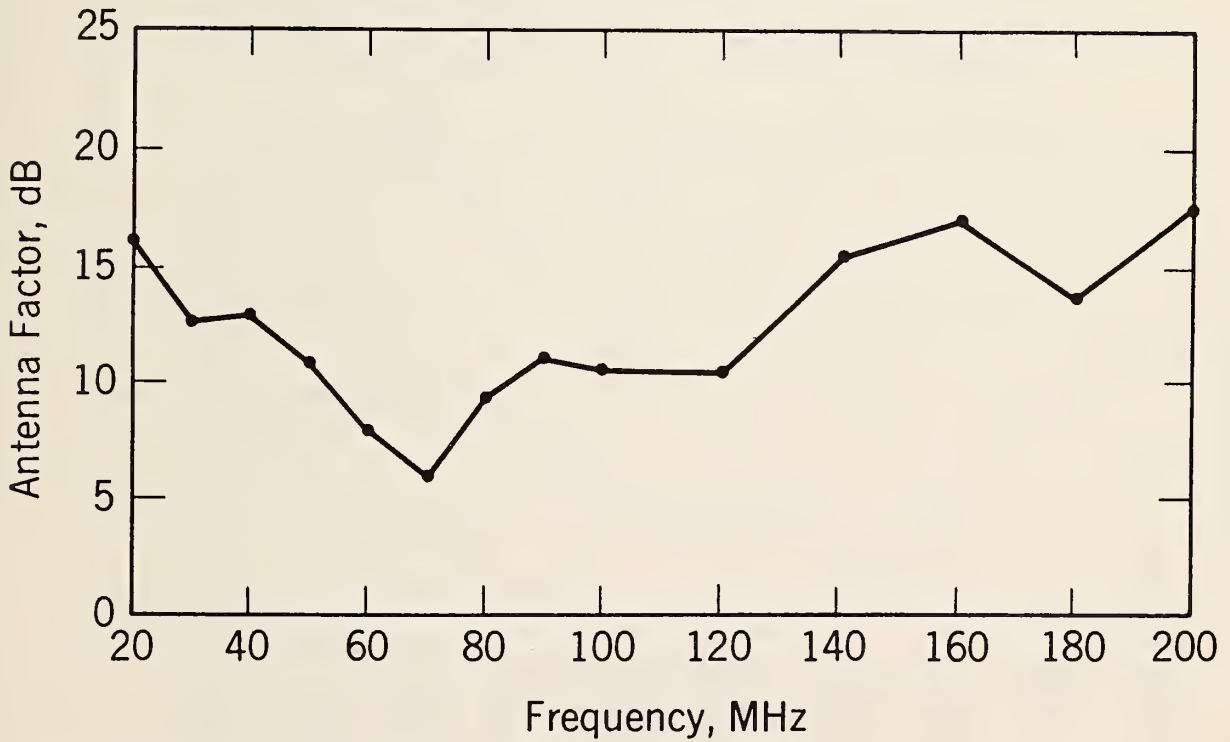


Figure 4-6. Antenna factor of a typical biconical dipole taken from the manufacturer's manual for a separation distance of 15 m and an antenna height of 3 m.

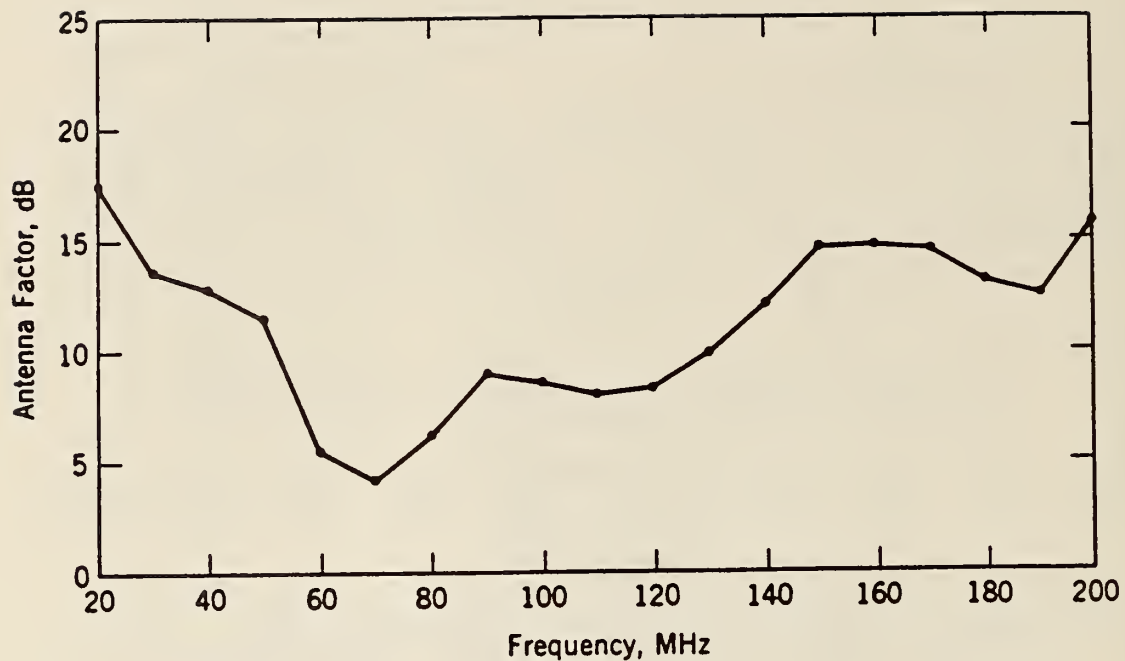


Figure 4-7. Antenna factor of Biconical No. 1 for a "far field" separation distance, as measured at NBS.

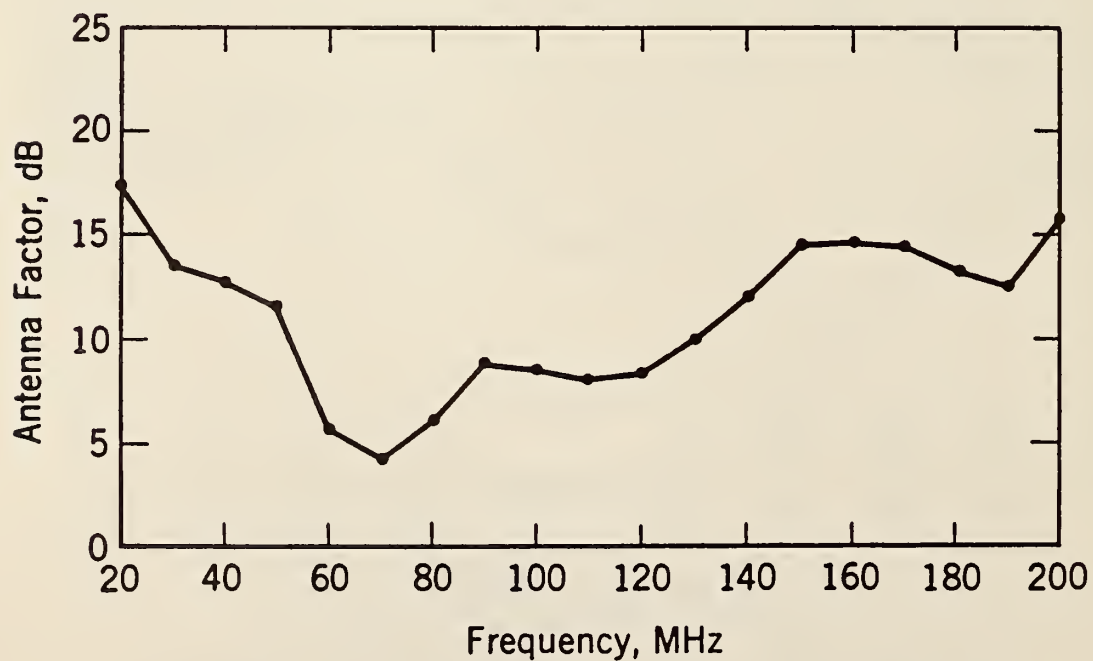


Figure 4-8. Antenna factor of Biconical No. 2 for a "far field" separation distance, as measured at NBS.

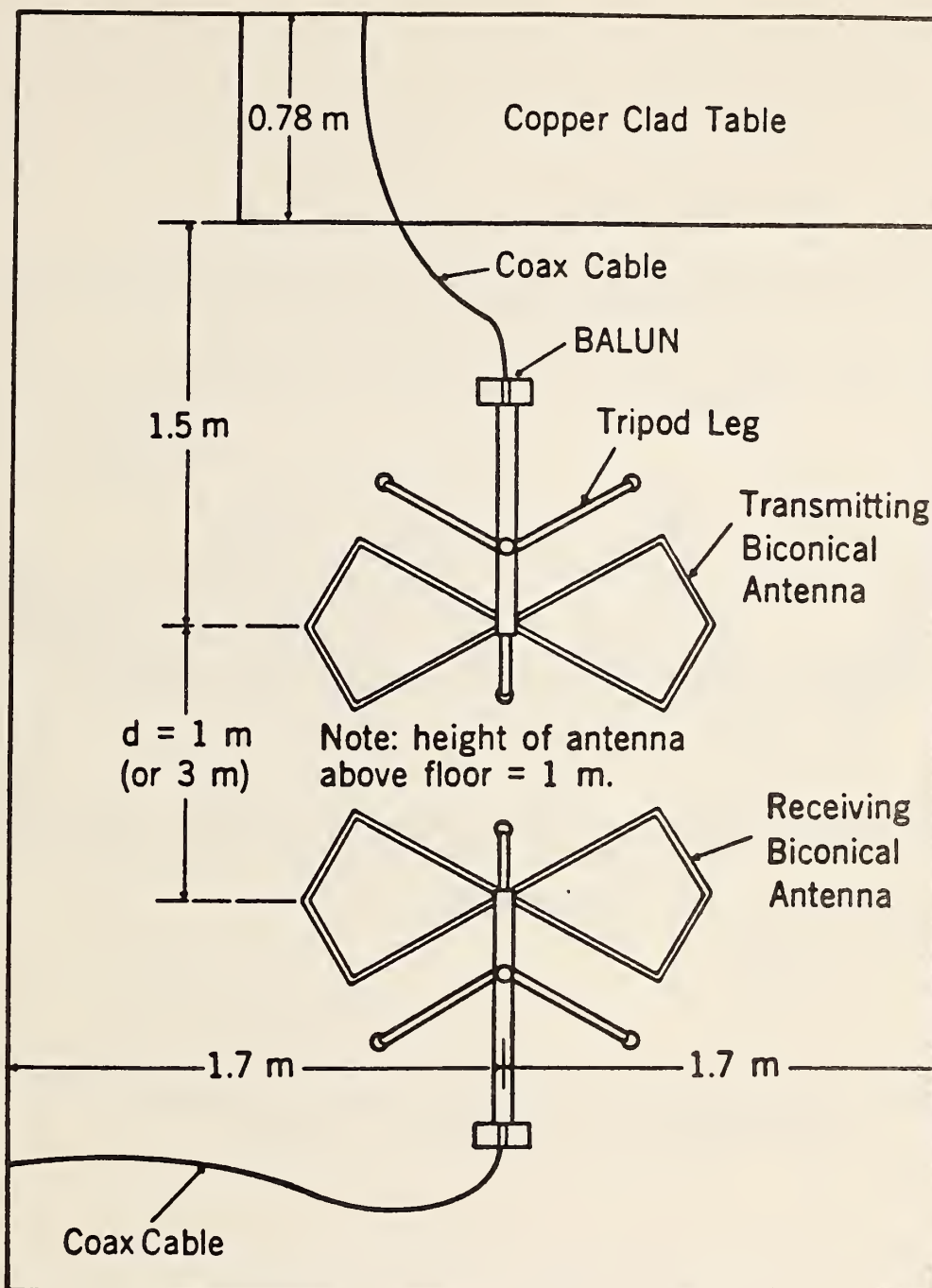


Figure 4-9. Placement of biconical antennas in NBS screenroom, position 1.

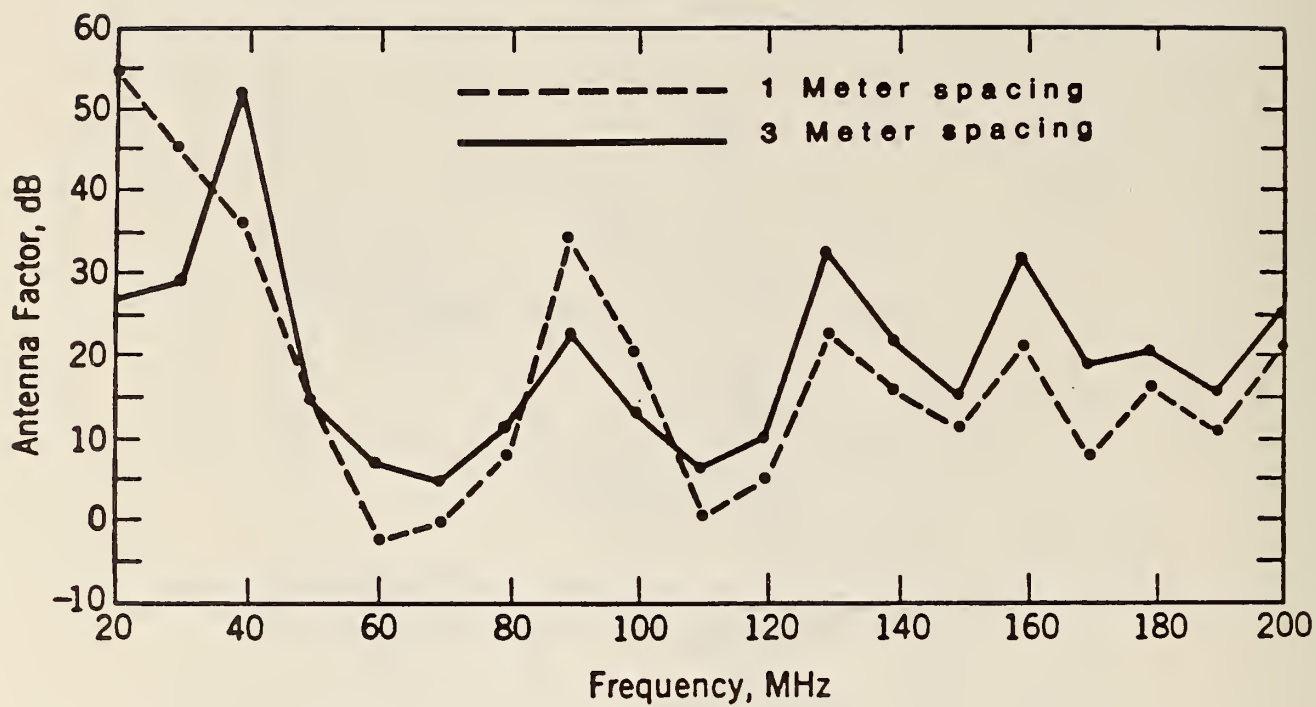


Figure 4-10. Antenna factors for biconical dipole calibrated in the NBS screenroom at spacings of 1 and 3 m.



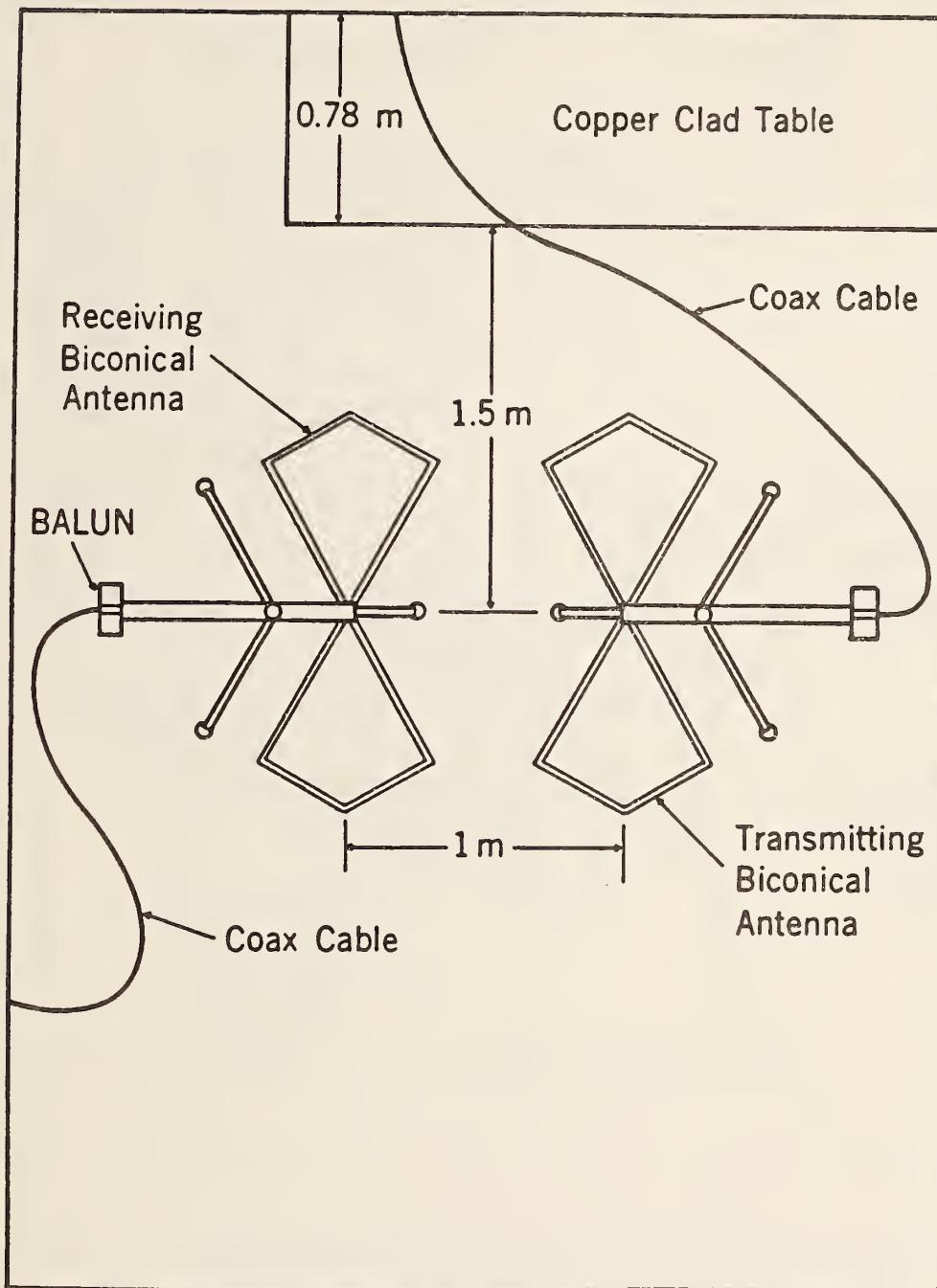


Figure 4-11. Placement of biconical antennas in NBS screenroom, position 2.

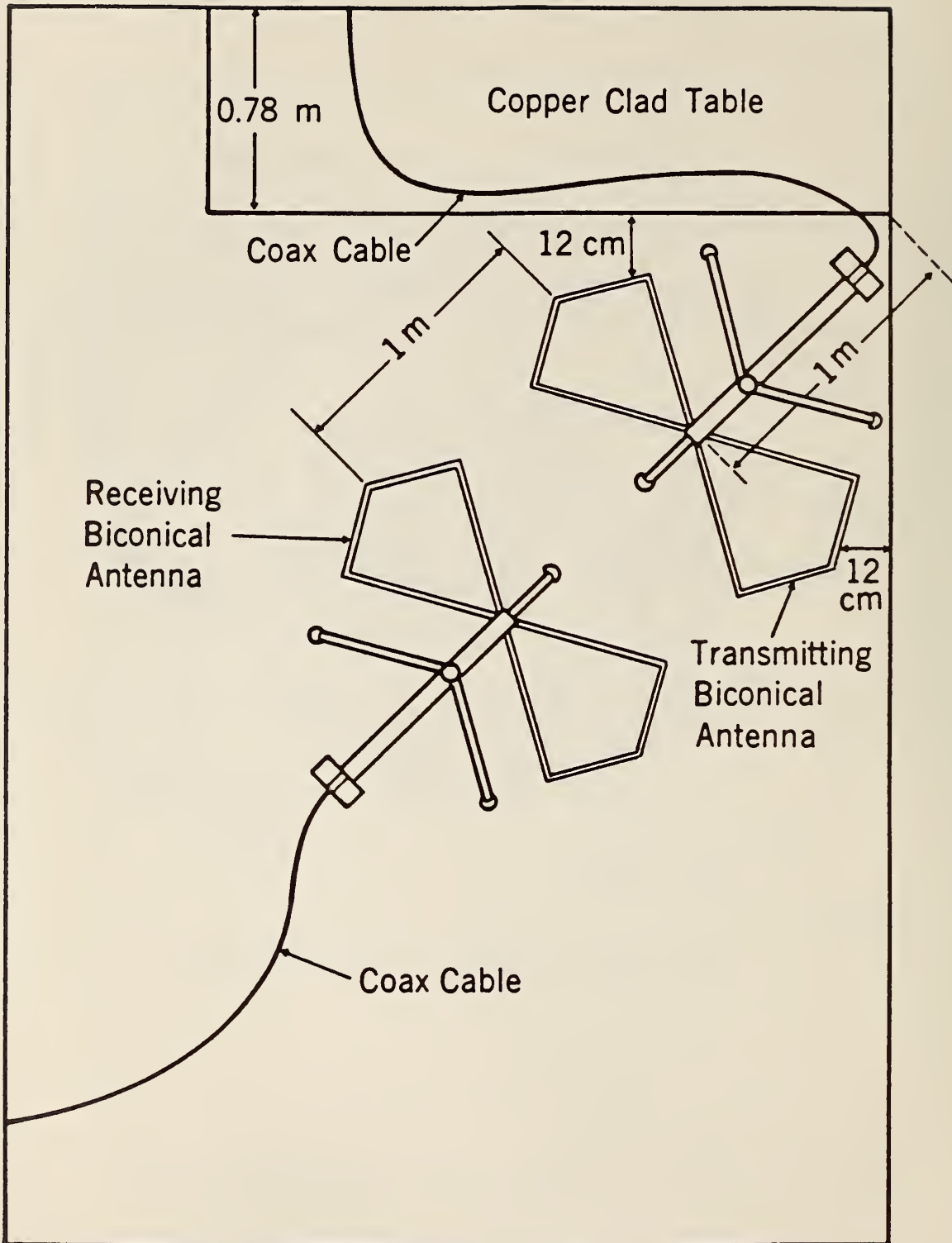


Figure 4-12. Placement of biconical antennas in NBS screenroom, position 3.

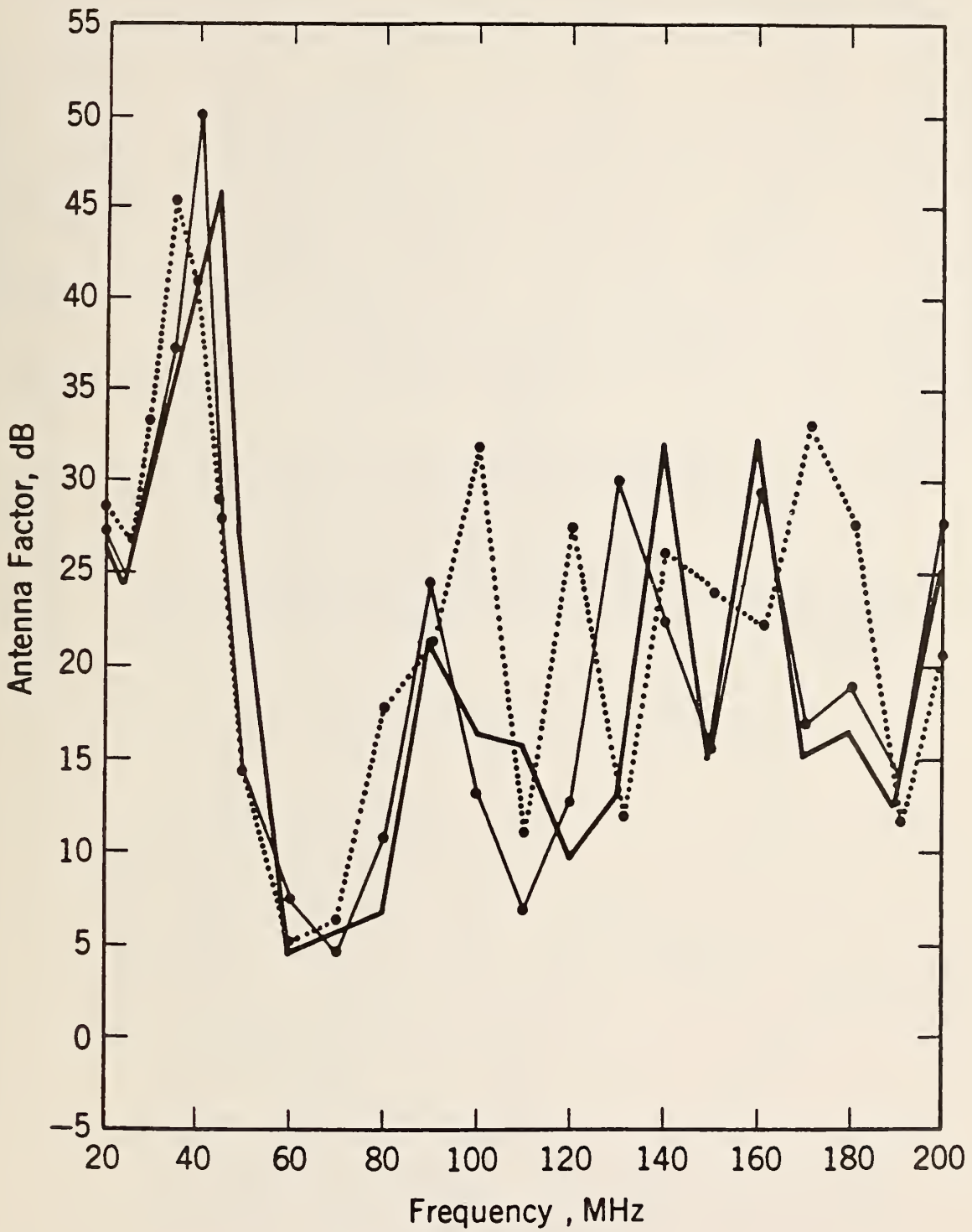


Figure 4-13. Measurement results of three screenroom placements with an antenna separation distance of 1 m.

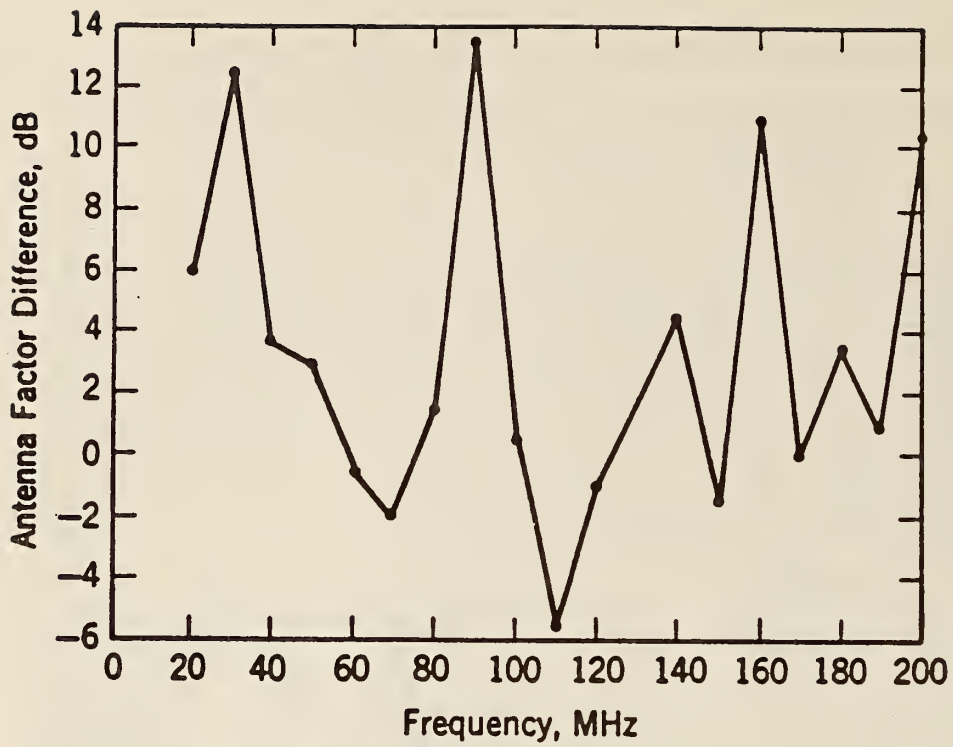


Figure 4-14 Difference between antenna factors measured in a screenroom and on the NBS field site for a biconical dipole.

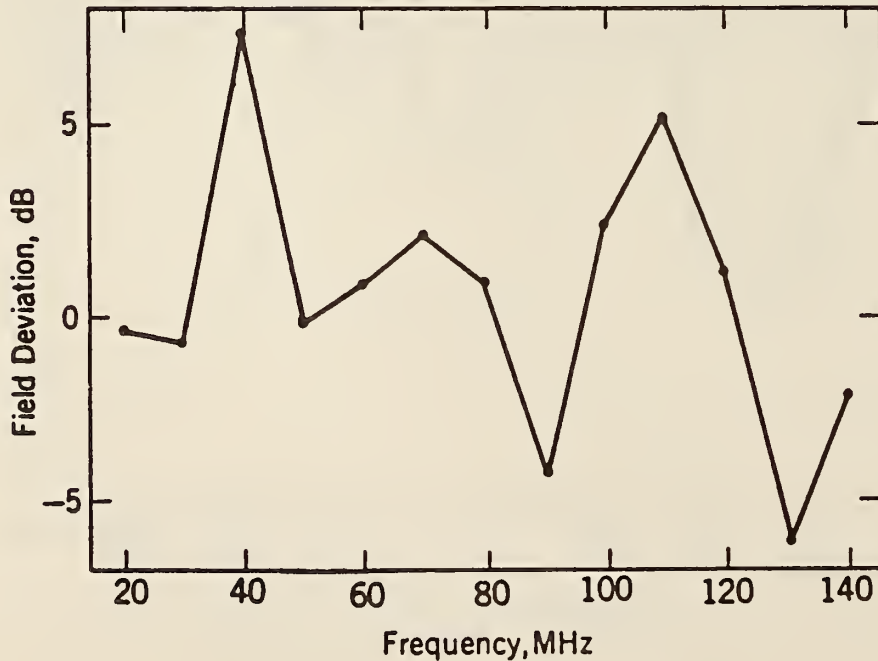


Figure 4-15. Difference between field strength measured with a calibrated transfer probe (EFM-5) and that measured with a biconical antenna calibrated by the MIL-STD-461A two-antenna method.



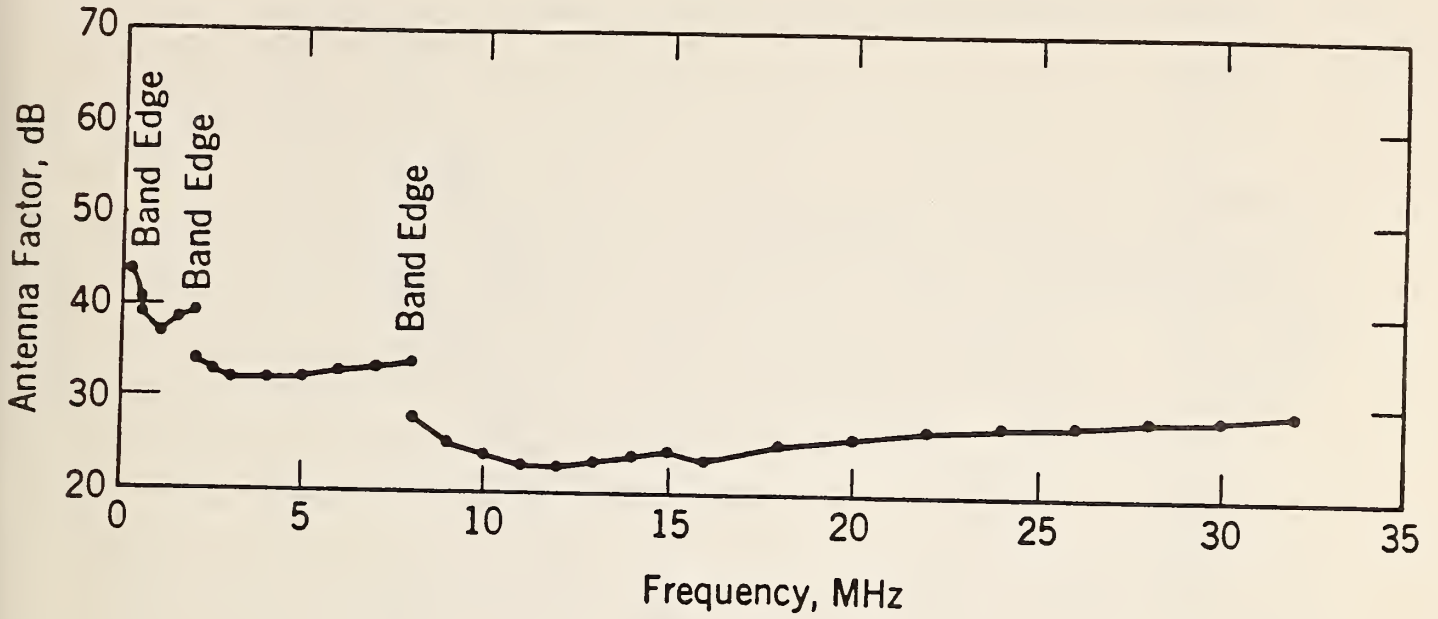


Figure 4-16. Antenna factor for typical 1.04 m vertical monopole taken from the manufacturer's manual.

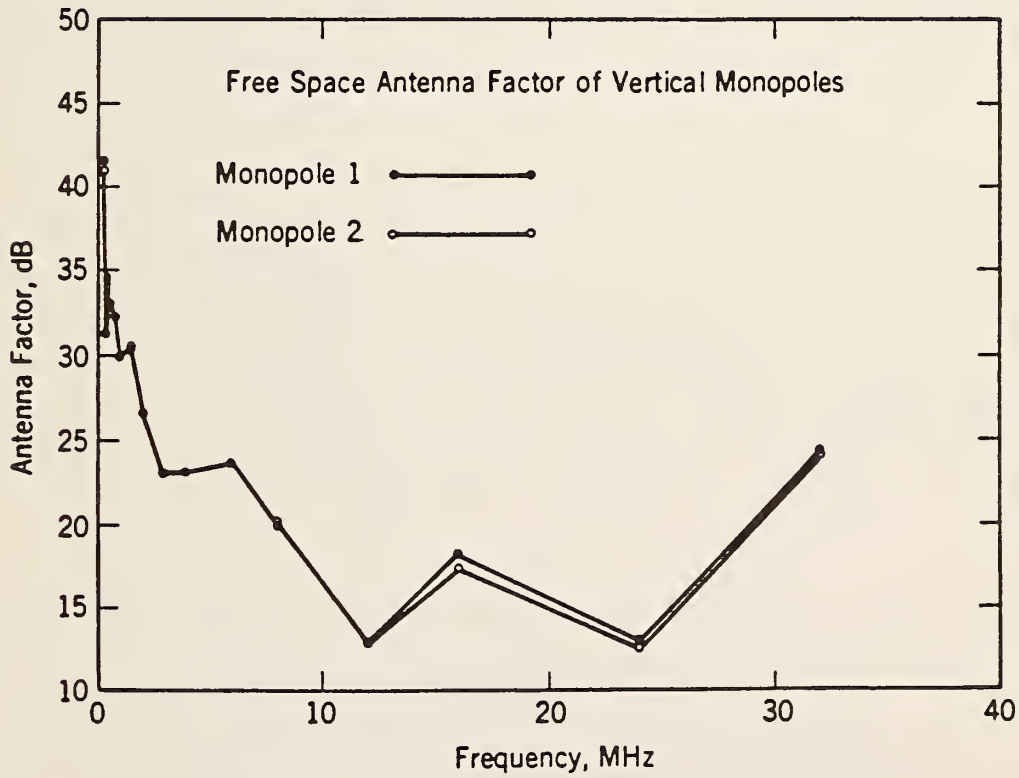


Figure 4-17. Free-space antenna factor of two vertical monopoles as calibrated at the NBS open-field site.

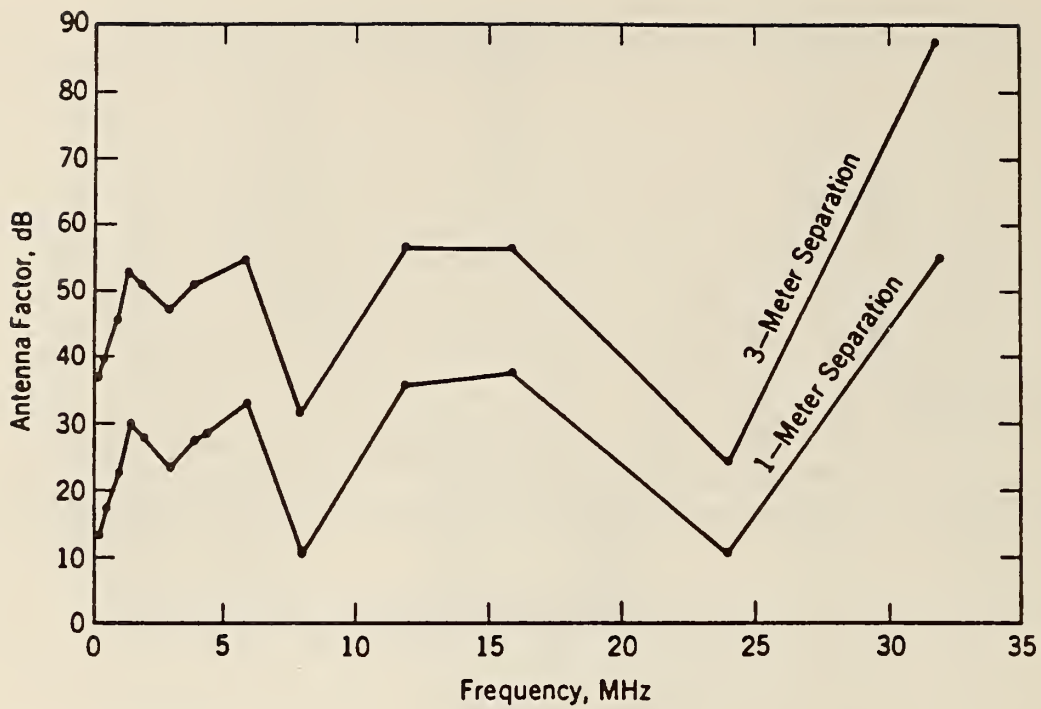


Figure 4-18. Antenna factor for 1.04 m vertical monopole calibrated in the NBS screenroom at different antenna spacings.

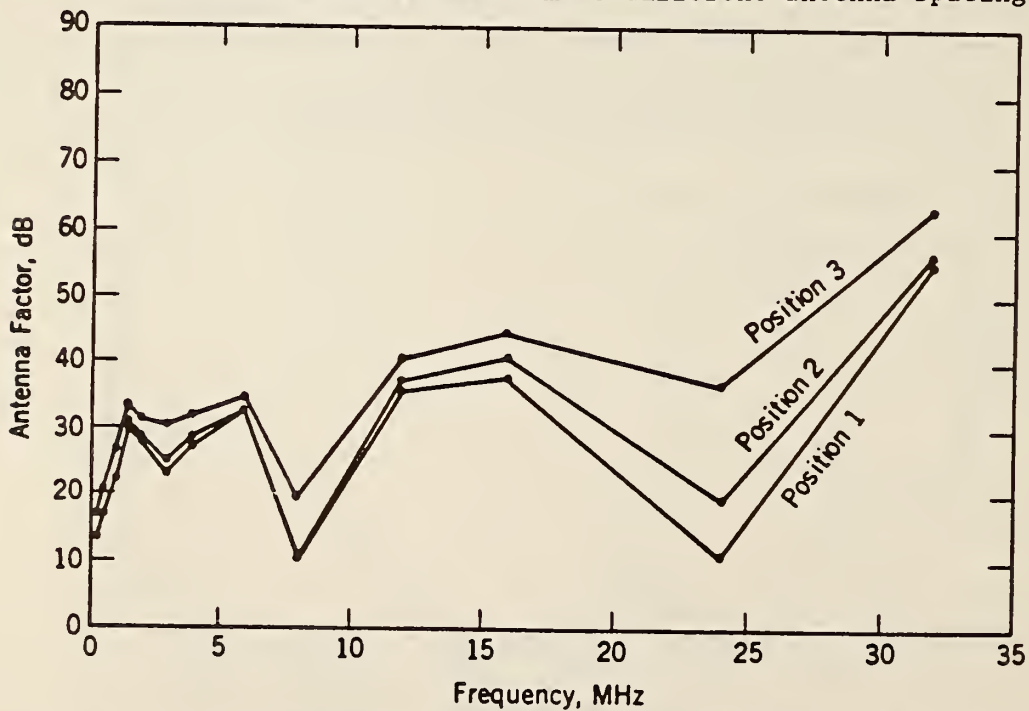


Figure 4-19. Antenna factor for 1.04 m vertical monopole calibrated in NBS screenroom at different antenna locations for a 1 m antenna separation.

## 5. Measurement of Broadband Impulsive Signals

### 5.1 Introduction

The impulse bandwidth (IBW) of an EMI receiver is used for measurement of broadband interference. The IBW may be determined by several different approaches. The spectrum amplitude of an impulse generator (IG) as a function of frequency,  $S(f)$ , may also be measured by several approaches. Four of these possible methods were evaluated at NBS for comparison purposes. The four techniques are defined and discussed in this chapter.

An RF signal is considered to be narrowband or broadband depending on whether its frequency spectrum is less than or greater than the bandwidth of the receiver. The overall bandwidth of a receiver is determined essentially by the selectivity of the IF amplifier strip and is typically of the order of 0.1 percent of the receiver tuned frequency. The term "cw" stands for a single-frequency sinusoid of constant amplitude. The term "impulse" is used for a baseband (DC) pulse or an RF burst (pulsed RF) whose time duration is short compared with the period of the receiver circuit which responds to the impulse. This period is approximately the reciprocal of the IF bandwidth for a well-designed EMI receiver.

A common practice is to divide broadband interference into two categories, which may be defined as follows: (1) Random noise consists of a large number of overlapping signals with random amplitude, frequency, and relative phases. Examples are thermal noise and shot noise. (2) Impulse noise consists of a single short pulse of voltage, or repetitive pulses, causing a signal with systematic relative phase and amplitude vs frequency. Examples are switching transients, automobile ignition noise, and interference from radar transmitters. The response of a receiver to either type of broadband signal is determined, partially, by the receiver bandwidth. This is because all frequency components of the input signal which fall outside the receiver bandwidth are rejected, or at least amplified less than the frequency components at the center of the passband.

Differences between the possible types of RF signals can be illustrated by comparing receiver response (indicated level) as a function of receiver bandwidth. For a cw signal, the response amplitudes for a peak-voltage, average-voltage, or RMS-voltage detector are independent of the receiver bandwidth. For random noise, the average voltage and RMS response values of a

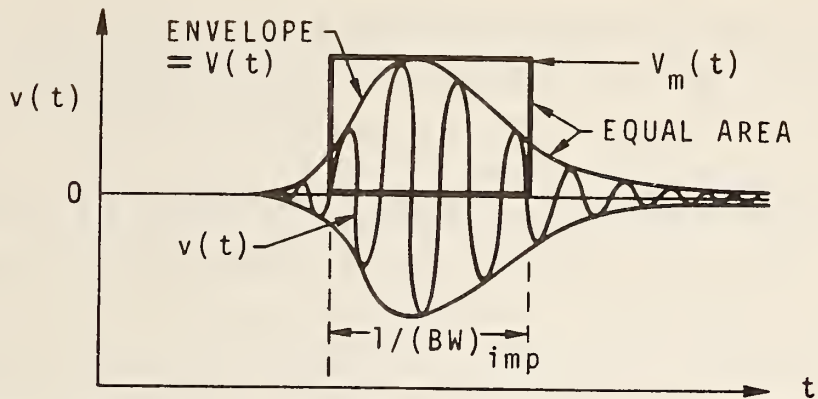
receiver are proportional to the square root of bandwidth. For impulse noise of low repetition rate, the average voltage is typically independent of bandwidth but the peak value is proportional to bandwidth (among other things). This proportionality factor makes it convenient to define an impulse bandwidth for a receiver. Actually, the response of a tuned receiver to an impulse, as measured with a peak-reading detector, depends not only on bandwidth but also on the shape of the bandpass curve and phase characteristics of the receiver. The response of ideal interference meters to various inputs, as a function of bandwidth, is summarized in table 5-1.

In most common approaches to impulse measurement, the impulse bandwidth of the receiver is a calibration factor determined by adjusting the output of a cw generator to give the same indication on the receiver output meter as the peak response to an impulse generator of known characteristics. The impulse bandwidth in MHz is then the output of the cw generator in  $\mu\text{V}$ , divided by the output of the impulse generator in  $\mu\text{V}/\text{MHz}$ . Some commonly used definitions relating to broadband interference are discussed in the next section.

## 5.2 Calibration of an EMI Receiver and Measurement of an Impulse Generator Using the Video Pulse Technique of MIL-STD-462

The video pulse technique involves application of a train of (nominally) identical repetitive pulses to an EMI receiver which has been designed with the "proper" shape of passband. This means that the receiver acts as a filter having a well-rounded (Gaussian shaped) passband, rather than a rectangular passband. The measurement approach is prescribed by MIL-STD-461/462 [5-1,5-2] and is unique in the sense that the EMI receiver itself is used to measure the impulse bandwidth of the receiver. That is, no calibrated external pulse standard is required to calibrate the receiver IBW. As specified in the MIL-STD, the area of the receiver response envelope and maximum envelope amplitude are each measured. From these measurements the receiver IBW and spectrum amplitude  $S(f)$  of the IG are determined. The calibrated receiver (with a calibrated antenna) can then be used to measure radiated impulsive interference. A sketch of the intermediate frequency (IF) output voltage  $v(t)$  of a typical EMI receiver is given as follows.





In the above sketch:

$v(t)$  = receiver IF voltage output in the time domain, RMS volts,  
 $V(t)$  = envelope of the receiver voltage response curve, RMS volts, and  
 $V_m(t)$  = maximum voltage value of the envelope of the receiver response curve, RMS volts.

Definitions of the terms involved are given as follows:

a. Receiver impulse bandwidth

$$(\text{IBW, Hz}) = \frac{V_m(t)}{\int_0^{\infty} V(t)dt} = \frac{\text{Maximum envelope height, volts}}{\text{Envelope area, volt}\cdot\text{sec}} \quad (5-1a)$$

$$= \frac{\text{Maximum envelope height, cm}}{(\text{Envelope area, cm}^2)(\text{Scope sweep speed, sec/cm})} \quad (5-1b)$$

or

$$(\text{IBW, Mhz}) = \frac{\text{Maximum envelope height, cm}}{(\text{Envelope area, cm}^2)(\text{Scope sweep speed, }\mu\text{sec/cm})}. \quad (5-1c)$$

b. Impulse spectrum amplitude

$$S(f), \text{ Volts/Hz} = (1/G_0) \int_0^{\infty} V(t)dt = \frac{\text{Envelope area, volt}\cdot\text{sec}}{\text{RCVR gain}}. \quad (5-2a)$$

Also

$$S(f), \text{ Volts/Hz} = \frac{V_m(t)}{(G_0)(\text{IBW})} = \frac{\text{Maximum envelope height, volts}}{(\text{RCVR gain, } G_0)(\text{RCVR IBW, Hz})}, \quad (5-2b)$$

or

$$S(f), \mu\text{V/MHz} = \frac{(\text{Maximum envelope height, cm})(\text{Scope gain, }\mu\text{v/cm})}{(\text{RCVR gain, } G_0)(\text{RCVR IBW, MHz})} \quad (5-2c)$$

$$= \frac{(\text{Envelope area, cm}^2)(\text{Scope sweep speed, }\mu\text{s/cm})(\text{Scope gain, }\mu\text{v/cm})}{\text{RCVR gain, } G_0}. \quad (5-2d)$$

A block diagram of the instrumentation used at NBS for the MIL-STD-462 approach for measuring impulse bandwidth of a receiver and spectrum amplitude of an impulse generator is given in figure 5-1. The EMI receiver used for our tests has a three-position bandwidth switch, with selectable bandwidths of 10 kHz, 100 kHz, or 1 MHz. This bandwidth switch was set in the 1 MHz position for all the data reported here. At each receiver tuned frequency tested, the receiver "CAL" knob (gain control) was adjusted to obtain a receiver dial indication of 40 dB $\mu$ V, with the receiver step attenuator in the 40 dB position. This corresponds to a voltage level of 80 dB $\mu$ V  $\equiv$  10 mV, which is the true receiver input signal level as determined by the calibrated voltmeter (1 V minus 40 dB = 80 dB $\mu$ V). The overall cw gain of the receiver,  $G_0$ , was determined by measuring the IF output with the oscilloscope shown in figure 5-1, and dividing this voltage by the 10 mV RMS input to the receiver. That is,

$$G_0 = \frac{(\text{cw peak-to-peak volts at IF output}) / (2\sqrt{2})}{10 \text{ mV}} . \quad (5-3)$$

As shown in figure 5-1, a commercially available impulse generator was used for our tests. It is specified by the manufacturer to produce a spectrum output that is flat within  $\pm 1$  dB from 60 kHz to 1000 MHz. The output amplitude is switch selectable from 10 to 101 dB $\mu$ V/MHz (RMS) in one-quarter dB steps. The IG was set to its maximum output level of 101 dB $\mu$ V/MHz for all the data included in this report. The receiver input level for impulsive signals should thus be 95 dB $\mu$ V/MHz, after the 6 dB insertion loss of the 50  $\Omega$  power splitter. Photographs of the receiver response envelopes (video pulses) are shown in figure 5-2. The data for the MIL-STD calibration of the EMI receiver and impulse generator are given in tables 5-2 and 5-3. A set of data was taken at frequencies near the top and bottom end of each of the eight receiver bands, plus measurements at the middle of the highest frequency band. It can be seen that the MIL-STD measurements of  $S(f)$  are within one-half dB of the IG nominal output value of 101 dB $\mu$ V/MHz at all the frequencies checked below 800 MHz. At higher frequencies the measured values of  $S(f)$  range from 101.9 to 103.6 dB $\mu$ V/MHz.

The definition of impulse bandwidth of a narrowband filter (receiver) is given in the IEEE dictionary of electronic terms [5-3] as follows: "The peak value of the response envelope divided by the spectrum amplitude of an applied

impulse." It is seen that this definition agrees with the MIL-STD approach [5-1,5-2,5-4]. A copy of Section 4.2.3.5 and 4.2.3.6 of MIL-STD-461 is quoted here for reference purposes.

Calibration of Measuring Equipment. All measuring equipment shall be calibrated in accordance with MIL-STD-461.

Impulse Generators. Impulse generators shall be calibrated as follows:

(a) Apply the output of an impulse generator to the input of an amplitude-linear receiver having synchronously tuned, less than critically coupled circuits. EMI receivers are satisfactory for this purpose if their impulse bandwidth is at least five times the repetition rate of the impulse generator. Any AGC system shall be disabled and the AGC line firmly referred to ground with a low impedance voltage source of appropriate value.

(b) Obtain an oscilloscope pattern of the overall receiver response at the IF output. The oscilloscope controls shall be so adjusted that the pattern is as large as possible within the calibrated area on the face plate. Either photograph or trace the pattern. Record the oscilloscope sweep speed setting. (The sweep speed shall be calibrated accurately.)

(c) Use a planimeter or other integrating device to determine the area of the pattern. This operation shall be carried out at least 10 times and the average of the readings taken as the area.

(d) Calculate the impulse bandwidth of the receiver in accordance with the following formula:

$$\text{IBW in Hz} = \frac{(\text{Pattern height in cm})}{(\text{Pattern area in cm}^2)(\text{Sweep speed in sec/cm})}$$

(e) Connect a sinewave generator to the receiver and at  $f_0$  adjust the output until the peak pattern height is the same as that obtained with the impulse generator.

(f) Connect an rf power meter to the signal generator and measure the power output. Calculate the rms voltage of the sinewave signal.

(g) The output of the impulse generator is now calculated by taking the rms voltage calculated in step (f) divided by the impulse bandwidth determined in step (d).

### 5.3 Measurement of an IG by the NBS FFT Calibration System

An impulse generator (IG) can be calibrated by measuring the train of output pulses with a sampling oscilloscope and then taking the Fast Fourier Transform (FFT) of the average time domain pulse. This approach is used as the basis for the NBS method of calibrating the spectrum amplitude of broadband impulse sources [5-5]. The technical literature relating to the term "spectrum amplitude" is confusing due to the use of several different names for the same quantity. Other names include spectral intensity, spectral density, voltage spectrum, and impulse strength. The name preferred by IEEE is spectrum amplitude, defined as double the magnitude of the Fourier transform of the time domain pulse. That is, the spectrum amplitude vs frequency,  $S(f)$ , is computed from the measured waveform of the time domain pulse,  $v(t)$ , using the basic IEEE definition [5-6], as follows:

$$S(f) = 2 |V(f)| \quad (5-4)$$

where

$$V(f) = \int_{-\infty}^{\infty} v(t) e^{-j2\pi ft} dt. \quad (5-5)$$

The unit of  $S(f)$  is volt·second, or its equivalent volts/hertz. The units commonly used by the EMC community are  $\mu\text{V}/\text{MHz}$  or  $\text{dB}\mu\text{V}/\text{MHz}$ . The decibel unit is defined as  $S(f)$  in decibels above  $1 \mu\text{V}/\text{MHz}$

$$20 \log_{10} \left[ \frac{S(f) \text{ in } \mu\text{V}/\text{MHz}}{1 \mu\text{V}/\text{MHz}} \right].$$



The NBS and IEEE definition given by eqs (5-4) and (5-5) differ by 3 dB from that used by the EMC community. Therefore, as will be seen in the measurement data, a 3 dB correction factor was applied to the NBS FFT data in order to compare these results with the MIL-STD-461 measurements. In the time domain, voltage pulses are measured with respect to zero volts. In the frequency domain, however, they are usually expressed in RMS voltages. For a sine wave, the peak value is  $\sqrt{2}$  times the RMS value. This  $\sqrt{2}$  factor causes a 3 dB difference between the two voltages. Consequently, when a peak responding receiver that has been calibrated in terms of the RMS sine-wave voltage is used to measure  $S(f)$ , the results will be 3 dB lower than if it were calibrated in terms of the peak value.

A block diagram of the NBS Automatic Pulse Measurement System (APMS) is given in figure 5-3. As shown, it consists basically of a sampling oscilloscope interfaced with a computer. The IG used in our tests does not provide trigger output pulses for the oscilloscope. Therefore, a trigger pick-off delay line was used, as shown in the figure. The 6 dB power splitter, 30 dB pad, and 30 dB amplifier insure that the IG and delay line are matched to the 50  $\Omega$  measurement system. The NBS APMS is described in detail in [5-7] and [5-8]. Briefly, NBS calibrates impulse generators by measuring the time domain waveform of an average pulse from a train of repetitive pulses, and then computes the frequency domain spectrum amplitude. The APMS consists of an 18 GHz bandwidth, 50  $\Omega$  sampling oscilloscope interfaced with a computer. The time domain waveform is digitized and stored in the computer memory. By acquiring many waveforms and signal averaging, it is possible to improve the signal-to-noise ratio of the measurement. The spectrum amplitude is then computed, using the fast Fourier transform, eqs (5-4) and (5-5).

Figure 5-4 is a photograph of the oscilloscope trace of the IG output pulse and a plot of the corrected pulse as supplied to the computer for FFT analysis of the spectrum amplitude. Table 5-4 is a list of the computed spectrum amplitude values as measured in the frequency range of 50 to 2400 MHz. Figure 5-5 is a graph of the data for frequencies up to 2 GHz. It can be seen that the measured values agree with the specified IG output of 101 dB $\mu$ V/MHz within about 1 dB for all frequencies up to 1 GHz.

#### 5.4 Approximations of IG Output in Terms of the Measured Area of the Pulses

Certain "idealized" types of pulses can be described mathematically and their spectrum amplitude can be readily calculated. The signal output of actual impulse generators approximates these ideal waveforms quite closely. This approach is used by many manufacturers of IGs. An example is the IG purchased for this project. Such "standard" IGs can be used to calibrate the IBW of a receiver, and are similar to the IG built into the usual field intensity meter for self calibration. That is, the receiver gain control is adjusted to obtain the correct indication (in dB<sub>μ</sub>V/MHz) at each receiver-tuned frequency.

A common type of receiver IG uses a pulse forming transmission line of known electrical length that is charged to a known (regulated) DC voltage. The repetitive transient spikes produced by discharging the line have a time duration of about one-half nanosecond each, and a repetition rate of typically 60 Hz. The spectrum of an IG having short (rectangular) pulses is quite flat at frequencies up to about  $(0.2/T_0)$ , with an amplitude given approximately by [5-9]

$$S(f) = 2A = 2 V_0 \cdot T_0 \quad (5-6)$$

where:  $S(f)$  = spectrum amplitude of the IG, volts/hertz,

$A$  = area of each pulse, volts·seconds,

$V_0$  = DC charging voltage on the line, volts, and

$T_0$  = pulse duration, seconds.

The above approximation, that  $S(f)$  is equal to double the area under the time domain curve of baseband pulses, is strictly true only for idealized delta-function impulses in which the pulse duration is zero and the pulse height is infinite. In this case the frequency spectrum  $V(f)$  has constant amplitude, independent of frequency. For pulses of finite duration,  $S(f)$  at low frequencies is also approximately twice the pulse area. Actually, the equation for the frequency spectrum of rectangular pulses is

$$S(f) = 2 V_0 T_0 \left| \frac{\sin(\pi f T_0)}{(\pi f T_0)} \right| \cdot \quad (5-7)$$

The equation for the frequency spectrum of triangular pulses is

$$S(f) = 2 V_0 T_0 \left| \frac{\sin(\pi f T_0)}{(\pi f T_0)} \right|^2. \quad (5-8)$$

Figure 5-6 shows graphs of both the time domain and frequency domain functions for three common (ideal) types of pulses. For short pulses and low frequencies, the  $(\sin x)/x$  function approaches 1, and  $S(f)$  is approximately  $2 V_0 T_0$  as given by eq (5-6). The IBW of a receiver to be used for measuring impulsive interference can then be calibrated with a "standard" IG in terms of the basic equation

$$IBW = \frac{V_m(t)}{G_0 S(f)} \approx \frac{V_m(t)}{2 G_0 V_0 T_0}, \quad (5-9)$$

where  $G_0$  = receiver system tuned-frequency cw gain.

The theoretical, approximate spectrum amplitude of the commercial IG, at frequencies up to 1 GHz, can thus be calculated by several approximations, as follows:

- a. Assuming that the IG pulses are rectangular, with a peak amplitude of  $V_0$  and a duration given by the time interval at the half-voltage point, but omitting the overshoot and oscillatory part at the end of the pulse (see figure 5-4), then

$$\begin{aligned} S(f) &= 2A = (2)(0.23 \text{ V})(450 \text{ ps}) + 50 \text{ dB attenuator pad} \\ &\quad + 6 \text{ dB power splitter} - 3\text{dB for the EMC definition} \\ &= (2)(0.23 \mu\text{V})(450 \mu\text{s}) + 53 \text{ dB} = 99.3 \text{ dB}\mu\text{V/MHz}. \end{aligned}$$

The above value can be compared with the approximate 100.5 dB $\mu$ V/MHz value measured with the NBS FFT system, as shown in figure 5-5, for frequencies up to 1 GHz.

- b. Assuming that the IG pulses are triangular in shape with a time duration measured at the base of the triangle, but omitting the negative and positive pieces of the pulse after the first triangle, then

$$S(f) = 2A = (0.23 \text{ V})(800 \text{ ps}) + 53 \text{ dB} = 98.3 \text{ dB}\mu\text{V/MHz}.$$

- c. Using the measured area of the first positive part of the pulse,



$$S(f) = 2A = 98.1 \text{ dB}_\mu\text{V/MHz.}$$

- d. Using the same approach as (c) above, but assuming that both the positive and negative parts of the pulse should be added,

$$S(f) = 2A = 100.7 \text{ dB}_\mu\text{V/MHz.}$$

The above value is in best agreement with  $S(f)$  as measured with the NBS FFT system and with the nominal 101 value of the commercial IG tested. Measurements of the built-in step attenuator of the IG were made for all step positions, at a frequency of 300 MHz. The attenuator was found to be accurate within  $\pm 0.2$  dB.

## 5.5 References

- [5-1] MIL-STD-461A. Military Standard, Electromagnetic Interference Characteristics, Requirements for Equipment; 1968 August 1. Also Notice 1, 1969 February 7; Notice 2, 1969 March 20; Notice 3, 1970 May 1; Notice 4, 1971 February 9; and MIL-STD-461B, Notice 1, draft, 1983 January 5.
- [5-2] MIL-STD-462. Military Standard, Electromagnetic Interference Characteristics, Measurement of; 1967 July 31. Also Notice 1; 1968 August 1, Notice 2; 1970 May 1, Notice 3; 1971 February 9, and MIL-STD-462A, draft; 1970 June 29.
- [5-3] IEEE Std 100-1972. IEEE Standard Dictionary of Electrical and Electronic Terms, the Institute of Electrical and Electronics Engineers, Inc. New York: John Wiley & Sons, Inc.; 1972.
- [5-4] MIL-STD-463. Military Standard, Definitions and Systems of Units, Electromagnetic Interference Technology; 1966 June 9. Also, Notice 1; 1972 March 2.
- [5-5] IEEE Std 376-1975. IEEE Standard for the Measurement of Impulse Strength and Impulse Bandwidth. The Institute of Electrical and Electronics Engineers, Inc.; 1975.
- [5-6] Andrews, J.R.; Arthur, M.G. Spectrum amplitude--definition, generation and measurement. Nat. Bur. Stand. (U.S.) Tech. Note 699; 1977 October. 96 p.
- [5-7] Gans, W. L.; Andrews, J. R. Time domain automatic network analyzer for measurement of rf and microwave components. Nat. Bur. Stand. (U.S.) Tech. Note 672; 1975 September.



- [5-8] Andrews, J. R. Impulse generator spectrum amplitude measurement techniques. IEEE Trans. Inst. & Meas., Vol. IM-25, No. 4: 380-384; 1976 December.
- [5-9] Larsen, E.B. Calibration of radio receivers to measure broadband interference. Nat. Bur. Stand. (U.S.) NBSIR 73-335; 1973 September. 75 p.

Table 5-1. Response of an ideal receiver to various types of input signals.

Type of Detector		Type of RF Signal		
		Sine Wave	Random Noise	Periodic Pulses
Average (voltage)	Receiver indication is:	Independent of bandwidth (BW)	Proportional to $\sqrt{BW}$	Independent of BW
Peak (voltage)	Receiver indication is:	Independent of bandwidth (BW)	--	Proportional to BW
RMS (voltage)	Receiver indication is:	Independent of bandwidth (BW)	Proportional to $\sqrt{BW}$	Proportional to $\sqrt{BW}$
Power	Receiver indication is:	Independent of bandwidth (BW)	Proportional to BW	Proportional to BW

Table 5-2. Calibration of receiver impulse bandwidth (IBW) and impulse generator spectrum amplitude S(f) using MIL-STD-462 technique, bands 1-4.

Photograph number	1	2	3	4	5	6	7	8
Receiver band, MHz	30-57	30-57	55-105	55-105	101-192	101-192	186-292	186-292
Receiver tuned frequency, MHz	31	56	56	103	103	189	189	288
Receiver bandwidth setting, MHz	1	1	1	1	1	1	1	1
Receiver attenuator step, dB	40	40	40	40	40	40	40	40
Impulse generator (IG) setting, dB $\mu$ V/MHz	101	101	101	101	101	101	101	101
Nominal IG level at receiver, dB $\mu$ V/MHz	95	95	95	95	95	95	95	95
Receiver indication of IG signal, dB $\mu$ V/MHz	91.0	91.9	91.4	91.9	91.0	91.0	92.0	91.8
Oscilloscope sweep speed, $\mu$ s/cm	0.5	0.5	0.5	0.5	0.5	0.5	0.5	0.5
Oscilloscope gain setting, mV/cm	20	20	20	20	20	20	20	20
Receiver impulse response envelope maximum height, cm	3.90	4.35	4.10	4.39	4.10	3.90	4.45	4.30
Weight of response envelope, gm	0.230	0.238	0.227	0.231	0.219	0.210	0.220	0.208
Envelope area from measured weight, cm <sup>2</sup>	8.81	9.07	8.65	9.02	8.35	8.19	8.56	8.18
Envelope area using a planimeter, cm <sup>2</sup>	8.75	8.94	8.70	9.22	8.82	8.26	8.73	8.47
Envelope area, average of 2 methods, cm <sup>2</sup>	8.78	9.01	8.68	9.12	8.59	8.23	8.65	8.33
Resulting receiver IBW, MHz	0.89	0.97	0.94	0.96	0.95	0.95	1.03	1.03
Measured cw gain of receiver, G <sub>0</sub>	1.50	1.48	1.48	1.50	1.48	1.48	1.51	1.49
Resulting S(f) at receiver, dB $\mu$ V/MHz	95.3	95.7	95.4	95.7	95.3	94.9	95.2	94.9
Resulting S(f) of IG, dB $\mu$ V/MHz	101.3	101.7	101.4	101.7	101.3	100.9	101.2	100.9
Average S(f) at each frequency, dB $\mu$ V/MHz	101.3		101.5		101.5		101.1	

Table 5-3. Calibration of receiver impulse bandwidth (IBW) and impulse generator spectrum amplitude  $S(f)$  using MIL-STD-462 technique, bands 5-8.

Photograph number	9	10	11	12	13	14	15	16	17
Receiver band, MHz	285-445	285-445	430-620	430-620	600-825	600-825	800-1000	800-1000	800-1000
Receiver tuned frequency, MHz	288	438	438	610	610	812	812	900	999
Receiver bandwidth setting, MHz	1	1	1	1	1	1	1	1	1
Receiver attenuator step, dB	40	40	40	40	40	40	40	40	40
Impulse generator (IG) setting, $\text{dB}_\mu\text{V}/\text{MHz}$	101	101	101	101	101	101	101	101	101
Nominal IG level at receiver, $\text{dB}_\mu\text{V}/\text{MHz}$	95	95	95	95	95	95	95	95	95
Receiver indication of IG signal, $\text{dB}_\mu\text{V}/\text{MHz}$	91.8	91.8	91.8	92.2	92.2	92.9	92.9	93.2	94.0
Oscilloscope sweep speed, $\mu\text{s}/\text{cm}$	0.5	0.5	0.5	0.5	0.5	0.5	0.5	0.5	0.5
Oscilloscope gain setting, $\text{mV}/\text{cm}$	20	20	20	20	20	20	20	20	20
Receiver impulse response envelope maximum height, cm	4.25	4.20	4.28	4.60	4.45	4.80	4.78	5.03	5.60
Weight of response envelope, gm	0.210	0.210	0.216	0.224	0.223	0.242	0.243	0.254	0.283
Envelope area from measured weight, $\text{cm}^2$	8.24	8.04	8.09	8.59	8.39	9.06	9.03	9.38	11.05
Envelope area using a planimeter, $\text{cm}^2$	8.45	8.03	8.17	8.61	8.45	8.91	9.26	9.60	10.88
Envelope area, average of 2 methods, $\text{cm}^2$	8.35	8.04	8.13	8.60	8.42	8.99	9.15	9.49	10.97
Resulting receiver IBW, MHz	1.02	1.04	1.05	1.07	1.06	1.07	1.04	1.06	1.02
Measured cw gain of receiver, $G_0$	1.45	1.41	1.43	1.45	1.45	1.45	1.47	1.43	1.45
Resulting $S(f)$ at receiver, $\text{dB}_\mu\text{V}/\text{MHz}$	95.2	95.1	95.1	95.5	95.3	95.8	95.9	96.4	97.6
Resulting $S(f)$ of IG, $\text{dB}_\mu\text{V}/\text{MHz}$	101.2	101.1	101.1	101.5	101.3	101.8	101.9	102.4	103.6
Average $S(f)$ at each frequency, $\text{dB}_\mu\text{V}/\text{MHz}$	101.1		101.1		101.4		101.9		103.6

Table 5-4. Spectrum amplitude of the commercial impulse generator, measured with the NBS FFT calibration system.

Frequency MHz	<u>S(f), dB<math>\mu</math>V/MHz</u>		Frequency MHz	<u>S(f), dB<math>\mu</math>V/MHz</u>	
	Using IEEE Definition	Using EMC Definition		Using IEEE Definition	Using EMC Definition
50	102.9	99.9	1250	102.6	99.6
100	103.5	100.5	1300	102.5	99.5
150	103.2	100.2	1350	101.5	98.5
200	103.5	100.5	1400	100.6	97.6
250	103.5	100.5	1450	99.2	96.2
300	103.7	100.7	1500	98.0	95.0
350	103.2	100.2	1550	95.7	92.7
400	103.5	100.5	1600	93.7	90.7
450	103.3	100.3	1650	92.0	89.0
500	103.4	100.4	1700	90.4	87.4
550	103.2	100.2	1750	87.7	84.7
600	103.6	100.6	1800	86.1	83.1
650	103.4	100.4	1850	83.1	80.1
700	103.7	100.7	1900	80.0	77.0
750	103.4	100.4	1950	81.7	78.7
800	103.4	100.4	2000	87.4	84.4
850	103.3	100.3	2050	87.0	84.0
900	103.9	100.9	2100	89.9	86.9
950	103.9	100.9	2150	89.1	86.1
1000	104.1	101.1	2200	89.0	86.0
1050	104.0	101.0	2250	82.3	79.3
1100	104.3	101.3	2300	78.1	75.1
1150	103.5	100.5	2350	79.6	76.6
1200	103.2	100.2	2400	83.1	80.1



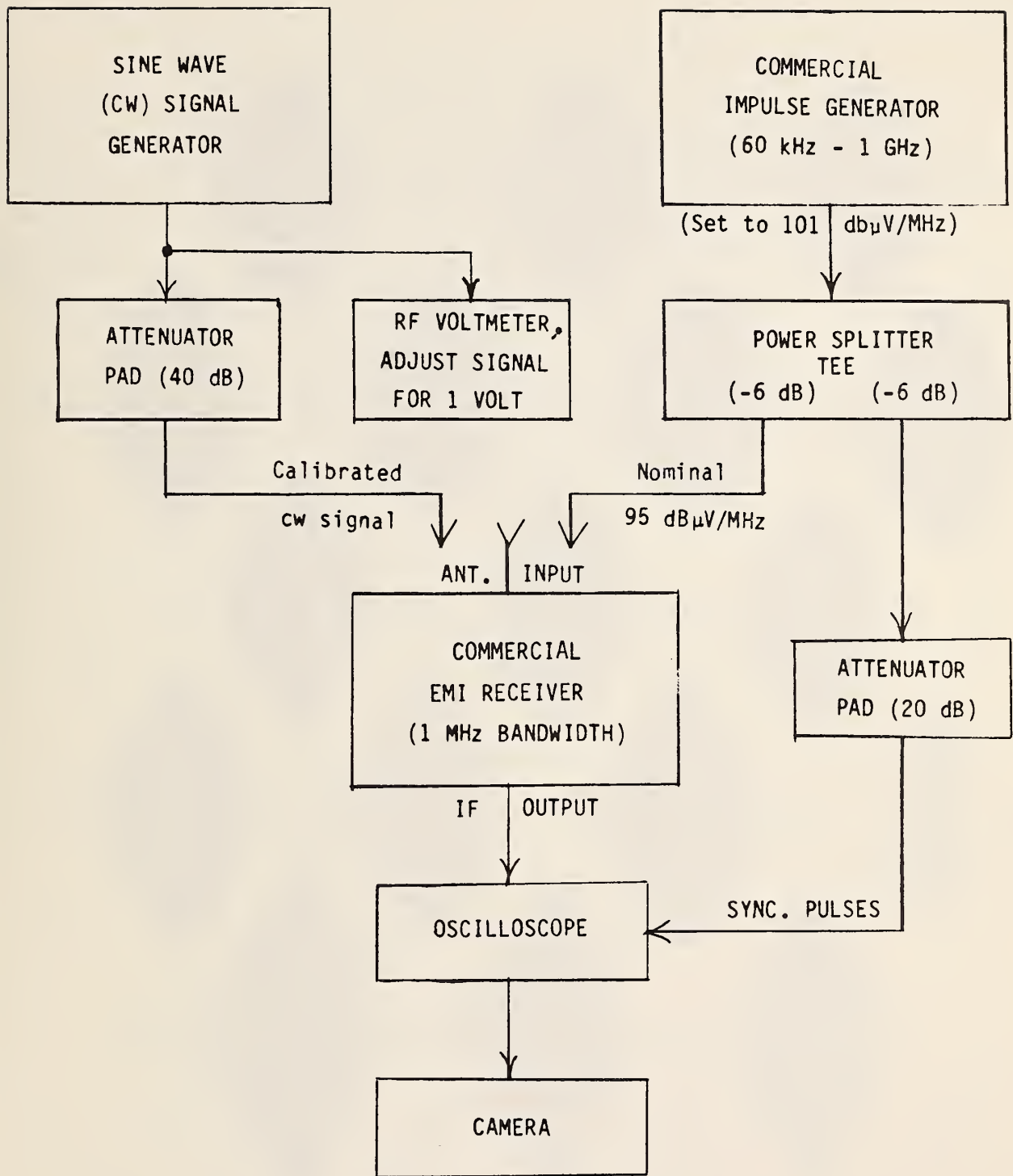


Figure 5-1. Instrumentation for testing the MIL-STD-461/462 approach for measuring impulse bandwidth of a receiver and spectrum amplitude of an impulse generator.

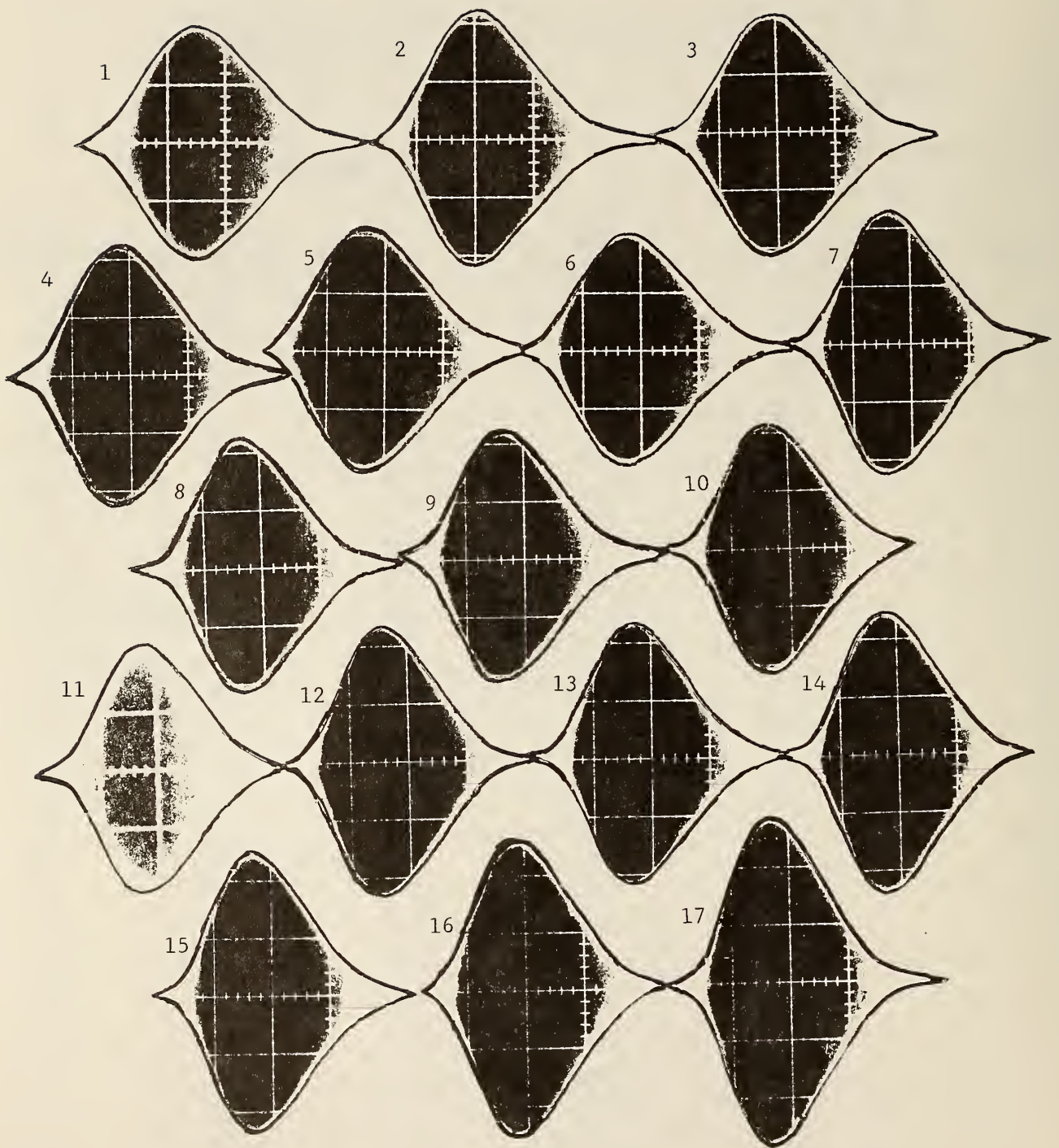


Figure 5-2. Photographs of the receiver impulse response envelopes (video pulses) measured at NBS.

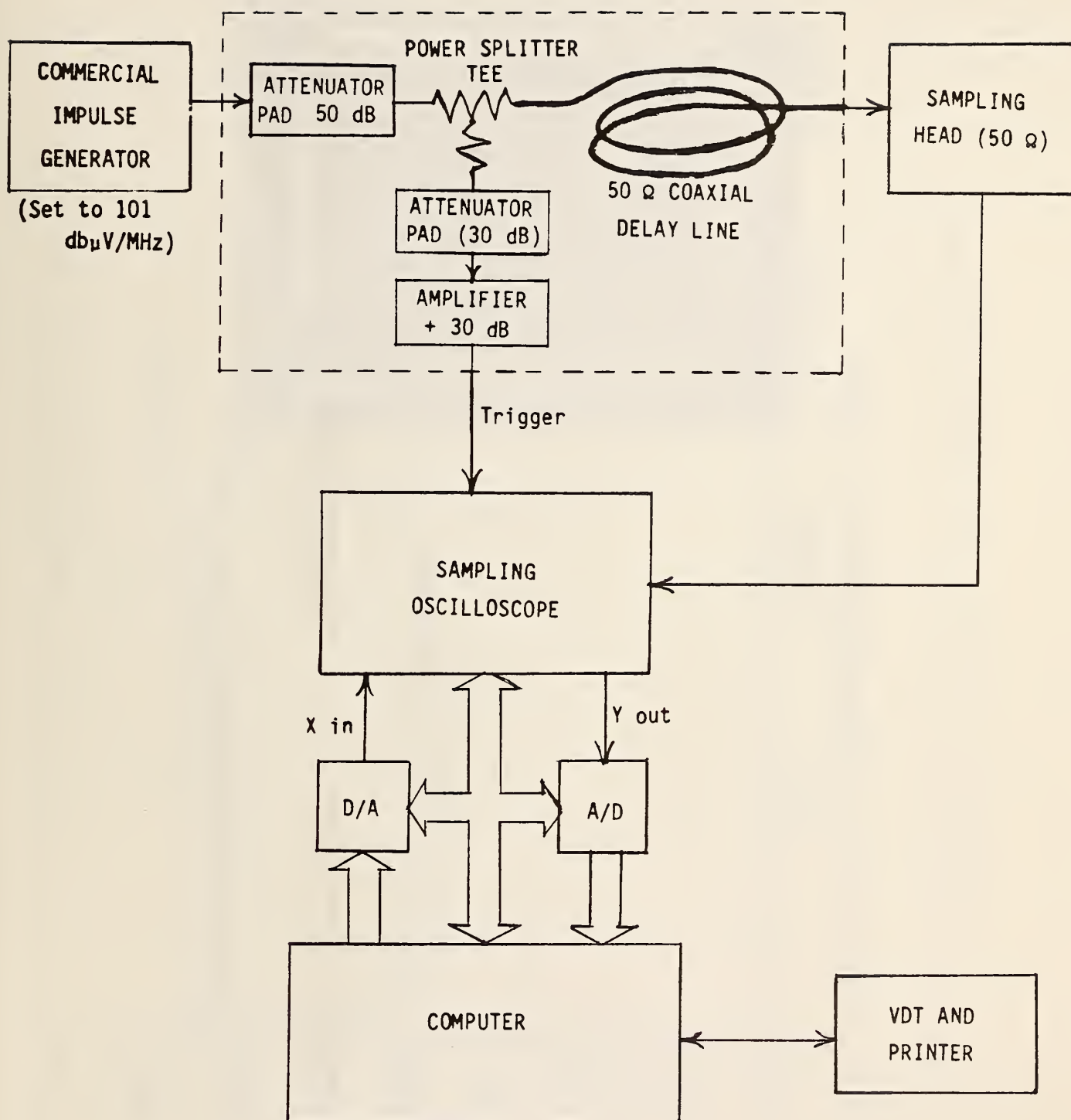


Figure 5-3. Instrumentation for the NBS automatic FFT pulse measurement system.

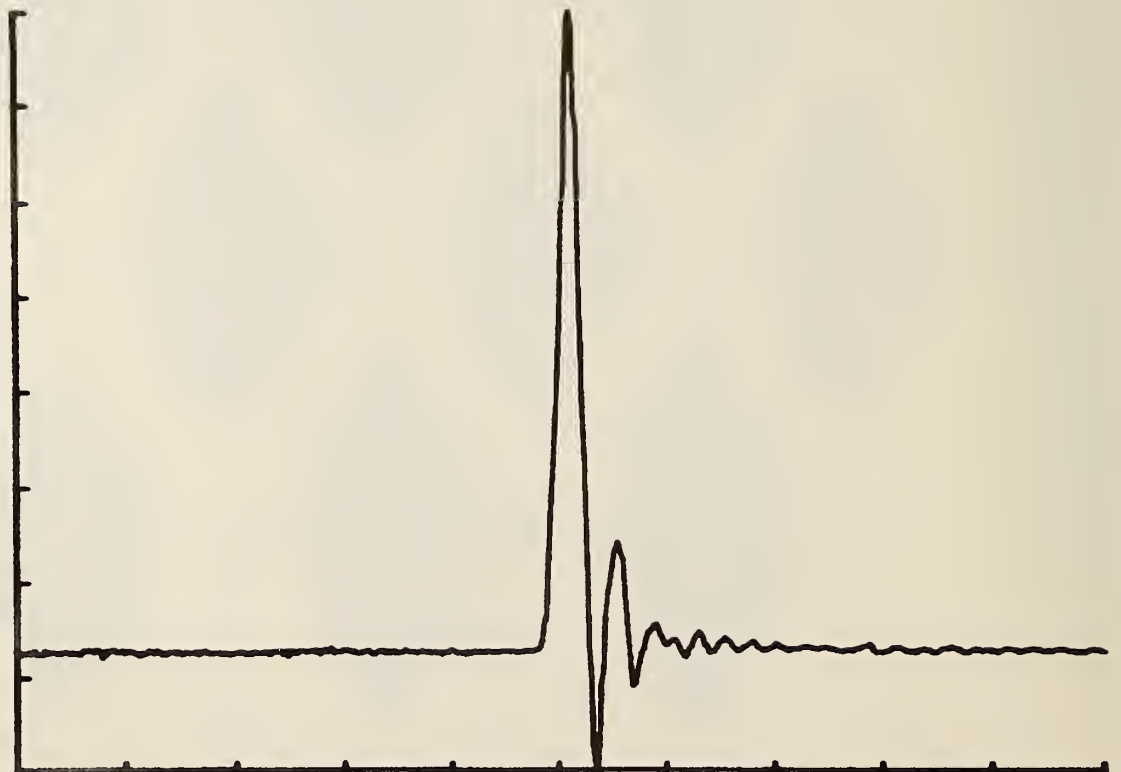
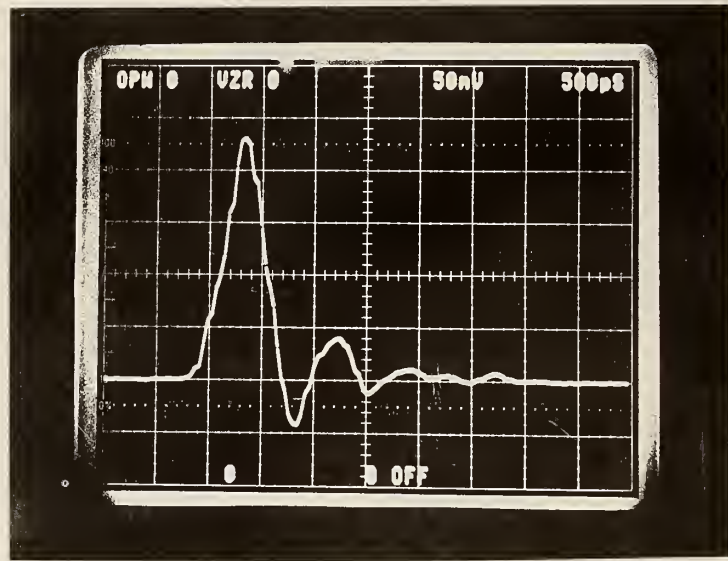


Figure 5-4. Photograph of sampling oscilloscope trace of the IG output pulse (top) and plot of the pulse supplied to the computer for the FFT (bottom).



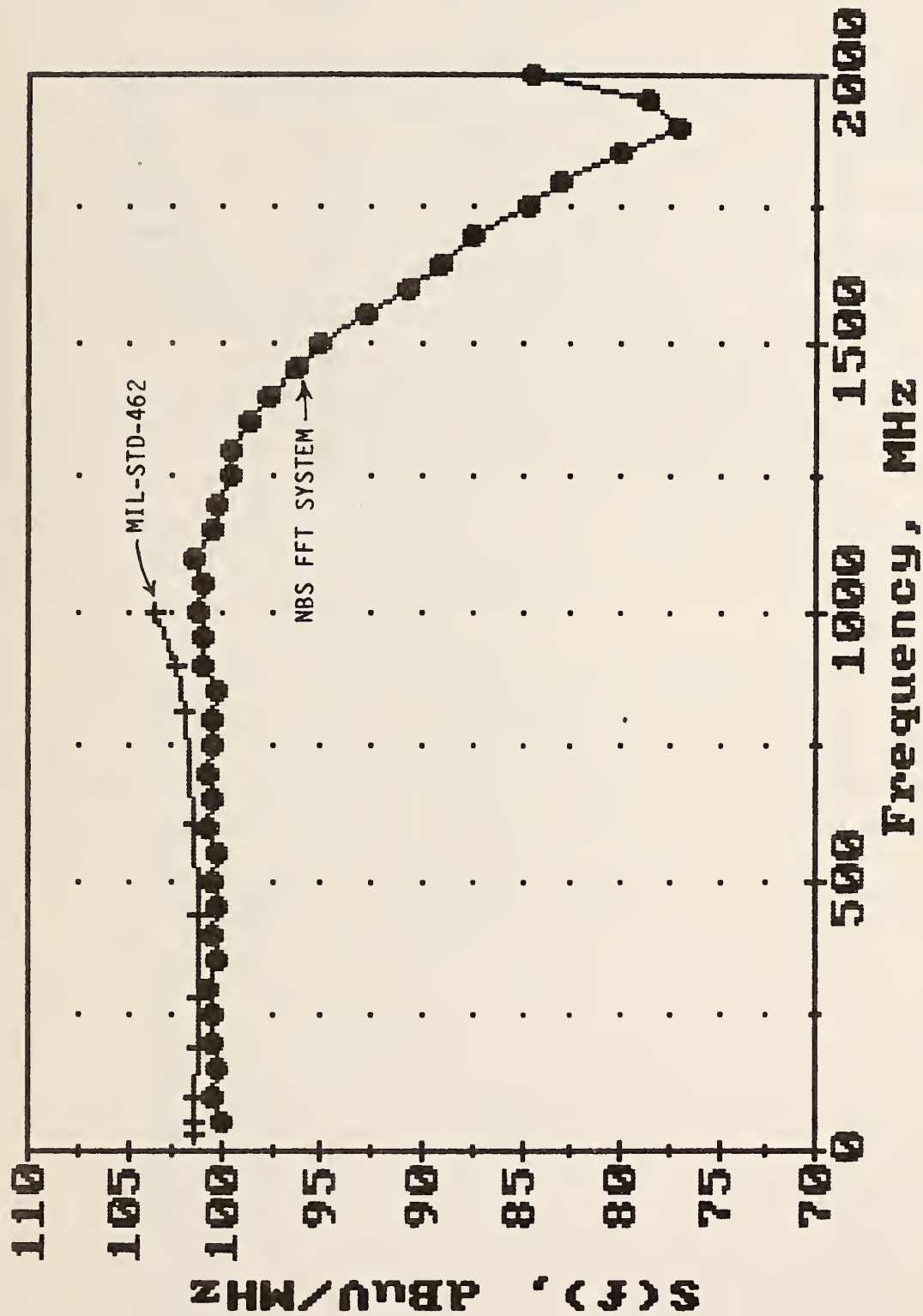


Figure 5-5. Graphs of the IG spectrum amplitude measured by two methods, MIL-STD-462 and the NBS FFT pulse measurement system.

Equation for  $S(f)$

Rectangular pulse

$$2V_0T_0 \left| \frac{\sin(\pi f T_0)}{(\pi f T_0)} \right|$$

Triangular pulse

$$2V_0T_0 \left| \frac{\sin(\pi f T_0)}{(\pi f T_0)} \right|^2$$

Sine squared pulse

$$2V_0T_0 \left| \frac{\sin(2\pi f T_0)}{(2\pi f T_0) [1 - (2f T_0)^2]} \right|$$

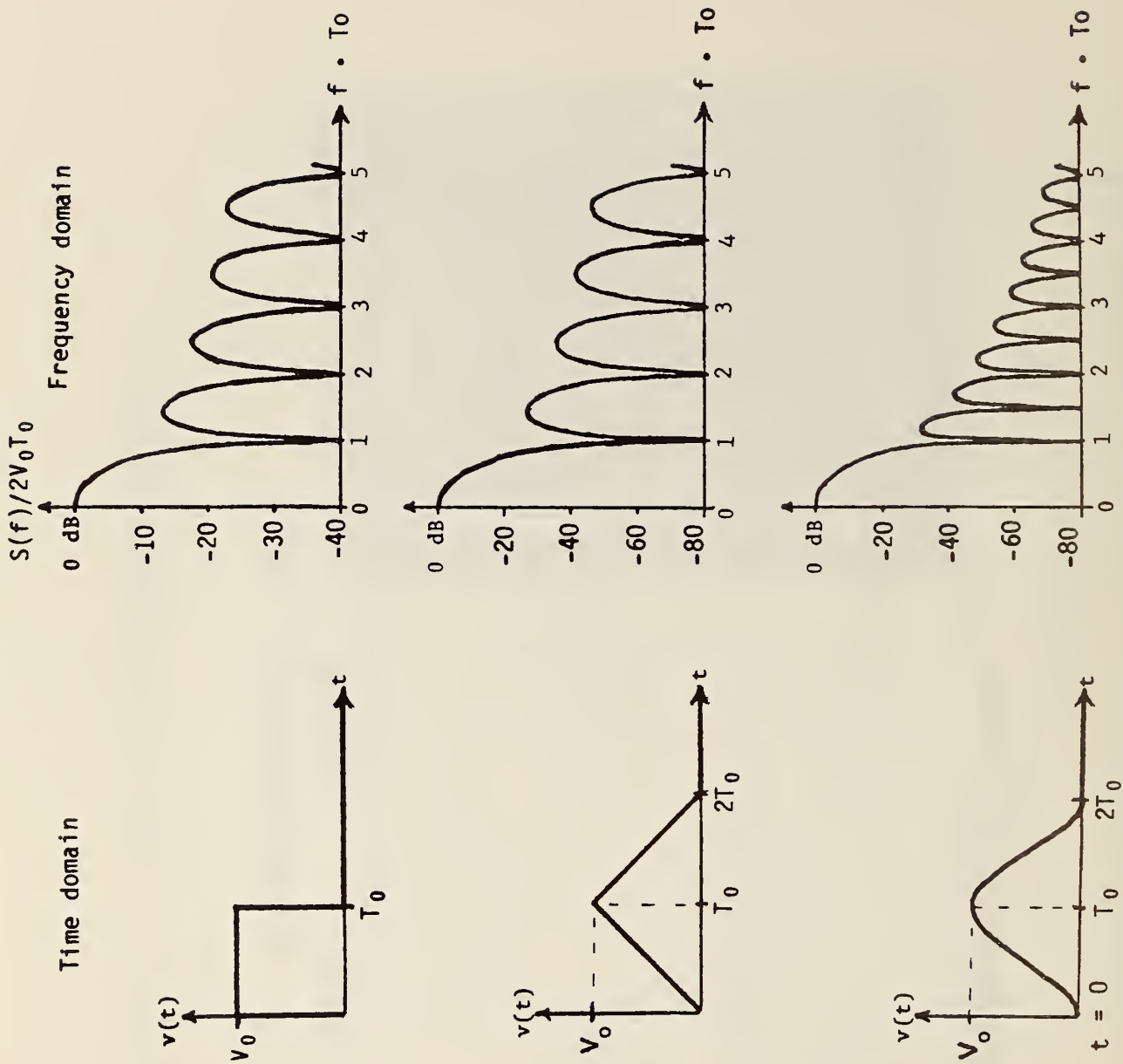


Figure 5-6. Sketches of the spectrum amplitude of three common pulse waveforms.

## 6. Overall Summary, Conclusions, and Recommendations

### 6.1 Field of a Parallel-Plate Transmission Line

MIL-STD-462 specifies the use of a parallel-plate transmission line (stripline) having a plate spacing of 0.457 m (1.5 ft), an upper plate width of 0.610 m (2 ft), and a lower plate width of 0.914 m (3 ft). This stripline is used for making radiated susceptibility tests of electronic equipment in a known EM field. The characteristic impedance ( $Z_C$ ) depends mainly on the plate spacing and width. It is also affected by its location, especially if the line is inside a shielded enclosure (high-Q cavity). Therefore, the optimum value of the terminating resistor for a stripline should be determined experimentally from tests of the E-field. The main criterion for a good standard-field setup is the level and uniformity of the generated field as a function of frequency. MIL-STD-462 states that the expected  $Z_C$  value for this line is 83  $\Omega$ . Several equations are given in the literature for calculating  $Z_C$  of parallel-plate lines. The line fabricated at NBS according to MIL-STD-462 has measured values ranging from 80 to 160  $\Omega$ .

Measurements were also made of the input impedance of the stripline, with the line terminated in two different values of resistance (83  $\Omega$  and 120  $\Omega$ ), for frequencies ranging from 1 to 100 MHz. The data show that the input impedance varies with frequency for both values of terminating resistance. The optimum value of terminating resistance appears to be in the neighborhood of 120  $\Omega$  rather than the 83  $\Omega$  specified in the MIL-STD.

Measurements of electric field strength vs signal frequency were made for two different locations of the stripline in the empty screenroom. The measured values of E-field at the center of the stripline, for both values of terminating resistance, were within 2 dB of the theoretically calculated values at all frequencies up to 40 MHz. The measured E-field at 30 MHz as a function of position along the line was correct within 2.3 dB and uniform within  $\pm 0.5$  dB over the 2 m length of the line. The effect of screenroom resonances on the behavior of the MIL-STD stripline is clearly evident from the measured excursions in impedance and field strength at frequencies above 40 MHz. These resonance effects would occur at lower frequencies if a larger screenroom were used.

A parallel-plate stripline can be operated without a resistive termination at frequencies up to 30 or 40 MHz. When the line is open circuited, it

produces a field with high wave impedance (high E/H ratio). High level E-fields can then be produced by connecting a broadband step-up transformer at the input of the line. Also, a high level E-field can be produced with a low power source if the line is resonated by means of an inductor. At higher frequencies (above 30 MHz) approaching self resonance of the system, it is necessary to measure the field strength at the calibrating point with a small transfer probe that has been calibrated previously in a small stripline or TEM cell. When a stripline or TEM cell is short circuited, it acts as a single turn loop, producing a high level H-field with low wave impedance (low E/H ratio).

## 6.2 Use of an Electrically Small Transfer Probe

An electrically small antenna (rf probe) can be used to test field level vs frequency and position in a MIL-STD-462 stripline. Such transfer probes can also be used to improve the construction and operation of other standard-field chambers by optimizing experimentally the value of terminating load impedance. Similarly, the E- or H-field in a screenroom that has been converted into a long-wire chamber can be determined more accurately with a transfer probe than by relying on theoretical equations. Measurements for this report were made with a calibrated NBS E-field probe (EFM-5) having dipole antennas 5 cm in length. Because of its design and small size, it does not perturb the field being measured.

## 6.3 Field of a Single-Wire Transmission Line

The long-wire antenna at NBS was installed in a shielded room. A No. 10 wire was suspended from the two end walls of the room, driven at one end and terminated at the other. The dimensions of the NBS screenroom are 7 m long x 3.7 m wide x 2.4 m high. The MIL-STD-462 equation for the characteristic impedance is stated as usable when the distance of the wire to the ceiling is less than one-third the room height. The calculated value according to this equation is 422  $\Omega$ . The final experimental determination of the optimum value was 380  $\Omega$ .

The field uniformity along the center line of the screenroom chamber was measured at 1 MHz, 15 MHz, and 30 MHz. The deviation with respect to the field at the midpoint of the chamber was less than  $\pm 0.3$  dB at 1 MHz, less than



$\pm 1$  dB at 15 MHz, and varied from +0 to -3 dB at 30 MHz. The data indicate that an acceptable uniformity can be achieved in the long-wire antenna chamber. However, terminating the antenna with the optimum resistance, as described in the MIL-STD, is necessary. The equation given in MIL-STD-462 was used to calculate the E field and compared with the measured values. The vertical component was measured at several distances below the long-wire for signal frequencies of 1, 2, 3, 5, 7.5, 15, 22, and 30 MHz. The distance below the center of the wire ranged from 0.2 to 0.8 m. The measured field varied both as a function of distance and frequency. The dB error in the calculated field was greater as the distance from the center conductor was increased. The data indicate that the average field strength produced in the long-wire chamber is uniform within 3 dB at frequencies up to 30 MHz, provided the long-wire is terminated in its characteristic impedance. However, it is recommended that a transfer probe be used to measure the field uniformity and absolute value at any desired location.

#### 6.4 Calibration of Antenna Factors for EMI Antennas

Measurements have been made at NBS of antenna factors in a screenroom, using the two antenna method described in MIL-STD-461A. An "in situ" antenna factor is determined for two identical antennas at specific locations in a given shielded enclosure. To determine antenna factors at an open field site, the standard antenna approach is used at NBS to calibrate dipoles for the horizontal component of electric field. The standard field method is used for calibrating monopoles for the vertical component of electric field. Two types of antennas were used for measurements of antenna factor--vertical monopoles and horizontal broadband dipoles (biconicals). The antenna factors determined by NBS open-site calibrations were compared with those determined in the screenroom by the MIL-STD approach.

The graph given in figure 2A of MIL-STD-461A for a typical biconical shows variation in antenna factor from a minimum of 7 dB at its resonance dip to a maximum of 18 dB. The antenna factor curves given in the manufacturer's manual show a variation from 4 dB (minimum) to 18 dB (maximum). The far-field antenna factors calibrated at the NBS field site had a total range of 4 dB (minimum) to 17 dB (maximum). In addition, all of the antenna factor curves for the two biconicals were within 3 dB of each other over the total frequency

range of 20-200 MHz.

The layout for measuring the effective gain of two biconical antennas in the NBS screenroom involved placing the two antennas on the center line (long dimension) of the room with both antennas at a height of 1 m above the floor. The dipoles were parallel to each other and horizontally polarized. Two different separation distances were checked, 1 m and 3 m. The effect of screenroom resonances and reflections on the measured antenna factor was much greater than any of those mentioned in the previous paragraph. The variation of antenna factor in the screenroom for a separation distance of 3 m was from 54.9 dB (maximum) to -2.3 dB (minimum). The variation for a 1 m separation distance was 50.1 dB (maximum) to 4.8 dB (minimum). The data also showed large effects of multipath reflections as a function of antenna placement in the screenroom. Our data indicate that using open-field-site antenna factors as permitted in MIL-STD-461A will lead to greater error in field strength measurements in a screenroom than using antenna factors as measured in-situ. Measurements of field strength determined from the measured screenroom antenna factors differ as much as 7 dB from the field measured with a calibrated transfer probe over the frequency range of 20-200 MHz.

Antenna factors of vertical monopoles are calibrated at NBS by immersing the receiving monopole in a known field above a groundscreen, about 20 m from a transmitting monopole. This is done at an outdoor field site which has a 30 x 60 m conducting mesh stretched over a concrete slab. The vertical E component of the calibrating field is calculated in terms of the base current in a thin transmitting monopole, at frequencies from 30 kHz to 300 MHz. The antenna factors measured at the NBS field site were compared with those given in the manufacturer's manual. The differences were as much as 10 dB at a given frequency. The antenna factors were also measured in the screenroom using a two-antenna method similar to that described for the biconicals. Again, two separation distances were used--1 and 3 m. The screenroom values of antenna factor obtained by the MIL-STD approach differed as much as 64 dB from that calibrated at the field site.

These measurements indicate that antenna factors determined in a screenroom are not an accurate parameter for subsequent measurement of field strength. It is concluded that large errors may occur due to room resonances, multiple reflections, and distortion of fields. The measurements depend on

the size of the enclosure, location of the test setup in the screenroom, and position of the antennas. Thus, determination of an in-situ antenna factor in a screenroom or using antenna factors which were determined in a free-space environment do not lead to accurate field strength measurements. To establish accurate EM fields in a screenroom, a small transfer probe should be used to measure the field produced by a radiating antenna.

## 6.5 Measurement of Broadband Impulsive Signals

The MIL-STD-462 approach for measuring impulse bandwidth, IBW, of a receiver and spectrum amplitude,  $S(f)$ , of an impulse generator was evaluated at NBS. The EMI receiver used has a selectable bandwidth which was set in the 1 MHz position for all the data reported here. At each receiver frequency tested, the gain control was adjusted to obtain a dial indication equal to the true cw signal level. The impulse generator used for our tests is specified to produce a spectrum output that is flat within  $\pm 1$  dB from 60 kHz to 1000 MHz. The IG was set to its maximum output level of 101 dB $\mu$ V/MHz. Photographs of the receiver response envelopes (video pulses) were used for the MIL-STD calibration of the EMI receiver. A set of data was taken for at least two frequencies in each of the eight receiver bands. It was found that the MIL-STD measurements of  $S(f)$  were within 0.5 dB of the IG nominal output value at all the frequencies checked below 800 MHz. At higher frequencies the measured values of  $S(f)$  were 0.9 to 2.6 dB above the nominal value.

An impulse generator can also be calibrated by measuring the train of output pulses with a sampling oscilloscope and taking the Fast Fourier Transform (FFT) of the average time domain pulse. This approach is used for the NBS method of calibrating the spectrum amplitude of broadband impulse sources. The  $S(f)$  of the IG was calibrated in the frequency range of 50-2400 MHz and these values agreed with the specified IG output within about 1 dB for all frequencies up to 1 GHz.

Certain "idealized" types of pulses can be described mathematically and their spectrum amplitude calculated. This approach is used by many manufacturers of IGs, including the IG purchased for these tests. Such "standard" IGs can be used to calibrate the IBW of a receiver, and are similar to the IG built into the usual field intensity meter. The IG uses repetitive transient spikes having a time duration of about 0.5 nanosecond each. The spectrum of

an IG having such short pulses is fairly flat at frequencies up to about 1 GHz, with an amplitude approximately double the area under the time domain curve of each pulse. It was found that this approximation and the NBS pulse calibration system using FFT both agreed with the MIL-STD-462 measurements within about 2 dB at all frequencies checked up to 1 GHz.



## 7. Acknowledgments

The authors wish to express their appreciation to all those who contributed time and interest during this NBS/Army project. We especially acknowledge the cooperation and assistance of Mr. Gilmore Krenner, Jr., the contract officer's representative. We are also grateful to Susan Macaskill and Michael CdeBaca of the NBS staff who accomplished most of the data gathering and analysis, both in the screenroom facility and at the various field sites used for obtaining comparison data.

U.S. DEPT. OF COMM. <b>BIBLIOGRAPHIC DATA SHEET</b> (See instructions)	<b>1. PUBLICATION OR REPORT NO.</b> NBS/TN-1300	<b>2. Performing Organ. Report No.</b>	<b>3. Publication Date</b> October 1986
<b>4. TITLE AND SUBTITLE</b> Assessment of Error Bounds for Some Typical MIL-STD-461/462 Types of Measurements			
<b>5. AUTHOR(S)</b> J.E. Cruz and E.B. Larsen			
<b>6. PERFORMING ORGANIZATION</b> (If joint or other than NBS, see instructions) NATIONAL BUREAU OF STANDARDS DEPARTMENT OF COMMERCE WASHINGTON, D.C. 20234		<b>7. Contract/Grant No.</b>	<b>8. Type of Report &amp; Period Covered</b>
<b>9. SPONSORING ORGANIZATION NAME AND COMPLETE ADDRESS</b> (Street, City, State, ZIP) U.S. Army Aviation Systems Command DRSAV-QE St. Louis, Missouri 63120			
<b>10. SUPPLEMENTARY NOTES</b>  <input type="checkbox"/> Document describes a computer program; SF-185, FIPS Software Summary, is attached.			
<b>11. ABSTRACT</b> (A 200-word or less factual summary of most significant information. If document includes a significant bibliography or literature survey, mention it here) This report deals with the instrumentation and equations for several systems used by the U.S. Army for electromagnetic compatibility (EMC) testing and calibrations. Most testing for MIL-STD-461/462 is performed in a shielded enclosure (screenroom) rather than at an open field site, which leads to uncertainty in the measurement of emissions from electronic equipment, or the susceptibility of equipment to radiation. Assessment of error bounds by the National Bureau of Standards (NBS) is covered in this report, and suggestions are given for improving the measurements. Four areas of concern were studied as follows: (a) electromagnetic (EM) fields generated in a parallel-plate transmission line (stripline), (b) EM fields beneath a single-wire transmission line in a screenroom (long-wire line), (c) determination of antenna factors for electromagnetic interference (EMI) antennas located in a screenroom, and (d) calibration of EMI receivers to measure broadband impulsive signals. Most EMC antennas at NBS are calibrated at an open field site or in an anechoic chamber. This report presents antenna factors determined in a typical screenroom using the two-antenna method, and comparison with those determined at an open field site. The video pulse technique prescribed in MIL-STD-462 for calibrating EMI receivers was also evaluated. Four different methods were tested for comparison with the MIL-STD approach. They are defined and discussed in this report.			
<b>12. KEY WORDS</b> (Six to twelve entries; alphabetical order; capitalize only proper names; and separate key words by semicolons) antenna factor; electromagnetic compatibility; field strength standards; impulse spectrum amplitude; military standards; screenroom measurements			
<b>13. AVAILABILITY</b> <input checked="" type="checkbox"/> Unlimited <input type="checkbox"/> For Official Distribution. Do Not Release to NTIS <input checked="" type="checkbox"/> Order From Superintendent of Documents, U.S. Government Printing Office, Washington, D.C. 20402. <input type="checkbox"/> Order From National Technical Information Service (NTIS), Springfield, VA. 22161		<b>14. NO. OF PRINTED PAGES</b> 108	<b>15. Price</b>

# NBS *Technical Publications*

## *Periodical*

---

**Journal of Research**—The Journal of Research of the National Bureau of Standards reports NBS research and development in those disciplines of the physical and engineering sciences in which the Bureau is active. These include physics, chemistry, engineering, mathematics, and computer sciences. Papers cover a broad range of subjects, with major emphasis on measurement methodology and the basic technology underlying standardization. Also included from time to time are survey articles on topics closely related to the Bureau's technical and scientific programs. Issued six times a year.

## *Nonperiodicals*

---

**Monographs**—Major contributions to the technical literature on various subjects related to the Bureau's scientific and technical activities.

**Handbooks**—Recommended codes of engineering and industrial practice (including safety codes) developed in cooperation with interested industries, professional organizations, and regulatory bodies.

**Special Publications**—Include proceedings of conferences sponsored by NBS, NBS annual reports, and other special publications appropriate to this grouping such as wall charts, pocket cards, and bibliographies.

**Applied Mathematics Series**—Mathematical tables, manuals, and studies of special interest to physicists, engineers, chemists, biologists, mathematicians, computer programmers, and others engaged in scientific and technical work.

**National Standard Reference Data Series**—Provides quantitative data on the physical and chemical properties of materials, compiled from the world's literature and critically evaluated. Developed under a worldwide program coordinated by NBS under the authority of the National Standard Data Act (Public Law 90-396).

NOTE: The Journal of Physical and Chemical Reference Data (JPCRD) is published quarterly for NBS by the American Chemical Society (ACS) and the American Institute of Physics (AIP). Subscriptions, reprints, and supplements are available from ACS, 1155 Sixteenth St., NW, Washington, DC 20056.

**Building Science Series**—Disseminates technical information developed at the Bureau on building materials, components, systems, and whole structures. The series presents research results, test methods, and performance criteria related to the structural and environmental functions and the durability and safety characteristics of building elements and systems.

**Technical Notes**—Studies or reports which are complete in themselves but restrictive in their treatment of a subject. Analogous to monographs but not so comprehensive in scope or definitive in treatment of the subject area. Often serve as a vehicle for final reports of work performed at NBS under the sponsorship of other government agencies.

**Voluntary Product Standards**—Developed under procedures published by the Department of Commerce in Part 10, Title 15, of the Code of Federal Regulations. The standards establish nationally recognized requirements for products, and provide all concerned interests with a basis for common understanding of the characteristics of the products. NBS administers this program as a supplement to the activities of the private sector standardizing organizations.

**Consumer Information Series**—Practical information, based on NBS research and experience, covering areas of interest to the consumer. Easily understandable language and illustrations provide useful background knowledge for shopping in today's technological marketplace.

*Order the above NBS publications from: Superintendent of Documents, Government Printing Office, Washington, DC 20402.*

*Order the following NBS publications—FIPS and NBSIR's—from the National Technical Information Service, Springfield, VA 22161.*

**Federal Information Processing Standards Publications (FIPS PUB)**—Publications in this series collectively constitute the Federal Information Processing Standards Register. The Register serves as the official source of information in the Federal Government regarding standards issued by NBS pursuant to the Federal Property and Administrative Services Act of 1949 as amended, Public Law 89-306 (79 Stat. 1127), and as implemented by Executive Order 11717 (38 FR 12315, dated May 11, 1973) and Part 6 of Title 15 CFR (Code of Federal Regulations).

**NBS Interagency Reports (NBSIR)**—A special series of interim or final reports on work performed by NBS for outside sponsors (both government and non-government). In general, initial distribution is handled by the sponsor; public distribution is by the National Technical Information Service, Springfield, VA 22161, in paper copy or microfiche form.

**U.S. Department of Commerce**  
National Bureau of Standards  
Gaithersburg, MD 20899

Official Business  
Penalty for Private Use \$300